Supplementary Information

Early-Stage Biosynthesis of Phenalinolactone Diterpenoids Involves Sequential Prenylation, Epoxidation, and Cyclization

*Tyler A. Alsup[1], Zining Li[1], Caitlin A. McCadden[1], Annika Jagels[1,2], Diana P. Łomowska-Keehner[1], Erin M. Marshall[1,2], Liao-Bin Dong[3], Sandra Loesgen[1,2], and Jeffrey D. Rudolf[1]**

[1]Department of Chemistry, University of Florida, Gainesville, Florida, USA

[2]Whitney Laboratory for Marine Bioscience, University of Florida, St. Augustine, FL, United States

[3]State Key Laboratory of Natural Medicines, School of Traditional Chinese Pharmacy, China Pharmaceutical University, Nanjing 211198, Jiangsu, China

*To whom correspondence should be addressed: jrudolf@chem.ufl.edu

Table of Contents

Material and Methods

Bacterial Strains, Plasmids, and Chemicals.

Strains, plasmids, and PCR primers used in this study are listed in Tables S1–S3. *E. coli* ET12567/pUZ8002 was used for all intergeneric conjugations. *E. coli* Turbo cells were used for general cloning. Enzymes and reagents for general cloning procedures including Q5 high fidelity DNA polymerase, restriction enzymes, buffers, and dNTPs were purchased from NEB and used according to the manufacturer's suggested protocols. Omega Bio-Tek gel extraction and plasmid isolation kits were used for the purification of digested plasmids, PCR fragments, and plasmids harboring the desired gene inserts. All media components, chemicals, and solvents were purchased at high quality from various commercial suppliers.

General Experimental Procedures.

All 1D (^{1}H and ^{13}C) and 2D (^{1}H-^{13}C HSQC, ^{1}H-^{1}H COSY, ^{1}H-^{13}C HMBC) NMR experiments were performed in $CDCl_3$ or CD_3OD on either a Bruker AVANCE III Ultrashield 600 or a Bruker AVANCE III HD 600 equipped with a 5 mm TXI CryoProbe, Bruker AVANCE III 800 equipped with a 5 mm TXI CryoProbe. All NMR chemical shifts in $CDCl_3$ were referenced to residual $CHCl_3$ at 7.26 ppm for ^{1}H or 77.00 ppm for ^{13}C, and all chemical shifts in CD_3OD were referenced to residual CH_3OH at 3.31 ppm for ^{1}H or 49.00 ppm for ^{13}C. For LC-MS analysis, an Agilent 1290 infinity II single quadrupole LC/MSD equipped with a GL Sciences C18 column (150 mm x 4.6 mm, 5 µm) was used. For high-resolution LC-MS analysis, an Agilent 1290 Infinity II LC/Q-TOF equipped with a Kinetex C18 column (50 mm x 2.1 mm, 2 µm) was used. For preparative reversed-phase chromatography, an Agilent 1260 Infinity LC system equipped with an Agilent Eclipse XDB-C18 column (250 mm × 21.2 mm, 7 µm) was used.

General Cloning.

The primers described in Table S3 were used to amplify genes from genomic DNA of *Streptomyces* sp. Tü 6071 or to subclone genes from previously assembled plasmids and were designed for T5 exonuclease-dependent assembly[1]. For generation of the plaT3(D67A) mutant, an initial PCR reaction was carried out using two primer sets to introduce a point mutation at the desired location followed by an overlap PCR to assemble the complete gene sequence with TEDA homology arms. PCR products were gel purified and cloned into pJR1090[2] linearized with *Nde*I and *Swa*I, or *Swa*I only, to afford plasmids pJR3001–pJR3008. In each plasmid, the *Swa*I cut site was preserved upstream of the terminator to facilitate insertion of additional genes. Sequences of all assembled plasmids were confirmed by DNA sequencing before being used for conjugation

into the selected *Streptomyces* hosts. See Fig. S16 for additional information on assembled constructs.

Culture Conditions.

E. coli strains harboring the plasmids described in Table S2 were grown in lysogeny broth (LB) with the appropriate antibiotics; apramycin (50 μg mL^{-1}), kanamycin (50 μg mL^{-1}), chloramphenicol (25 μg mL^{-1}). *Streptomyces* strains were grown on solid ISP4 medium or liquid tryptic soy broth (TSB) with antibiotics as needed; apramycin (50 μg mL^{-1}) and nalidixic acid (25 μg mL^{-1}). *E. coli-Streptomyces* conjugations were plated onto solid ISP4 medium supplemented with either 20 mM $MgCl_2$ or 20 mM $CaCl_2$. Fermentation of *Streptomyces* strains harboring empty vector (*S. albus* UFJR3000 and *S. venezuelae* UFJR3009) or various combinations of *pla* core genes (*S. albus* UFJR3001–UFJR3008 and *S. venezuelae* UFJR3009–UFJR3017) were carried out in HA medium (4 g L^{-1} glucose, 4 g L^{-1} yeast extract, 10 g L^{-1} malt extract, in deionized water, pH 7.2).

Small Scale Screening and LC-MS Analysis.

For initial screening of *Streptomyces* strains harboring either empty vector or various combinations of *pla* genes, 250-mL baffled flasks containing 50 mL of HA medium and ~30 glass beads (3 mm) were inoculated with 4% (v/v) of 48-hour old seed cultures. Small scale fermentations were maintained at 28 °C with shaking at 250 rpm for 7 days. From each flask, a 5 mL aliquot was taken, mixed with 5 mL of EtOAc with vigorous vortexing, and centrifuged at 3900 rpm for 15 mins. The organic layer was then dried under air before being reconstituted in 500 μL of CH_3OH and analyzed by LC-MS. Briefly, the sample was loaded onto a C18 column (150 mm x 4.6 mm, 5 μm) and liquid chromatography was carried out at 0.5 mL min^{-1} starting from 5% CH_3CN in H_2O for 5 mins, followed by a 20 min solvent gradient from 5–98% CH_3CN in H_2O, and ending with a 15 min hold at 98% CH_3CN in H_2O. Purified compounds were analyzed via high resolution LC-MS using a C18 column (50 mm x 2.1 mm, 2 μm), and liquid chromatography was carried out at 0.4 mL min^{-1} starting from 10 % CH_3CN in H_2O for 0.25 mins, followed by a 9.75 min solvent gradient from 10–95 % CH_3CN in H_2O, and ending with a 3 min hold at 95% CH_3CN. Mobile phases for low- and high-resolution LC-MS contained 0.1% (v/v) formic acid.

Isolation of compounds 1 – 7 and 10.

For isolation of compounds from *S. venezuelae*::*plaT431*, a large scale fermentation (18 L) was carried out in thirty-six 2-L baffled flasks containing 500 mL of HA production media and inoculated

with 4% (v/v) of 48-hour old TSB seed cultures. The fermentation was carried out for 7 days at 28 °C with shaking at 200 rpm. After 7 days, the broth and mycelia were separated by centrifugation at 6500 rpm for 30 min. The clarified culture broth was adjusted to pH 3.0, extracted with EtOAc three times, and concentrated in vacuo to afford 8.6 g of crude extract. The crude extract was adsorbed onto silica gel and fractionated via column chromatography over a gradient of hexanes:EtOAc (100:0 – 0:100) to afford 11 fractions (Fr01–Fr11). Putative terpene intermediates eluted in fractions Fr03–Fr06 (each 500–600 mg).

Individually, Fr03–Fr06 were subjected to preparative reversed-phase HPLC with a flow rate of 20 mL min^{-1} starting from 5% CH_3CN in H_2O for 5 mins, followed by a 20 min solvent gradient from 5–98% CH_3CN in H_2O, and ending with a 15 min hold at 98% CH_3CN in H_2O. Fr03 was purified to obtain **4** (18 mg, t_R = 23.2 min). Fr04–Fr05 were purified to obtain **5** (18.7 mg, t_R = 22.5 min), **6** (30.5 mg, t_R = 19.5 min), and **7** (9.2 mg, t_R = 21.1 min). Fr06 was purified to obtain **3** (11 mg, t_R = 17.3 min).

For isolation of compounds from *S. albus*::*plaT4321*, the same large scale fermentation (18 L) and extraction procedure was carried out as above to afford 7.5 g of crude extract. The crude extract was adsorbed onto silica gel and fractionated via column chromatography over a gradient of hexanes:EtOAc (100:0 – 0:100) and EtOAc:CH_3OH (100:0 – 0:100) to afford 13 fractions (Fr01–Fr13). Putative cyclized diterpenoids eluted in fractions Fr07–Fr09, which were combined and fractionated again via silica column over a gradient of EtOAc:CH_3OH (100:0 – 0:100) to afford 12 subfractions (Fr0701–Fr0712).

Subfractions Fr0707–Fr0708 (480 mg) were subjected to preparative reversed-phase HPLC with a flow rate of 20 mL min^{-1} starting from 15% CH_3CN in H_2O for 2 mins, followed by a 38 min solvent gradient from 15–50% CH_3CN in H_2O, and ending with a 2 min hold at 50% CH_3CN in H_2O. This gave **1** (10 mg, t_R = 25.8 min) and **2** (1.2 mg, t_R = 21.9 min).

For isolation of compounds from *S. albus*::*plaT431*, the same large scale fermentation (18 L) and extraction procedure was carried out as above to afford 4.5 g of crude extract. The crude extract was adsorbed onto silica gel and fractionated via column chromatography over a gradient of hexanes:EtOAc (100:0 – 0:100) and EtOAc:CH_3OH (100:0 – 0:100) to afford 9 fractions (Fr01–Fr09). Putative terpene intermediates eluted in fraction Fr05 (260 mg).

Fr05 was subjected to preparative reversed-phase HPLC with a flow rate of 20 mL min^{-1} starting from 5% CH_3CN in H_2O for 5 mins, followed by a 30 min solvent gradient from 5–98% CH_3CN in H_2O, and ending with a 15 min hold at 98% CH_3CN in H_2O. Fr05 was purified to obtain **10** (12 mg, t_R = 26.4 min).

17-Amino-17-deoxo-15,16-dihydrophenalinolactone CD7 (**1**): yellowish white solid, R_f = 0.24 (methanol:ethyl acetate = 1:1); $[\alpha]_D^{22}$ = +13.55° (*c* 0.70, CH_3OH); IR (cm^{-1}): 2934, 1700, 1582, 1397, 749, 576; UV (acetonitrile:water = 37:63): λ_{max} = 210 nm; ^1H and ^{13}C NMR data, see Table S4 and Figs. S4–S9; HRESIMS affording the $[M + H]^+$ ion at *m/z* 376.2852 (calcd $[M + H]^+$ ion for $C_{23}H_{38}NO_3$ at 376.2846, 1.6 ppm).

17-Amino-17-deoxo-15,16-dihydrophenalinolactone CD6 (**2**): yellowish white solid, R_f = 0.76; $[\alpha]_D^{22}$ = +3.24° (*c* 0.05, CH_3OH); IR (cm^{-1}): 3410, 2929, 1710, 1580, 1390, 1075, 936; UV (acetonitrile:water = 17:33): λ_{max} = 210 nm; ^1H and ^{13}C NMR data, see Table S5 and Figs. S10–S15; HRESIMS affording the $[M + H]^+$ ion at *m/z* 378.3010 (calcd $[M + H]^+$ ion for $C_{23}H_{40}NO_3$ at 378.3003, 1.8 ppm).

PL TA3 (**3**): light brown solid, R_f = 0.26 (methanol:ethyl acetate = 1:1); $[\alpha]_D^{22}$ = +7.65° (*c* 0.55, CH_3OH); IR (cm^{-1}): 3310, 2922, 2853, 1709, 1580, 1514, 1445, 1400, 1074, 909; UV (acetonitrile:water = 3:2): λ_{max} = 210 nm; ^1H and ^{13}C NMR data, see Table S6 and Figs. S18–S22; HRESIMS affording the $[M + H]^+$ ion at *m/z* 396.3113 (calcd $[M + H]^+$ ion for $C_{23}H_{42}NO_4$ at 396.3108, 1.3 ppm).

PL TA4 (**4**): yellow/brown oil, R_f = 0.31 (hexanes:ethyl acetate = 1:1); $[\alpha]_D^{22}$ = +7.45° (*c* 0.19, CH_2Cl_2); IR (cm^{-1}): 3417, 2923, 1709, 1554, 1445, 1377, 1267, 1189, 1071, 936; UV (acetonitrile:water = 9:1): λ_{max} = 210 nm; ^1H and ^{13}C NMR data, see Table S7 and Figs. S23–S27; HRESIMS affording the $[M - H]^-$ ion at *m/z* 365.2698 (calcd $[M - H]^-$ ion for $C_{22}H_{37}O_4$ at 365.2697, 0.3 ppm).

PL TA5 (**5**): yellowish oil, R_f = 0.28 (hexanes:ethyl acetate = 1:1); $[\alpha]_D^{22}$ = +9.46° (*c* 0.46, CH_2Cl_2); IR (cm^{-1}): 3413, 2963, 2154, 1708, 1449, 1403, 1377, 1289, 1230, 1073; UV (acetonitrile:water = 7:3): λ_{max} = 210 nm; ^1H and ^{13}C NMR data, see Table S8 and Figs. S28–S32; HRESIMS affording the $[M - H]^-$ ion at *m/z* 339.2547 (calcd $[M - H]^-$ ion for $C_{20}H_{35}O_4$ at 339.2541, 1.8 ppm).

PL TA6 (**6**): yellow/brown oil, R_f = 0.27 (hexanes:ethyl acetate = 1:1); $[\alpha]_D^{22}$ = +12.24° (*c* 1.02, CH_2Cl_2); IR (cm^{-1}): 3421, 2967, 2927, 2871, 1707, 1456, 1377, 1162, 1072, 940, 887; UV (acetonitrile:water = 29:11): λ_{max} = 210 nm; ^1H and ^{13}C NMR data, see Table S9 and Figs. S33–

S38; HRESIMS affording the $[M - H]^-$ ion at *m/z* 355.2490 (calcd $[M - H]^-$ ion for $C_{20}H_{35}O_5$ at 355.2490, 0 ppm).

PL TA7 (**7**): yellow/brown oil, R_f = 0.33 (hexanes:ethyl acetate = 1:1); $[\alpha]_D^{22}$ = +12.94° (*c* 0.49, CH_2Cl_2); IR (cm^{-1}): 3420, 2969, 2926, 2870, 1714, 1455, 1377, 1174, 1076, 1023, 951, 888; UV (acetonitrile:water = 4:1): λ_{max} = 210 nm; ^1H and ^{13}C NMR data, see Table S10 and Figs. S39–S43; HRESIMS affording the $[M - H]^-$ ion at *m/z* 381.2647 (calcd $[M - H]^-$ ion for $C_{22}H_{37}O_5$ at 381.2646, 0.3 ppm).

PL TA8 (**10**): yellowish oil, R_f = 0.26 (hexanes:ethyl acetate = 1:1); $[\alpha]_D^{22}$ = +15.38° (*c* 0.52, CH_2Cl_2); IR (cm^{-1}): 3423, 2959, 2925, 2858, 2134, 1713, 1440, 1381, 1284, 1076; UV (acetonitrile:water = 29:11): λ_{max} = 210 nm; ^1H and ^{13}C NMR data, see Table S11 and Figs. S45–S49; HRESIMS affording the $[M - H]^-$ ion at *m/z* 339.2546 (calcd $[M - H]^-$ ion for $C_{20}H_{35}O_4$ at 339.2541, 1.5 ppm). A structurally similar compound (melidianolic acid B)[3] was previously reported from *Aphanamixis grandifolia;* however, the reported chemical shifts for C2–C4 were 4–7 ppm upfield of our values for **10**. In addition, the optical rotation of **10** had an opposite sign compared with that of melidianolic acid B.[3]

Table S1. Bacterial strains used in this study.

Strain	Description	Source [Reference]
E. coli NEB Turbo	Host for general cloning	New England Biolabs
E. coli BL21 Star (DE3)	Host for protein expression	Invitrogen
E. coli ET12567/pUZ8002	Host for conjugal transfer	[4]
Streptomyces sp. Tü 6071	Native phenalinolactone producer, used for isolation of genomic DNA and for expression of additional copies of *pla* genes	[5,6]
Streptomyces venezuelae ATCC 10712	Host for heterologous expression	ATCC
Streptomyces albus J1074	Host for heterologous expression	[7]
Streptomyces albus UFJR3000	*S. albus* J1074 harboring pJR01090 (empty pSET-sp44)	This study
Streptomyces albus UFJR3001	*S. albus* J1074 harboring pJR3001 (*plaT4*)	This study
Streptomyces albus UFJR3002	*S. albus* J1074 harboring pJR3002 (*plaT4* and *plaT1*)	This study
Streptomyces albus UFJR3003	*S. albus* J1074 harboring pJR3003 (*plaT4* and *plaT3*)	This study
Streptomyces albus UFJR3004	*S. albus* J1074 harboring pJR3004 (*plaT4* and *plaT3(D67A)* mutant)	This study
Streptomyces albus UFJR3005	*S. albus* J1074 harboring pJR3005 (*plaT4*, *plaT2*, and *plaT1*)	This study
Streptomyces albus UFJR3006	*S. albus* J1074 harboring pJR3006 (*plaT4*, *plaT3*, and *plaT2*)	This study
Streptomyces albus UFJR3007	*S. albus* J1074 harboring pJR3007 (*plaT4*, *plaT3*, and *plaT1*)	This study
Streptomyces albus UFJR3008	*S. albus* J1074 harboring pJR3008 (*plaT4*, *plaT3*, *plaT2*, and *plaT1*)	This study
Streptomyces venezuelae UFJR3009	*S. venezuelae* harboring pJR01090 (empty pSET-sp44)	This study
Streptomyces venezuelae UFJR3010	*S. venezuelae* harboring pJR3001 (*plaT4*)	This study
Streptomyces venezuelae UFJR3011	*S. venezuelae* harboring pJR3002 (*plaT4* and *plaT1*)	This study
Streptomyces venezuelae UFJR3012	*S. venezuelae* harboring pJR3003 (*plaT4* and *plaT3*)	This study
Streptomyces venezuelae UFJR3013	*S. venezuelae* harboring pJR3004 (*plaT4* and *plaT3(D67A)* mutant)	This study
Streptomyces venezuelae UFJR3014	*S. venezuelae* harboring pJR3005 (*plaT4*, *plaT2*, and *plaT1*)	This study
Streptomyces venezuelae UFJR3015	*S. venezuelae* harboring pJR3006 (*plaT4*, *plaT3*, and *plaT2*)	This study
Streptomyces venezuelae UFJR3016	*S. venezuelae* harboring pJR3007 (*plaT4*, *plaT3*, and *plaT1*)	This study
Streptomyces venezuelae UFJR3017	*S. venezuelae* harboring pJR3008 (*plaT4*, *plaT3*, *plaT2*, and *plaT1*)	This study

Table S2. Plasmids used in this study.

Plasmid	Description	Source [Reference]
pJR1090	Plasmid for heterologous expression of genes in *Streptomyces*. Derived from pSET152 and equipped with a synthetic sp44* constitutive promoter and sr40 ribosome binding site.	[2]
pJR3001	pSET-sp44 harboring *plaT4*	This study
pJR3002	pSET-sp44 harboring *plaT4* and *plaT1*	This study
pJR3003	pSET-sp44 harboring *plaT4* and *plaT3*	This study
pJR3004	pSET-sp44 harboring *plaT4* and *plaT3(D67A)* mutant	This study
pJR3005	pSET-sp44 harboring *plaT4*, *plaT2*, and *plaT1*	This study
pJR3006	pSET-sp44 harboring *plaT4*, *plaT3*, and *plaT2*	This study
pJR3007	pSET-sp44 harboring *plaT4*, *plaT3*, and *plaT1*	This study
pJR3008	pSET-sp44 harboring *plaT4*, *plaT3*, *plaT2*, *plaT1*	This study

Table S3. Primers used in this study.

Primer	Sequence	Purpose
T4-F	cttgtcaaaggagtgtccatatgcatgccgagacggca	Amplification of *plaT4* (for pJR3001)
T4-R	acaaaactttagatatttaaattcaatggttccgattggagaggtagttg	
T3-F	tctccaatcggaaccattgaatgggcgggcacgggctc	Amplification of *plaT3* (for pJR3003) or *plaT3(D67A)* (for pJR3004)
T3-R	cacataacgaaccgtcctcctcaggaaaagcgggccggtg	
T41-F	caatcggaaccattgaatttatgacgaccggacagccgga	Amplification of *plaT1* (for pJR3002)
T41-R	acaaaactttagatatttaaattcaatccctctgtccgttgtctcgg	
T421-F	caatcggaaccattgaatttggaggacggttcgttatgtgc	Amplification of *plaT2* and *plaT1* (for pJR3005)
T421-R	acaaaactttagatatttaaattcaatccctctgtccgttgtc	
T432-F	ggcccgcttttcctgaatttggaggacggttcgttatgtgctcagacgt	Amplification of *plaT2* (for pJR3006)
T432-R	cgacaaaactttagatattttcatgacgcctcccgtcgcg	
T3-D67A-F1	atgcatgccgagacggcagc	Amplification of *plaT3*(D67A) fragment 1
T3-D67A-R1	gagctcgcgggcgagatagtcg	
T3-D67A-F2	cgactatctcgcccgcgagctc	Amplification of *plaT3*(D67A) fragment 2
T3-D67A-R2	tcaggaaaagcgggccggtg	
T431-F	ggcccgcttttcctgaatttatgacgaccggacagccg	Amplification of *plaT1* (for pJR3007)
T431-R	cgacaaaactttagatattttcaatccctctgtccgttgtctcg	
T4321-F	ggcccgcttttcctgaatttggaggacggttcgttatgtgctcag	Amplification of *plaT2* and *plaT1* (for pJR3008)
T4321-R	cgacaaaactttagatatttaaattcaatccctctgtccgttgtct	

Table S4. ^{1}H NMR (600 MHz) and ^{13}C NMR (151 MHz) data for **1** in methanol-d_4 (δ in ppm, *J* in Hz). Chemical structure of **1** and key ^{1}H-^{1}H COSY, HMBC, and NOESY correlations are included.

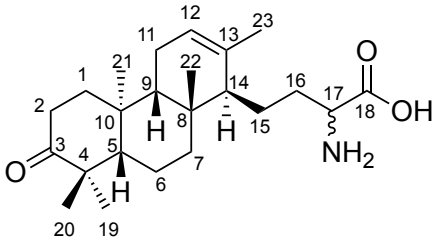

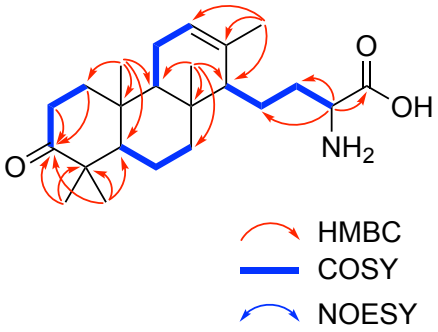

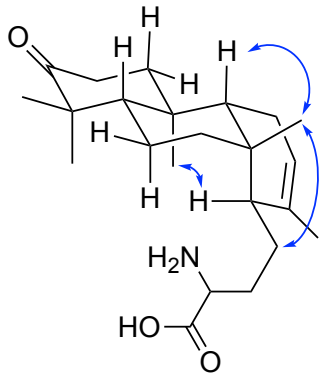

No.	1	
	δ_C	δ_H
1, CH_2	40.58	1.48 (m, H_a) 1.98 (ddd, *J* = 13.1, 7.9, 5.0, H_b)
2, CH_2	35.01	2.45 (m, H_a) 2.49 (m, H_b)
3, qC	221.07	-
4, qC	48.20	-
5, CH	56.06	1.59 (m, 1H)
6, CH_2	20.87	1.47 (m, H_a) 1.59 (m, H_b)
7, CH_2	38.51	1.15 (m, H_a)* 2.10 (m, H_b)
8, qC	38.20	-
9, CH	55.62	1.17 (d, *J* = 7.6, 1H)*
10, qC	38.90	-
11, CH_2	25.10	1.39 (tdd, *J* = 12.5, 7.1, 4.6, H_a) 1.64 (m, H_b)
12, CH	123.17	5.36 (m, 1H)
13, qC	136.79	-
14, CH	43.52	2.14 (m, 1H)
15, CH_2	23.83	2.02 (m, H_a) 2.27 (m, H_b)
16, CH_2	35.10	1.82 (ddt, *J* = 19.1, 13.0, 5.1, H_a) 2.16 (m, H_b)
17, CH	56.78	3.52 (t, *J* = 5.9, 1H)
18, qC	174.51	-
19, CH_3	27.68	1.08 (s, 3H)
20, CH_3	21.48	1.03 (s, 3H)
21, CH_3	15.76	0.94 (s, 3H)
22, CH_3	27.12	0.89 (s, 3H)
23, CH_3	23.01	1.75 (s, 3H)

*These signals overlapped, but the multiplicity and coupling constant of H-9 could still be determined.

Table S5. ^{1}H NMR (600 MHz) and ^{13}C NMR (151 MHz) data for **2** in methanol-d_4 (δ in ppm, *J* in Hz). Chemical structure of **2** and key ^{1}H-^{1}H COSY, HMBC, and NOESY correlations are included.

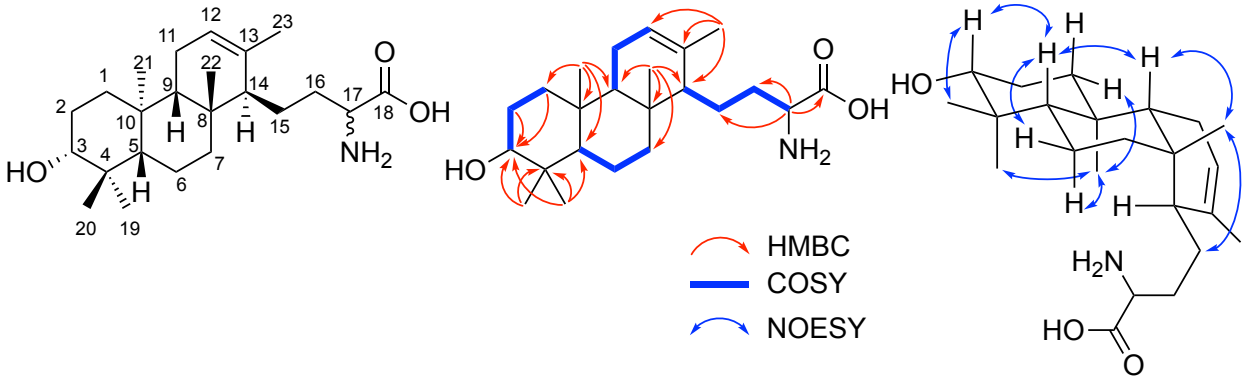

No.	**2**	
	δ_C	δ_H
1, CH_2	40.32	0.93 (m, H_{ax}) 1.80 (m, H_{eq})
2, CH_2	28.08	1.57 (dq, *J* = 13.3, 4.0, H_{eq}) 1.63 (m, H_{ax})
3, CH	79.70	3.13 (dd, *J* = 11.8, 4.7, H_{ax})
4, qC	39.91	-
5, CH	57.21	0.84 (dd, *J* = 15.0, 2.3, 1H)*
6, CH_2	19.54	1.45 (qd, *J* = 13.5, 2.8, H_{ax}) 1.53 (dq, *J* = 13.6, 3.2, H_{eq})
7, CH_2	39.50	2.08 (m, H_{eq}) 1.08 (td, *J* = 13.5, 3.9, H_{ax})
8, qC	39.44	-
9, CH	56.74	0.99 (d, *J* = 7.6, 1H)
10, qC	38.26	-
11, CH_2	23.55	2.01 (m, dd, *J* = 18.9, 5.5, H_a) 2.16 (m, H_b)
12, CH	123.49	5.34 (m, 1H)
13, qC	136.83	-
14, CH	43.91	2.08 (m, 1H)
15, CH_2	25.18	1.37 (tdd, *J* = 12.6, 7.0, 4.6, H_a) 1.62 (m, H_b)
16, CH_2	35.37	1.80 (m, H_a) 2.14 (m, H_b)
17, CH	56.84	3.50 (t, *J* = 6.0)
18, qC	174.69	-
19, CH_3	16.31	0.76 (s, 3H_{ax})
20, CH_3	28.81	0.96 (s, 3H_{eq})
21, CH_3	14.99	0.92 (s, 3H)
22, CH_3	27.37	0.85 (s, 3H)*
23, CH_3	22.98	1.73 (s, 3H)

*These signals overlapped, but the multiplicity and coupling constant of H-5 could still be determined.

Table S6. ^{1}H NMR (600 MHz) and ^{13}C NMR (151 MHz) data for **3** in methanol-d_4 (δ in ppm, J in Hz). Chemical structure of **3** and key ^{1}H-^{1}H COSY and HMBC correlations are included.

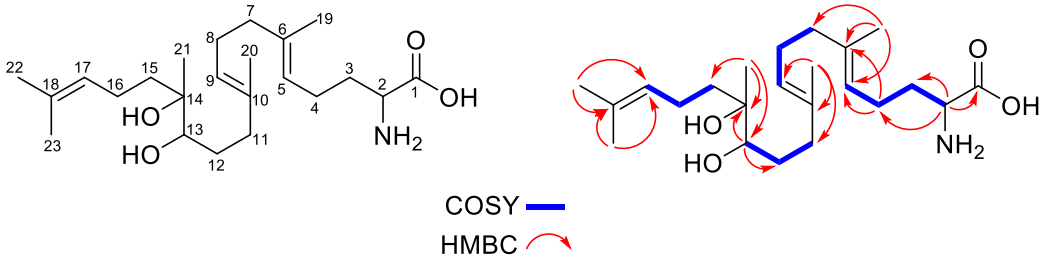

No.	**3**	
	δ_C	δ_H
1, qC	174.39	-
2, CH	56.05	3.53 (dd, J = 7.0, 5.1, 1H)
3, CH_2	32.62	1.81 (ddd, J = 12.7, 8.4, 6.4, H_a) 1.90 (td, J = 9.3, 7.9, 5.2, H_b)
4, CH_2	24.83	2.14 (m, 2H)
5, CH	123.82	5.16 (m, 1H)
6, qC	137.81	-
7, CH_2	40.78	2.02 (m, H_a) 2.11 (m, H_b)
8, CH_2	27.56	2.03 (m, H_a) 2.11 (m, H_b)
9, CH	125.40	5.18 (m, 1H)
10, qC	136.27	-
11, CH_2	37.98	2.02 (m, H_a) 2.24 (ddd, J = 14.2, 10.0, 4.7, H_b)
12, CH_2	30.57	1.36 (m, H_a) 1.74 (dddd, J = 13.7, 10.1, 6.8, 1.7, H_b)
13, CH	78.14	3.27 (dd, J = 10.6, 1.7, 1H)
14, qC	75.42	-
15, CH_2	39.50	1.45 (ddd, J = 13.8, 11.8, 5.3, H_a) 1.53 (ddd, J = 13.7, 11.7, 5.0, H_b)
16, CH_2	22.96	2.04 (m, H_a) 2.10 (m, H_b)
17, CH	126.05	5.12 (m, 1H)
18, qC	131.97	-
19, CH_3	16.17	1.65 (s, 3H)
20, CH_3	16.20	1.62 (s, 3H)
21, CH_3	21.92	1.10 (s, 3H)
22, CH_3	17.72	1.62 (s, 3H)
23, CH_3	25.89	1.67 (s, 3H)

Table S7. ^{1}H NMR (600 MHz) and ^{13}C NMR (151 MHz) data for **4** in chloroform-*d* (δ in ppm, *J* in Hz). Chemical structure of **4** and key ^{1}H-^{1}H COSY and HMBC correlations are included.

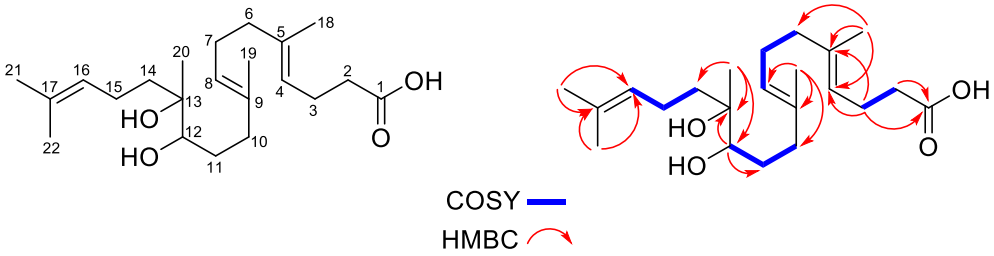

No.	**4**	
	δ_C	δ_H
1, qC	177.36	-
2, CH_2	34.57	2.30 (m, H_a) 2.36 (m, H_b)
3, CH_2	23.56	2.36 (m, H_a) 2.38 (m, H_b)
4, CH	122.99	5.11 (m, 1H)
5, qC	135.92	-
6, CH_2	38.95	2.06 (d, *J* = 6.6, 2H)
7, CH_2	24.98	2.13 (m, 2H)
8, CH	124.82	5.12 (m, 1H)
9, qC	134.28	-
10, CH_2	36.18	2.09 (m, H_a) 2.17 (m, H_b)
11, CH_2	28.79	1.41 (m, H_a) 1.57 (m, H_b)
12, CH	77.08	3.34 (d, *J* = 10.3, 1H)
13, qC	75.55	-
14, CH_2	35.67	1.39 (m, H_a) 1.64 (m, H_b)
15, CH_2	22.05	2.05 (m, H_a) 2.13 (m, H_b)
16, CH	124.48	5.12 (m, 1H)
17, qC	131.93	-
18, CH_3	15.94	1.60 (s, 3H)
19, CH_3	15.66	1.58 (s, 3H)
20, CH_3	23.17	1.16 (s, 3H)
21, CH_3	17.68	1.62 (s, 3H)
22, CH_3	25.71	1.69 (s, 3H)

Table S8. ^{1}H NMR (600 MHz) and ^{13}C NMR (151 MHz) data for **5** in chloroform-*d* (δ in ppm, *J* in Hz). Chemical structure of **5** and key ^{1}H-^{1}H COSY and HMBC correlations are included.

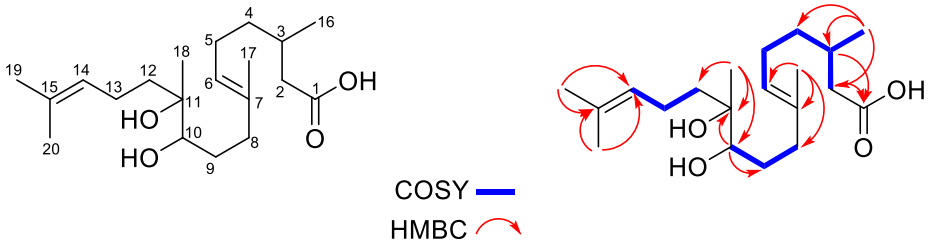

No.	**5**	
	δ_C	δ_H
1, qC	178.19	-
2, CH_2	41.82	2.16 (m, H_a) 2.28 (dd, *J* = 15.0, 6.6, H_b)
3, CH	29.59	1.94 (h, *J* = 8.6, 7.8)
4, CH_2	36.41	1.36 (m, H_a) 1.63 (m, H_b)
5, CH_2	25.17	2.03 (m, 2H)
6, CH	125.46	5.18 (t, *J* = 7.3, 1H)
7, qC	134.80	-
8, CH_2	36.68	2.12 (m, H_a) 2.19 (m, H_b)
9, CH_2	28.85	1.44 (m, H_a) 1.58 (m, H_b)
10, CH	77.78	3.40 (d, *J* = 10.4, 1H)
11, qC	74.96	-
12, CH_2	35.52	1.36 (m, H_a) 1.62 (m, H_b)
13, CH_2	22.03	2.04 (m, H_a) 2.12 (m, H_b)
14, CH	124.63	5.13 (t, *J* = 7.3, 1H)
15, qC	131.81	-
16, CH_3	19.66	0.96 (d, *J* = 6.6, 3H)
17, CH_3	15.73	1.60 (s, 3H)
18, CH_3	23.36	1.15 (s, 3H)
19, CH_3	17.66	1.62 (s, 3H)
20, CH_3	25.70	1.68 (s, 3H)

Table S9. ^{1}H NMR (600 MHz) and ^{13}C NMR (151 MHz) data for **6** in methanol-d_4 (δ in ppm, *J* in Hz). Chemical structure of **6** and key ^{1}H-^{1}H COSY and HMBC correlations are included.

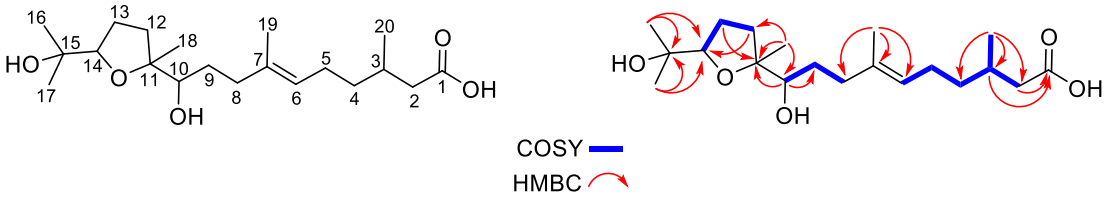

No.	**6**	
	δ_C	δ_H
1, qC	177.17	-
2, CH_2	42.63	2.08 (m, H_a) 2.29 (dd, *J* = 14.8, 6.9, H_b)
3, CH	31.01	1.94 (m, 1H)
4, CH_2	37.91	1.25 (m, H_a) 1.39 (m, H_b)
5, CH_2	26.35	2.04 (m, H_a)
6, CH	125.68	5.19 (m, H_b)
7, qC	136.16	-
8, CH_2	37.57	2.04 (m, H_a) 2.23 (ddd, *J* = 14.0, 9.1, 4.7, H_b)
9, CH_2	31.11	1.36 (m, H_a) 1.74 (m, H_b)
10, CH	77.09	3.39 (dd, *J* = 10.3, 1.9, 1H)
11, qC	86.77	-
12, CH_2	34.83	1.60 (m, H_a) 2.04 (m, H_b)
13, CH_2	27.77	1.84 (m, 2H)
14, CH	88.09	3.75 (dd, *J* = 9.6, 5.9, 1H)
15, qC	72.24	-
16, CH_3	25.21	1.14 (s, 3H)
17, CH_3	26.33	1.16 (s, 3H)
18, CH_3	22.89	1.12 (s, 3H)
19, CH_3	16.09	1.63 (s, 3H)
20, CH_3	20.04	0.96 (d, *J* = 6.6, 3H)

Table S10. ^{1}H NMR (600 MHz) and ^{13}C NMR (151 MHz) data for **7** in methanol-d_4 (δ in ppm, *J* in Hz). Chemical structure of **7** and key ^{1}H-^{1}H COSY and HMBC correlations are included.

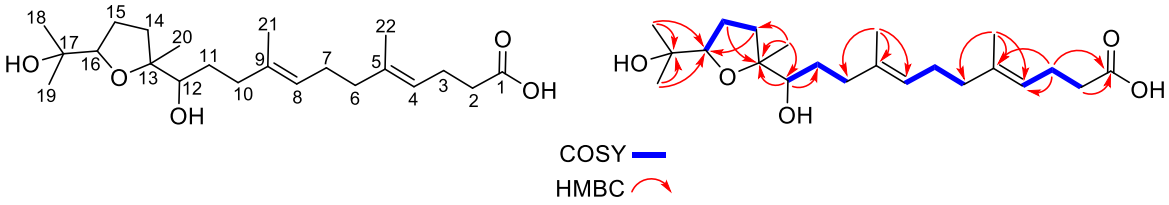

No.	7	
	δ_C	δ_H
1, qC	178.29	-
2, CH_2	35.97	2.28 (m, 2H)
3, CH_2	24.91	2.29 (m, 2H)
4, CH	124.22	5.15 (m, 1H)
5, qC	137.18	-
6, CH_2	40.82	2.03 (m, H_a) 2.12 (m, H_b)
7, CH_2	27.75	2.02 (m, H_a) 2.11 (m, H_b)
8, CH	125.53	5.17 (tq, *J* = 7.12, 1.34, 1H)
9, qC	136.03	-
10, CH_2	37.58	2.06 (m, H_a) 2.25 (m, H_b)
11, CH_2	31.10	1.34 (m, H_a) 1.72 (dddd, *J* = 13.9, 9.4, 7.4, 1.9, H_b)
12, CH	77.18	3.39 (dd, *J* = 10.4, 1.9, 1H)
13, qC	86.79	-
14, CH_2	34.78	1.62 (m, H_a) 2.06 (m, H_b)
15, CH_2	27.78	1.81 (m, H_a) 1.84 (m, H_b)
16, CH	88.12	3.75 (dd, *J* = 9.6, 5.9, 1H)
17, qC	72.23	-
18, CH_3	25.23	1.14 (s, 3H)
19, CH_3	26.34	1.16 (s, 3H)
20, CH_3	22.95	1.12 (s, 3H)
21, CH_3	16.11	1.61 (s, 3H)
22, CH_3	16.05	1.64 (s, 3H)

Table S11. ^{1}H NMR (600 MHz) and ^{13}C NMR (151 MHz) data for **10** in chloroform-*d* (δ in ppm, *J* in Hz). Chemical structure of **10** and key ^{1}H-^{1}H COSY and HMBC correlations are included.

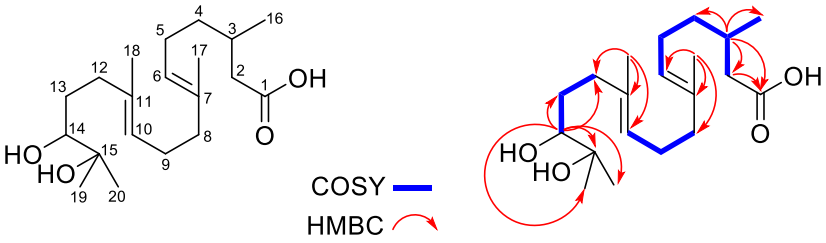

No.	**10**	
	δ_C	δ_H
1, qC	177.36	-
2, CH_2	41.65	2.15 (m, H_a) 2.29 (dd, *J* = 14.7, 6.2, H_b)
3, CH	29.58	1.98 (m, 1H)
4, CH_2	36.39	1.25 (m, H_a) 1.40 (m, H_b)
5, CH_2	25.06	2.02 (m, 2H)
6, CH	124.68	5.09 (t, *J* = 6.7, 1H)
7, qC	134.68	-
8, CH_2	39.33	2.02 (m, H_a) 2.10 (m, H_b)
9, CH_2	25.77	2.10 (m, 2H)
10, CH	124.56	5.16 (t, *J* = 6.7, 1H)
11, qC	134.67	-
12, CH_2	36.76	2.01 (m, H_a) 2.25 (ddd, *J* = 14.6, 9.2, 5.1, H_b)
13, CH_2	29.74	1.39 (m, H_a) 1.58 (m, H_b)
14, CH	78.48	3.37 (d, *J* = 10.1, 1H)
15, qC	73.34	-
16, CH_3	19.52	0.96 (d, *J* = 6.7, 3H)
17, CH_3	15.79	1.59 (s, 3H)
18, CH_3	15.96	1.60 (s, 3H)
19, CH_3	23.23	1.16 (s, 3H)
20, CH_3	26.34	1.20 (s, 3H)

Figure S1. Cyclization mechanisms of terpene cyclases. Canonical type I TCs possess a DDxxD and NSE/DTE motif which facilitate ionization of the polyprenyl substrate via abstraction of the diphosphate. Canonical type II TCs possess a DxDD motif which initiates ionization of the polyprenyl substrate via protonation, while the diphosphate remains intact. Noncanonical type II TCs, such as the oxidosqualene cyclases, lack the highly conserved DxDD motif present in canonical type II TCs and initiate ionization by protonation of an epoxide.

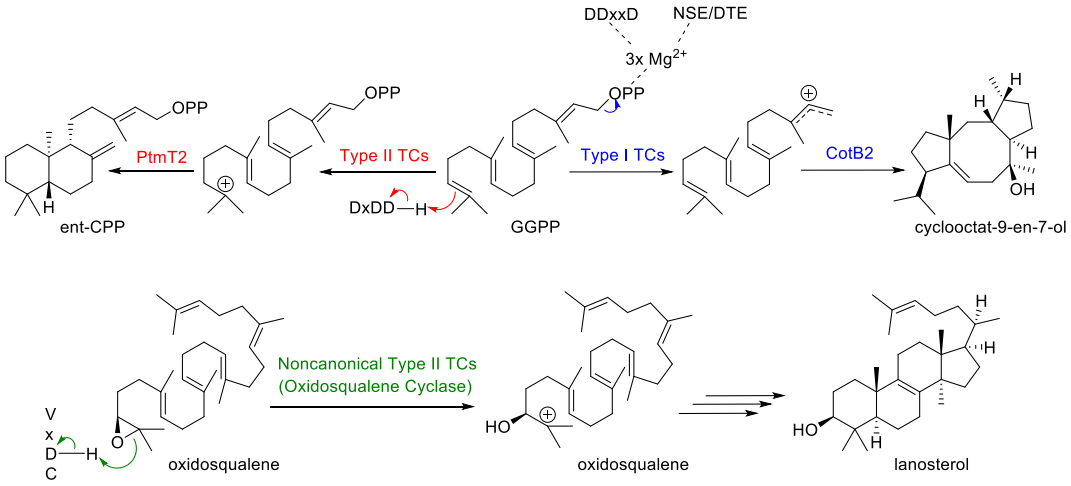

Figure S2. Construction of the four-gene *plaT1–plaT4* cassette in pSET-sp44. This figure also serves as an example workflow for the assembly of all expression plasmids. PCR amplfied gene fragments were cloned into linearized plasmids. The *Swa*I cut site upstream of the terminator was conserved to facilitate digestion and insertion of additional genes. Not drawn to scale.

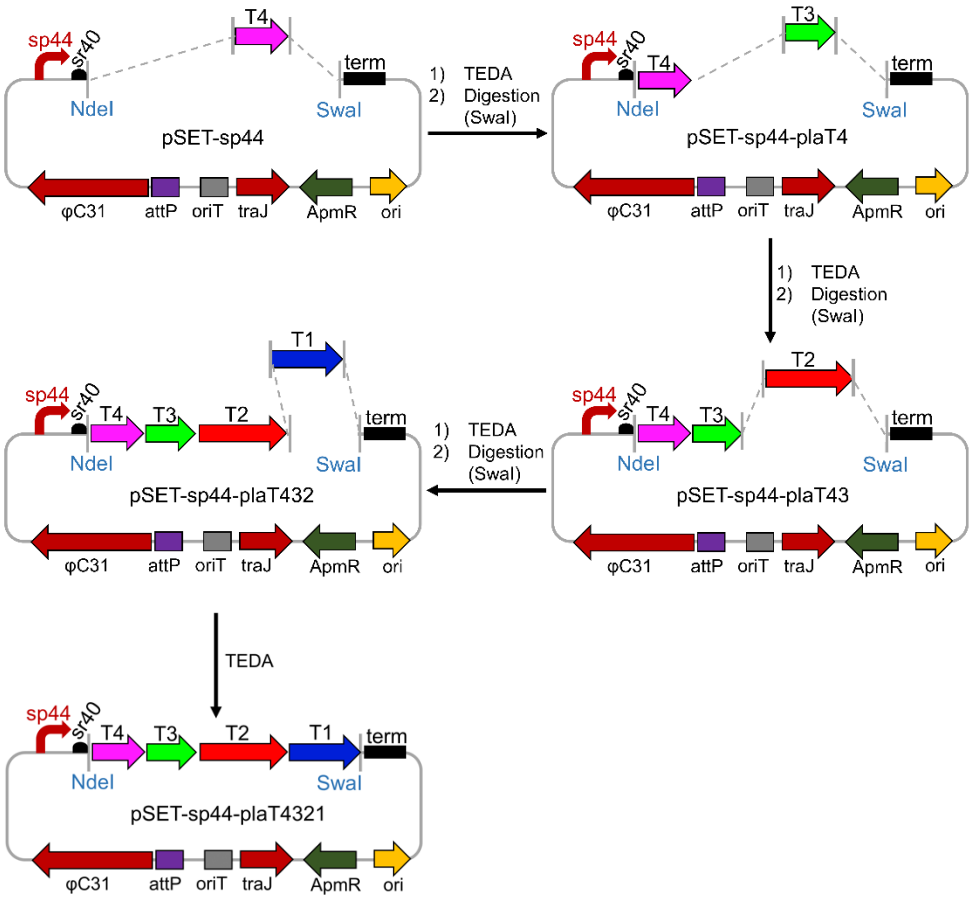

Figure S3. HRESIMS of **1** and **2** (positive mode).

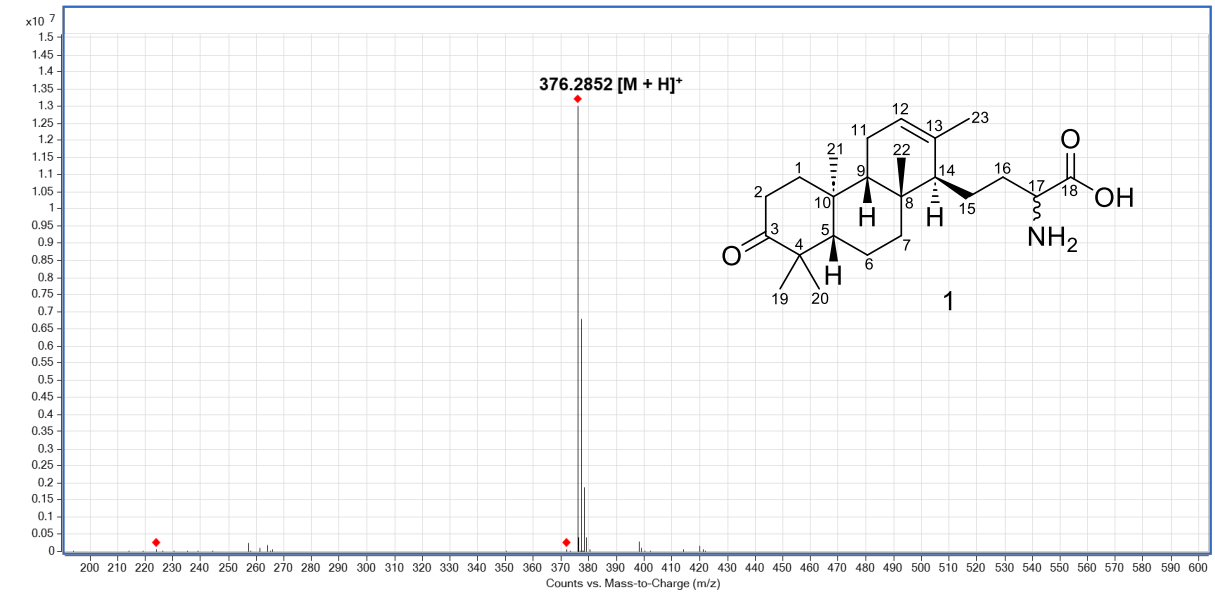

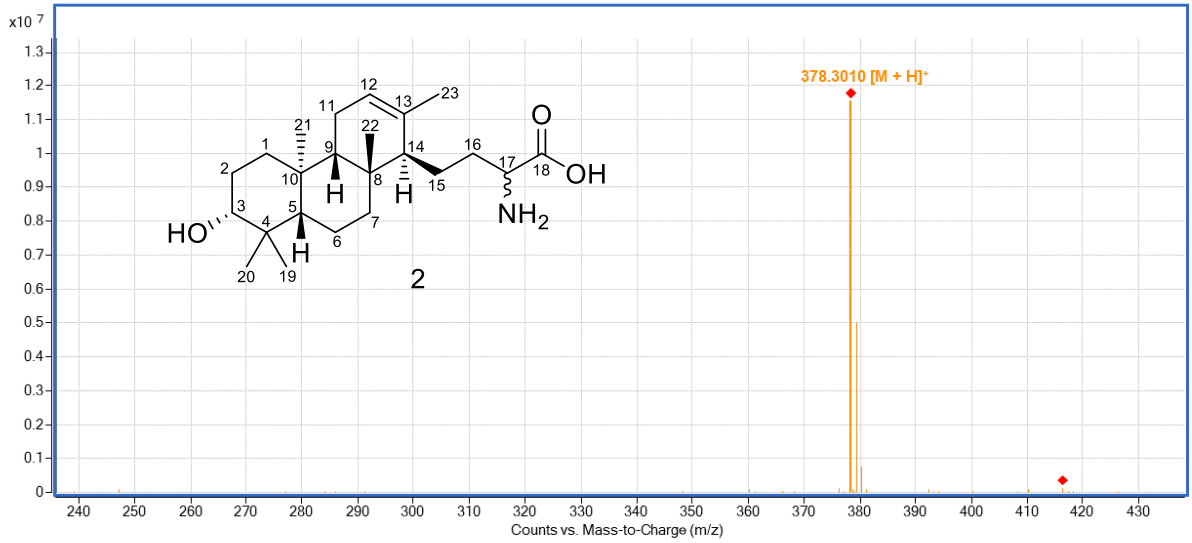

Figure S4. ^{1}H NMR spectrum of **1** in CD_3OD (600 MHz).

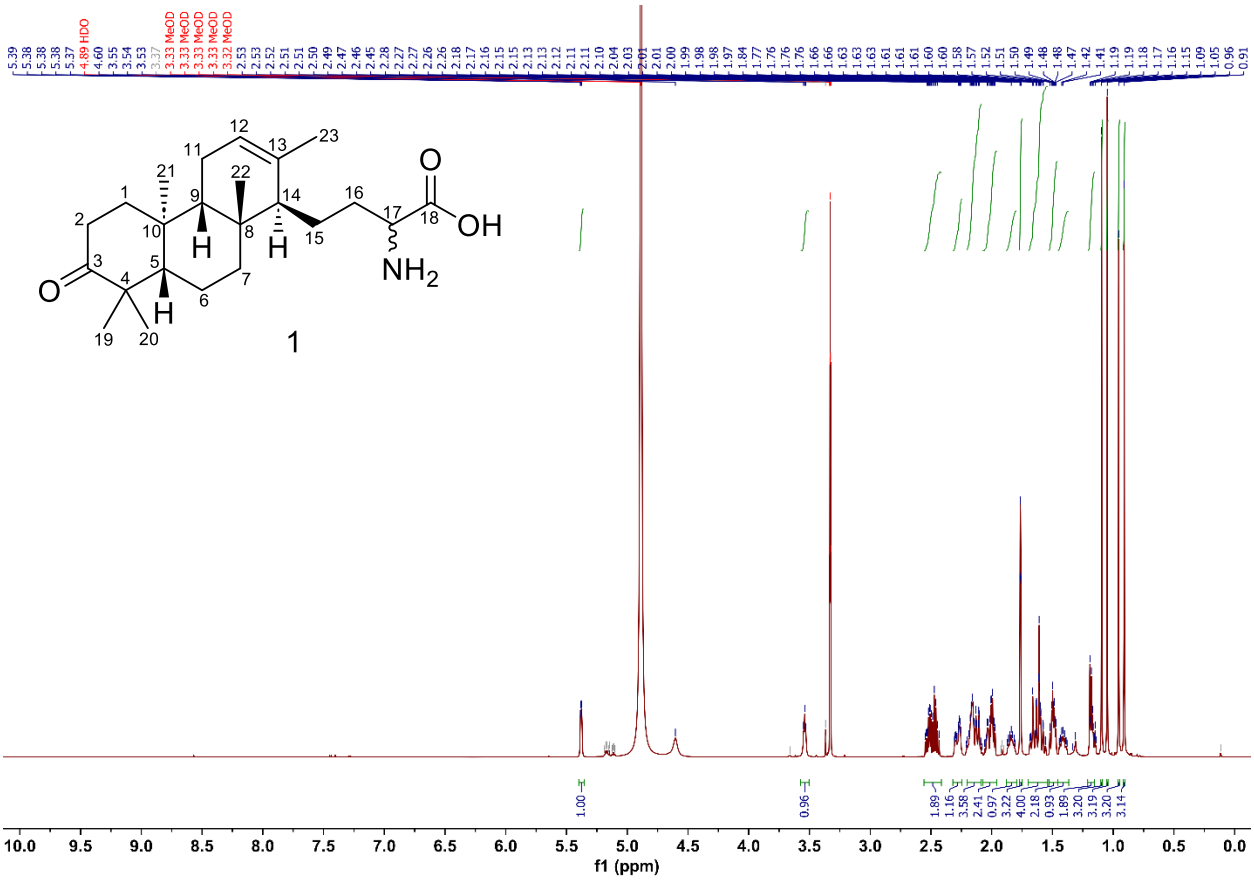

Figure S5. ^{13}C NMR spectrum of **1** in CD_3OD (151 MHz).

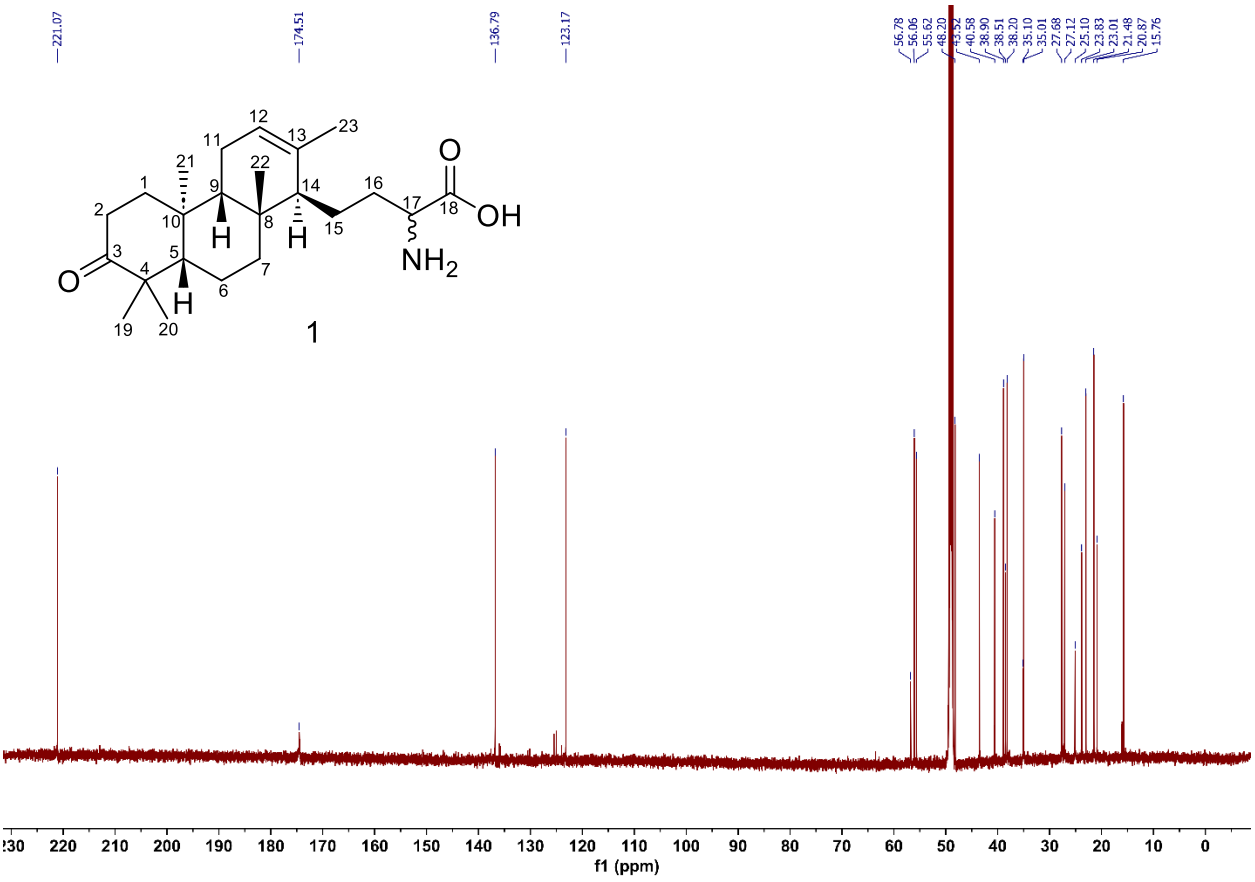

Figure S6. ^{1}H-^{13}C HSQC spectrum of **1** in CD_3OD.

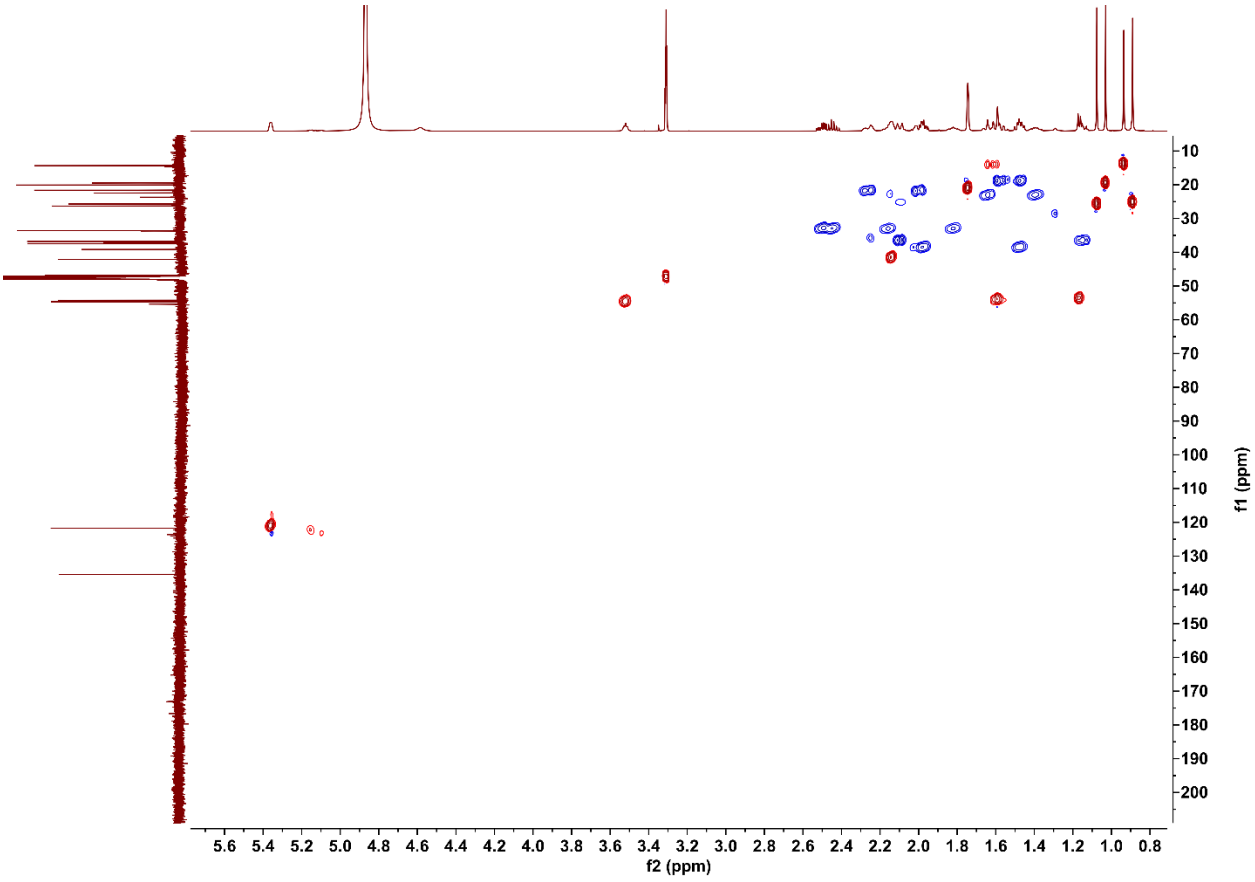

Figure S7. ^{1}H-^{13}C HMBC spectrum of **1** in CD_3OD.

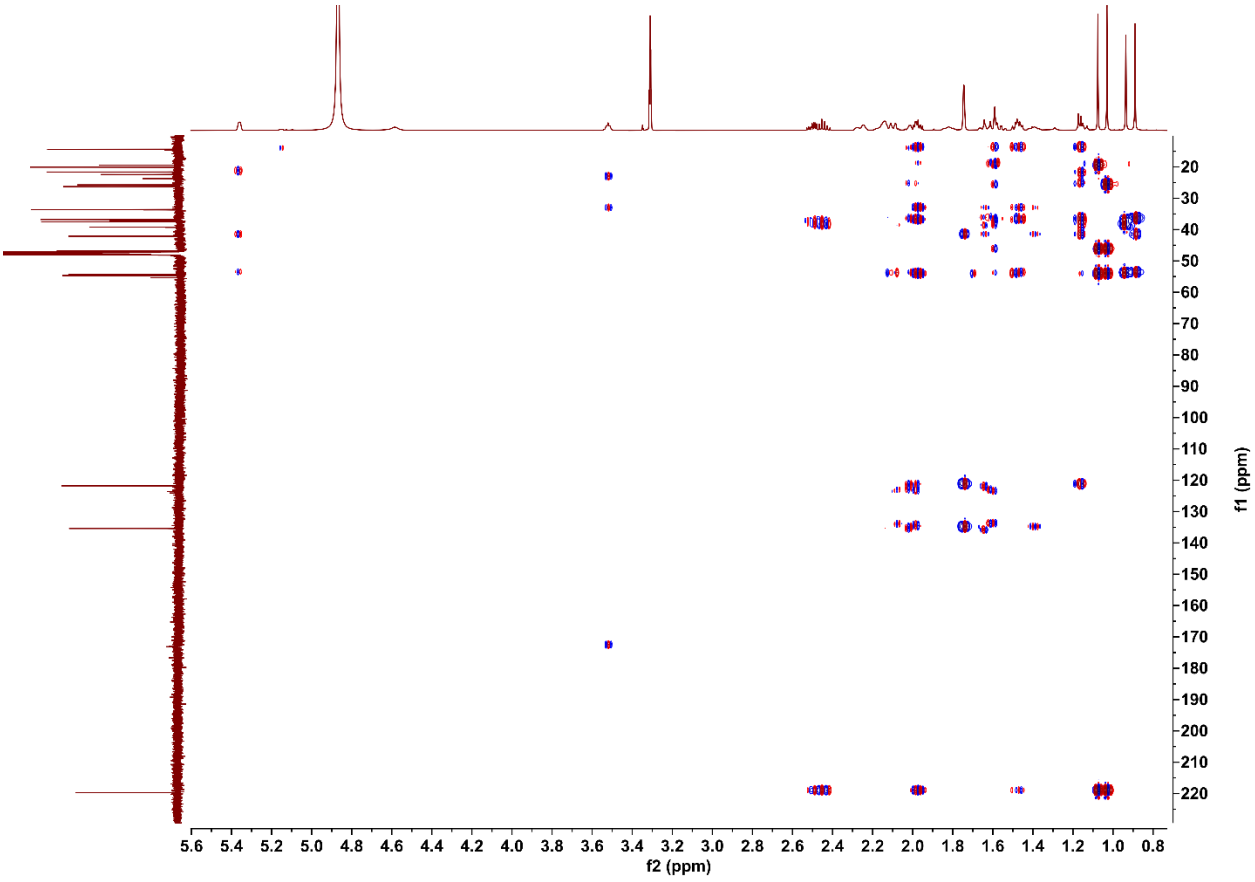

Figure S8. ^{1}H-^{1}H COSY spectrum of **1** in CD_3OD.

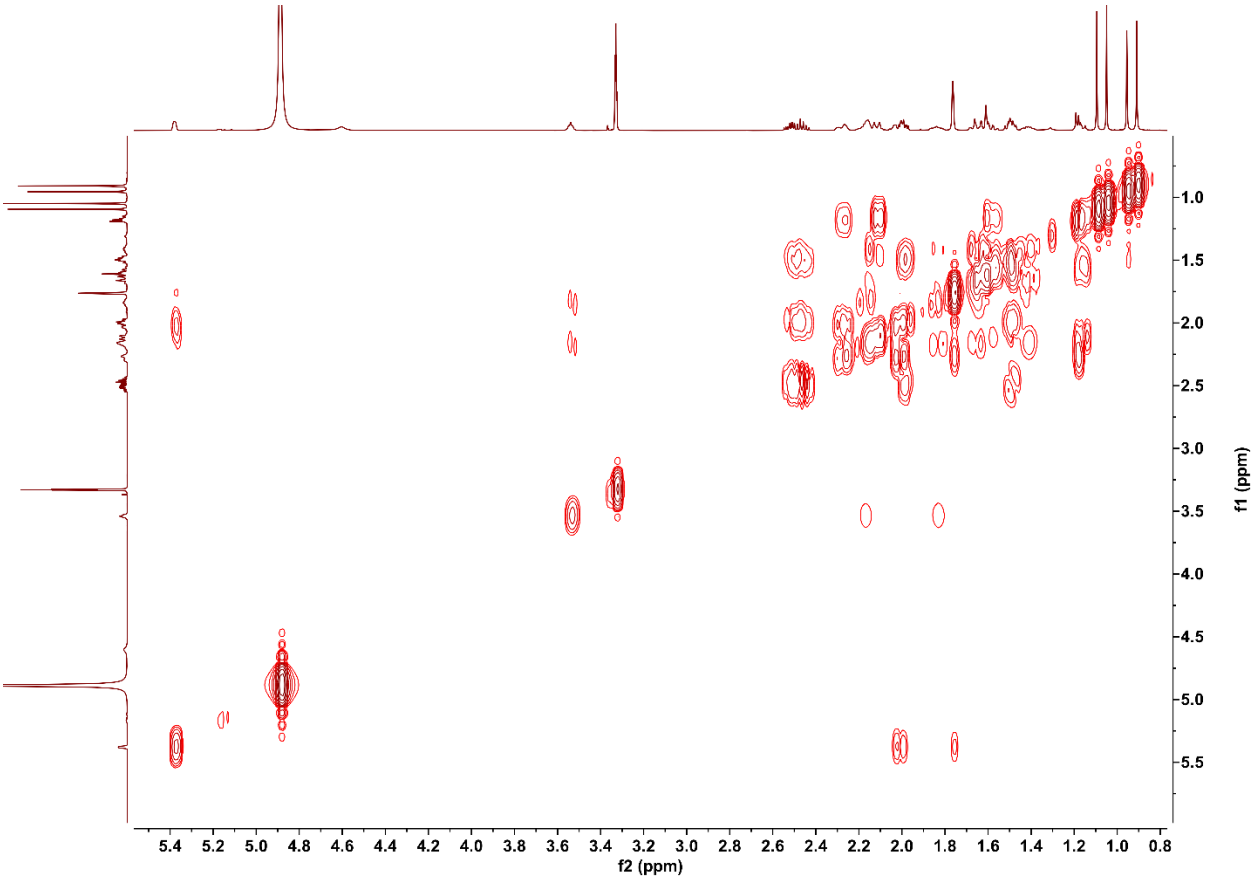

Figure S9. ^{1}H-^{1}H NOESY spectrum of **1** in CD_3OD.

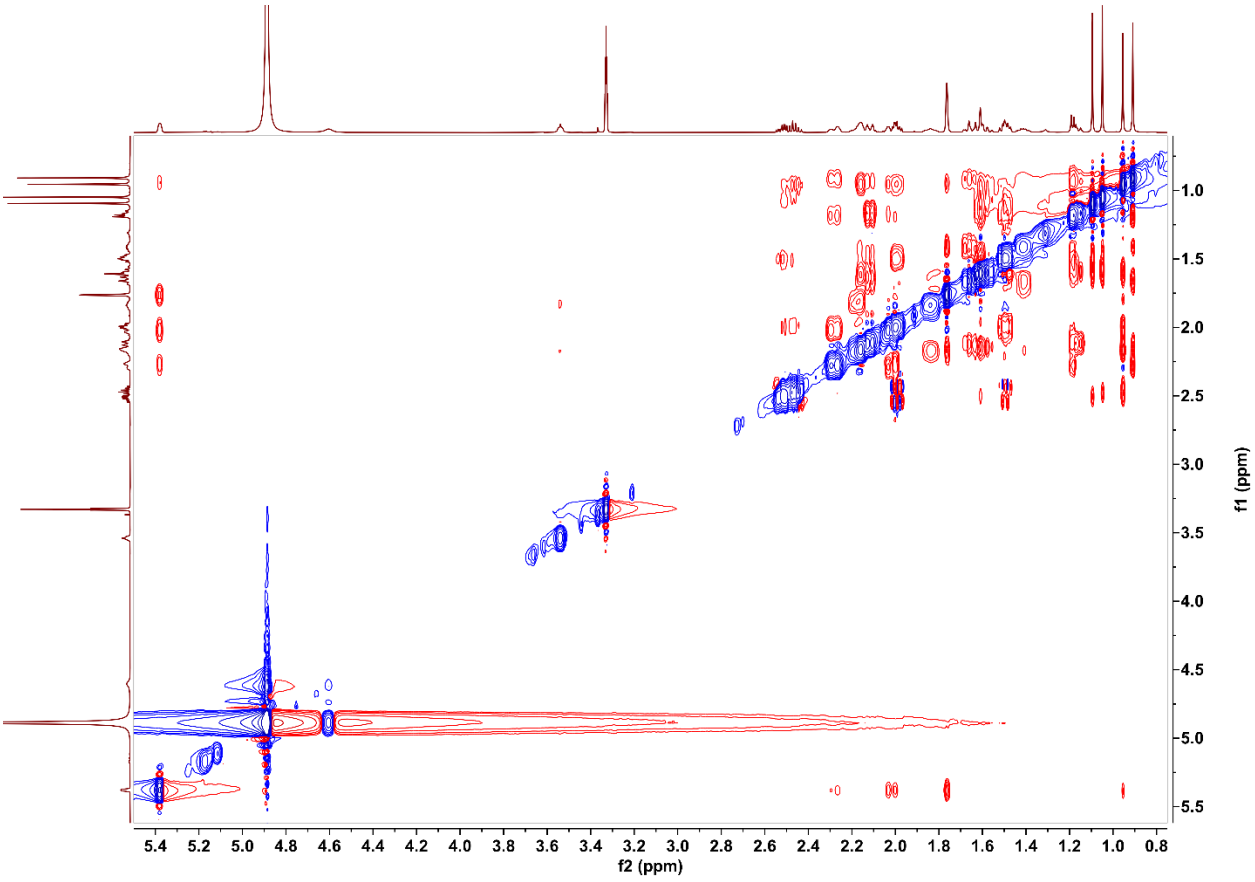

Figure S10. ^{1}H NMR spectrum of **2** in CD_3OD (800 MHz).

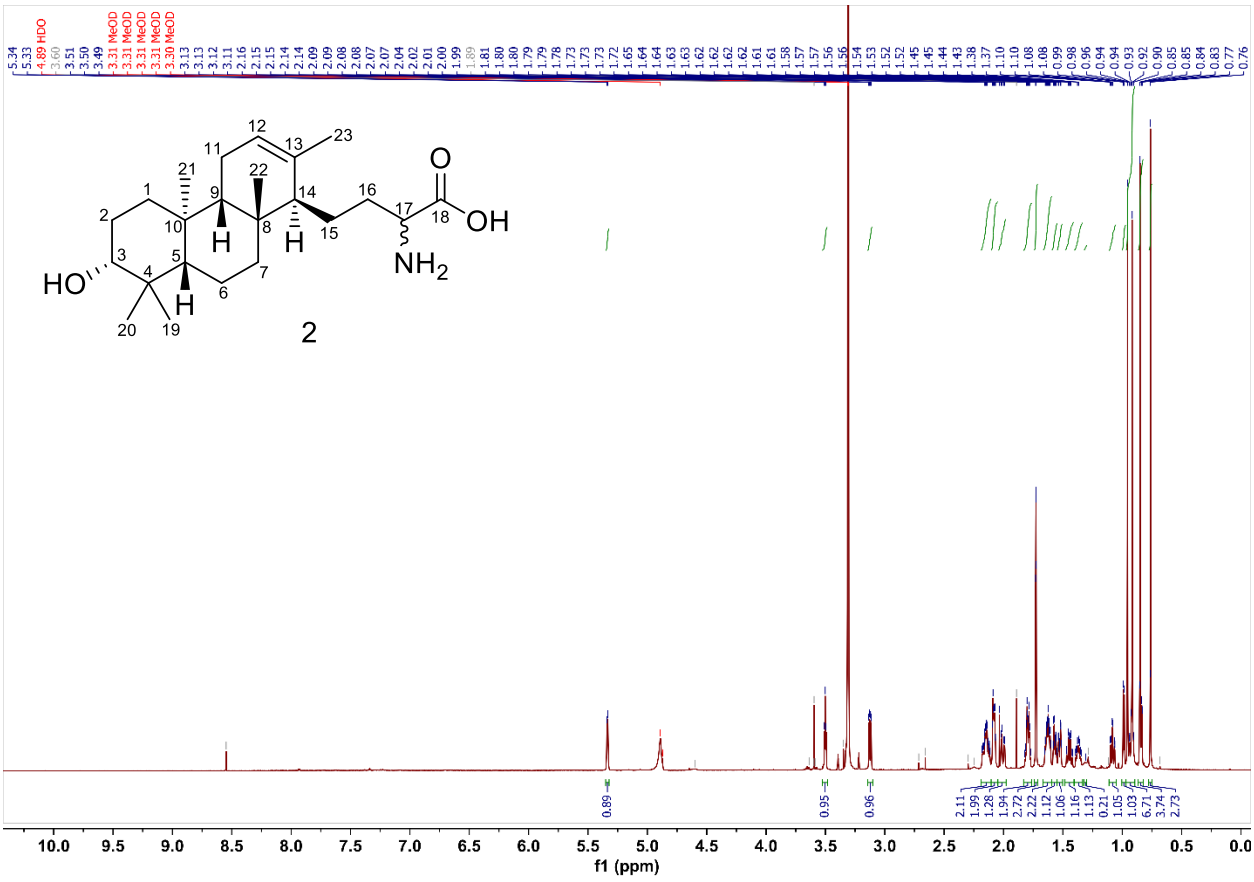

Figure S11. ^{13}C NMR spectrum of **2** in CD_3OD (151 MHz).

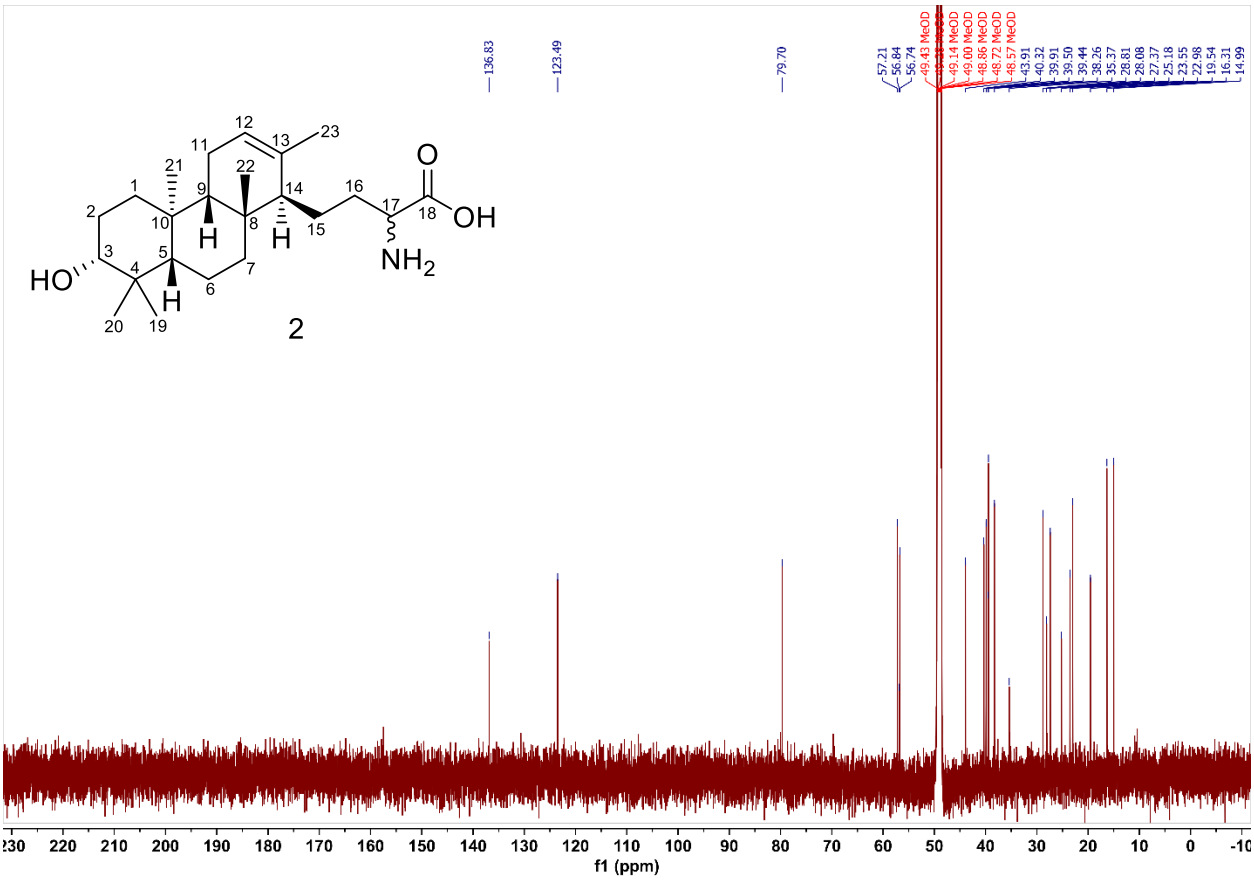

Figure S12. ^{1}H-^{13}C HSQC spectrum of **2** in CD_3OD (800 MHz).

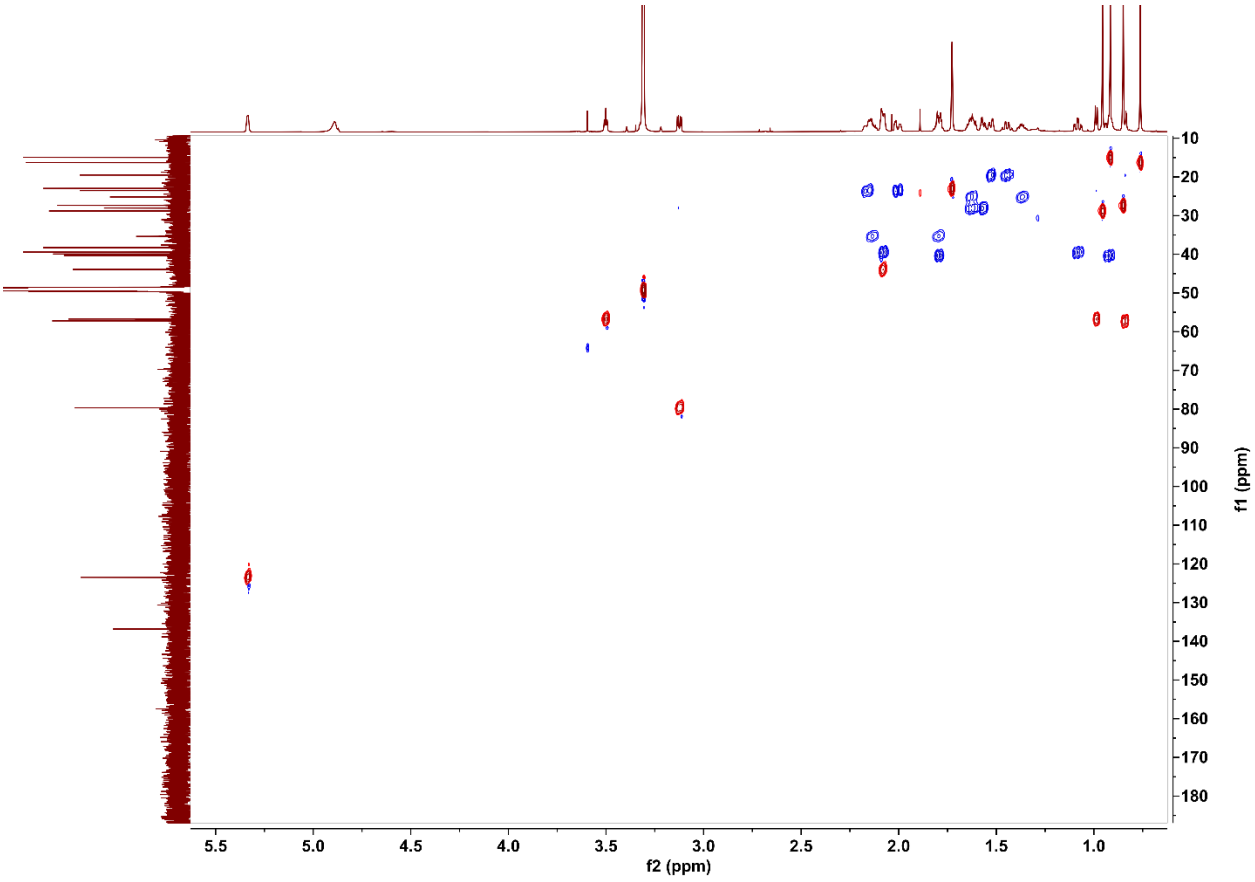

Figure S13. ^{1}H-^{13}C HMBC spectrum of **2** in CD_3OD (800 MHz).

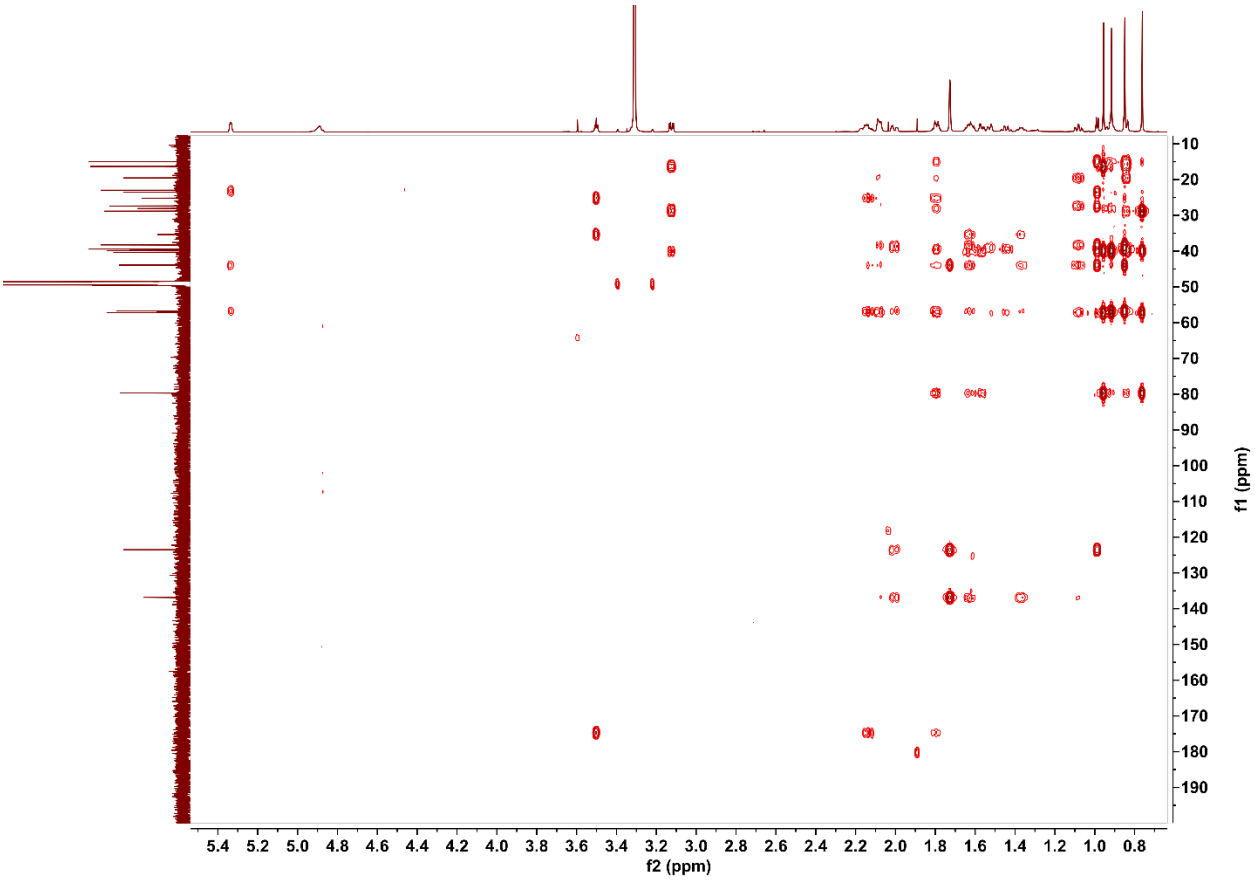

Figure S14. ^{1}H-^{1}H COSY spectrum of **2** in CD_3OD (800 MHz).

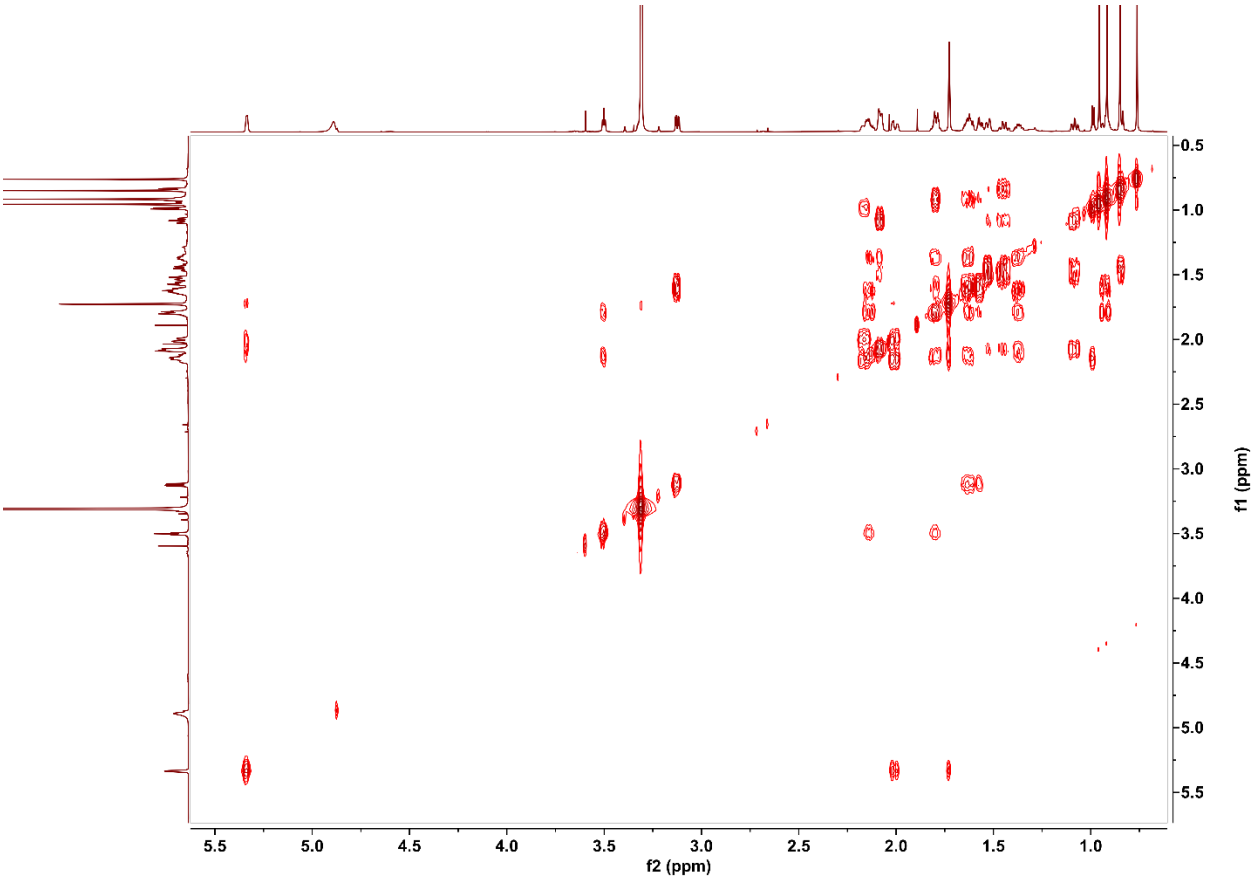

Figure S15. ^{1}H-^{1}H NOESY spectrum of **2** in CD_3OD (800 MHz).

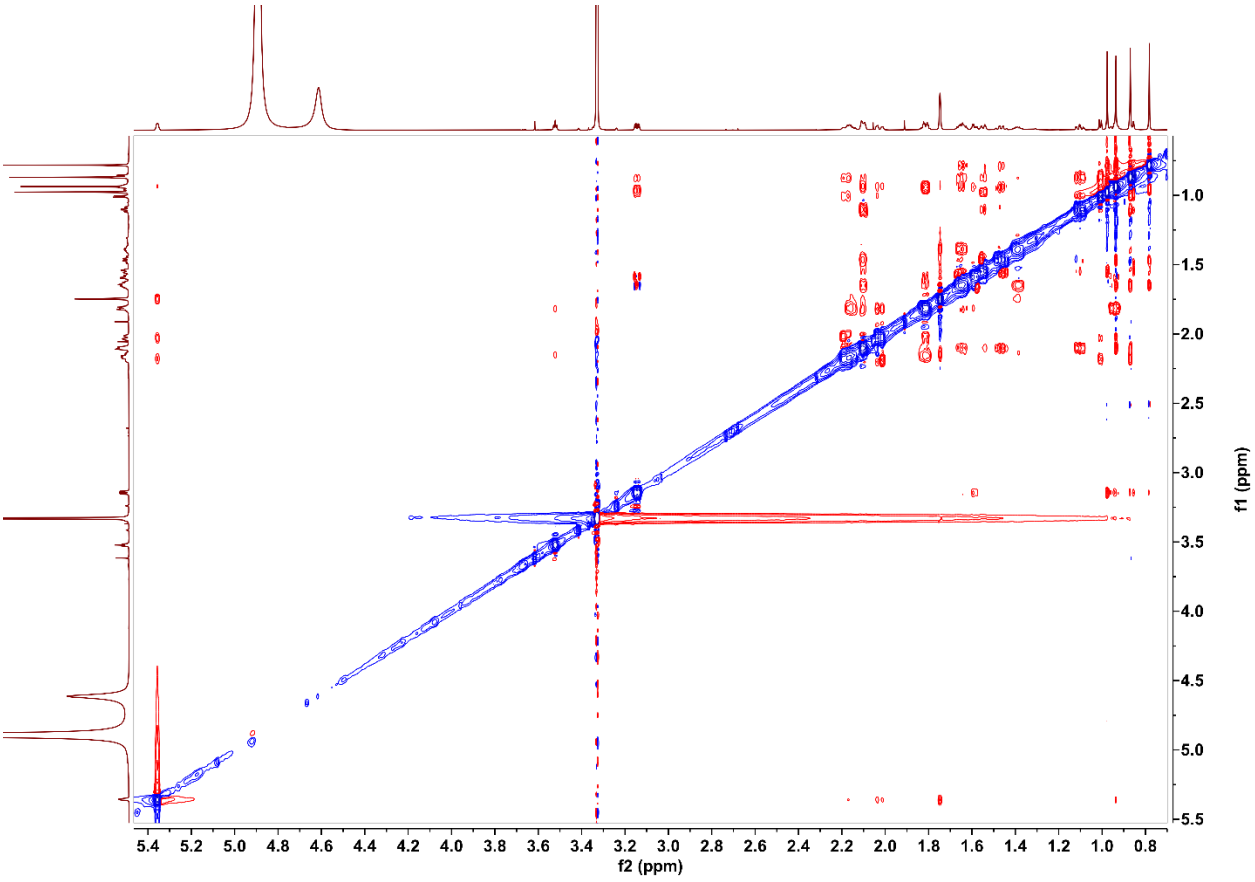

Figure S16. Plasmid maps of assembled constructs for heterologous expression. Constructs were assembled for expression under a single constitutive promoter and rbs. Not drawn to scale.

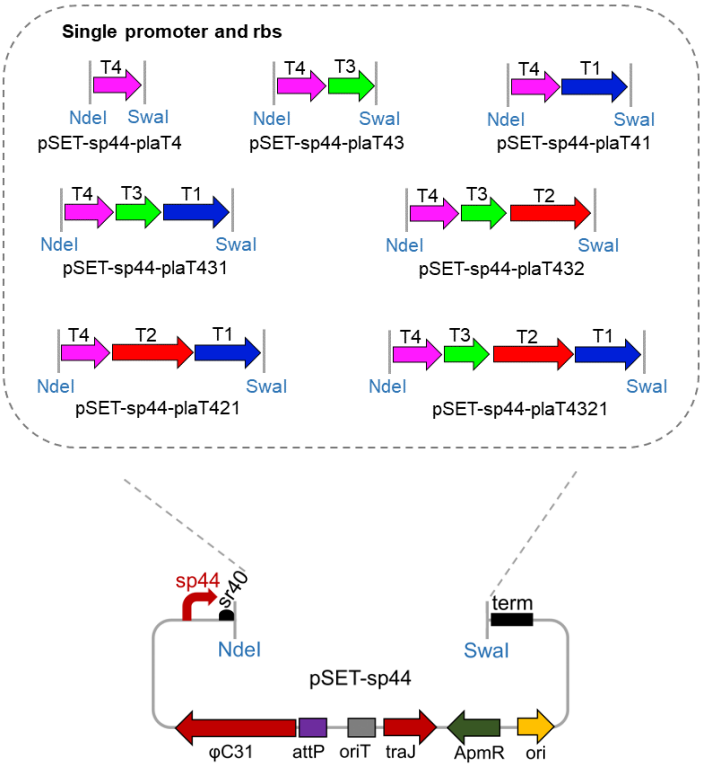

Figure S17. HRESIMS of **3** (positive mode), **4** and **5** (negative mode).

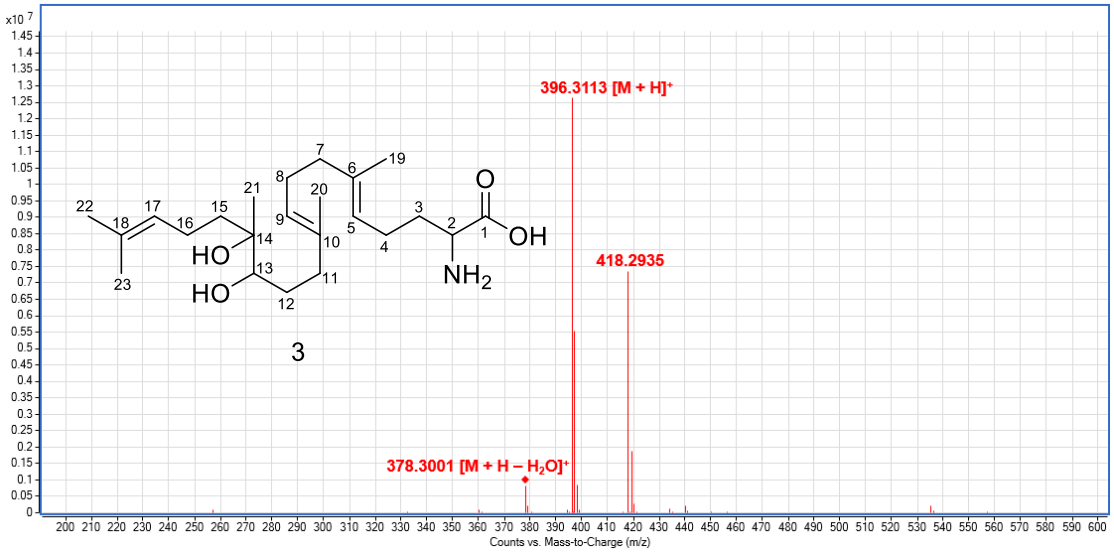

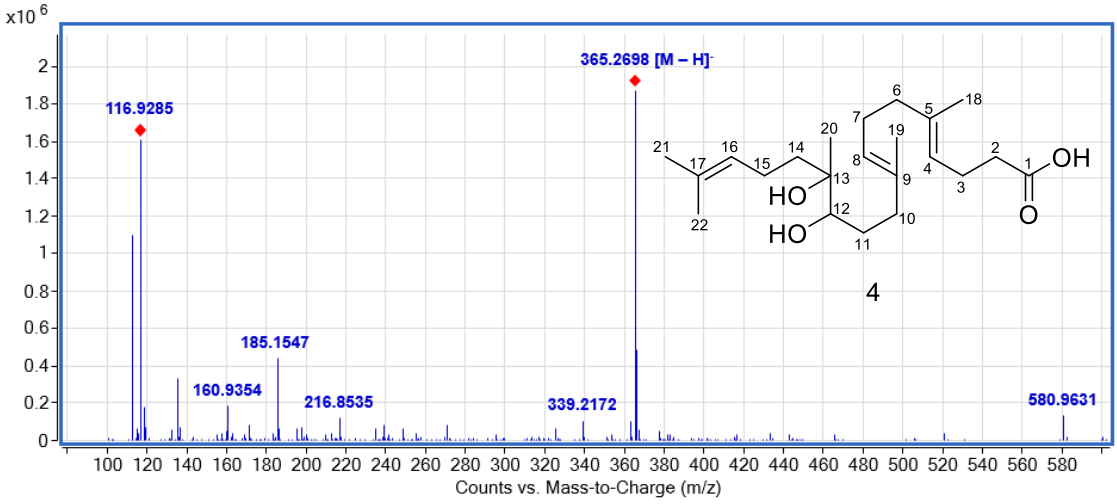

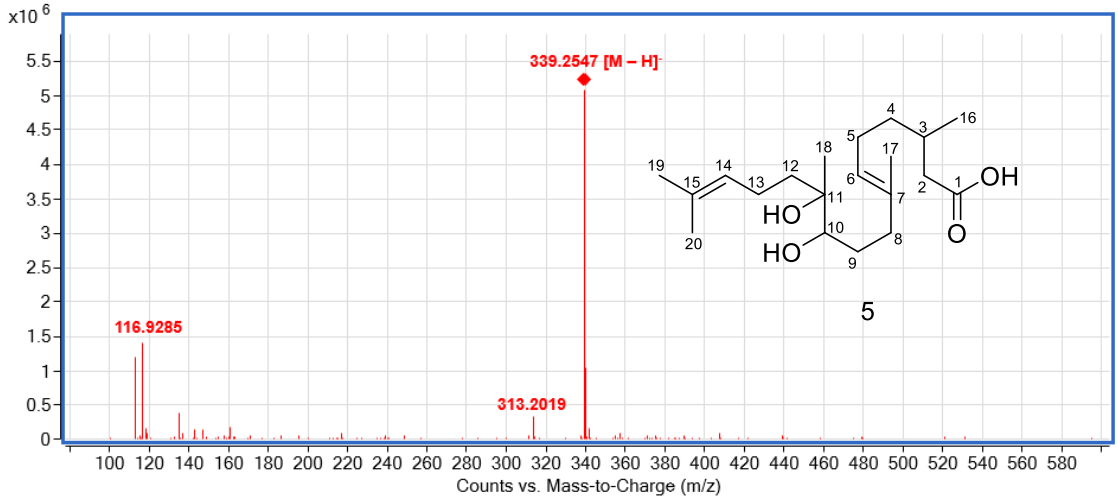

Figure S18. ^{1}H NMR spectrum of **3** in CD_3OD (600 MHz).

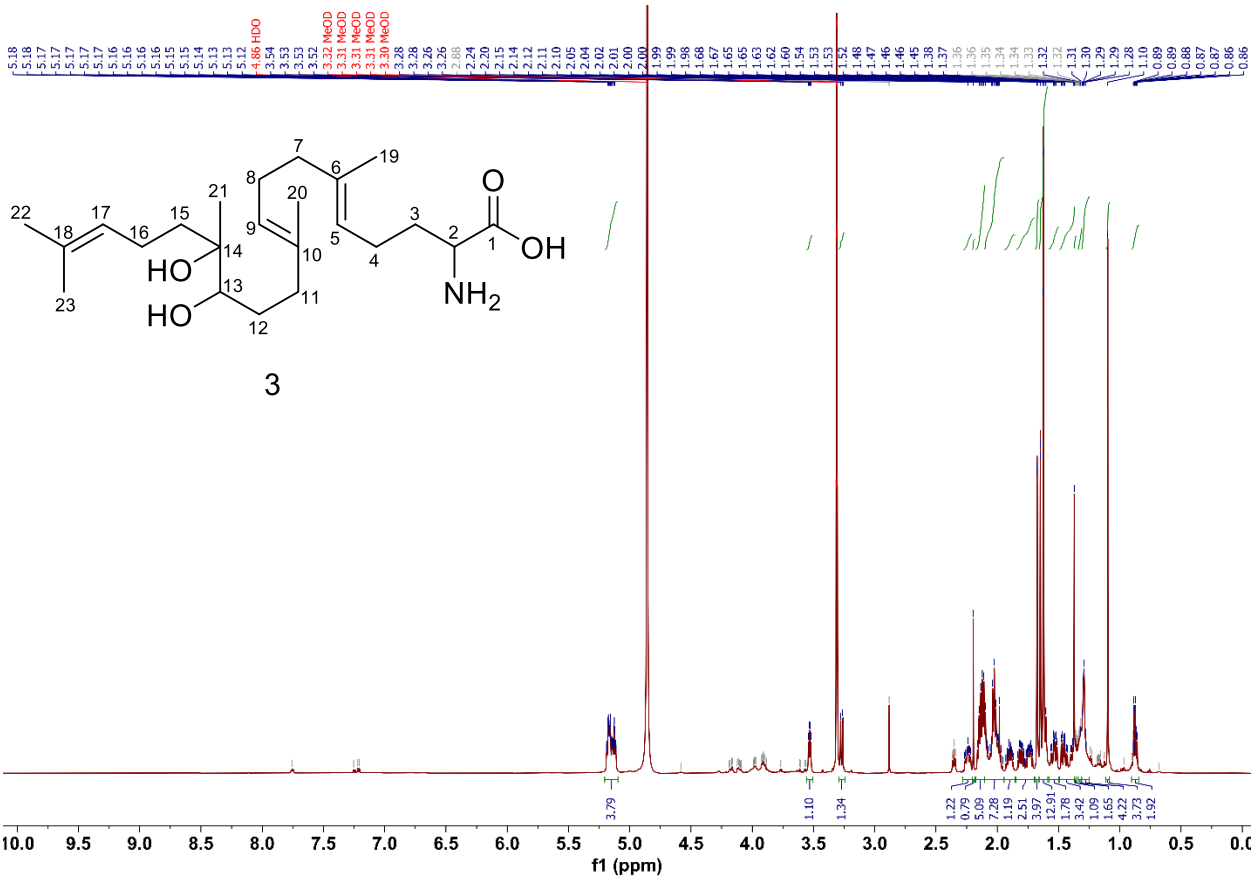

Figure S19. ^{13}C NMR spectrum of **3** in CD_3OD (151 MHz).

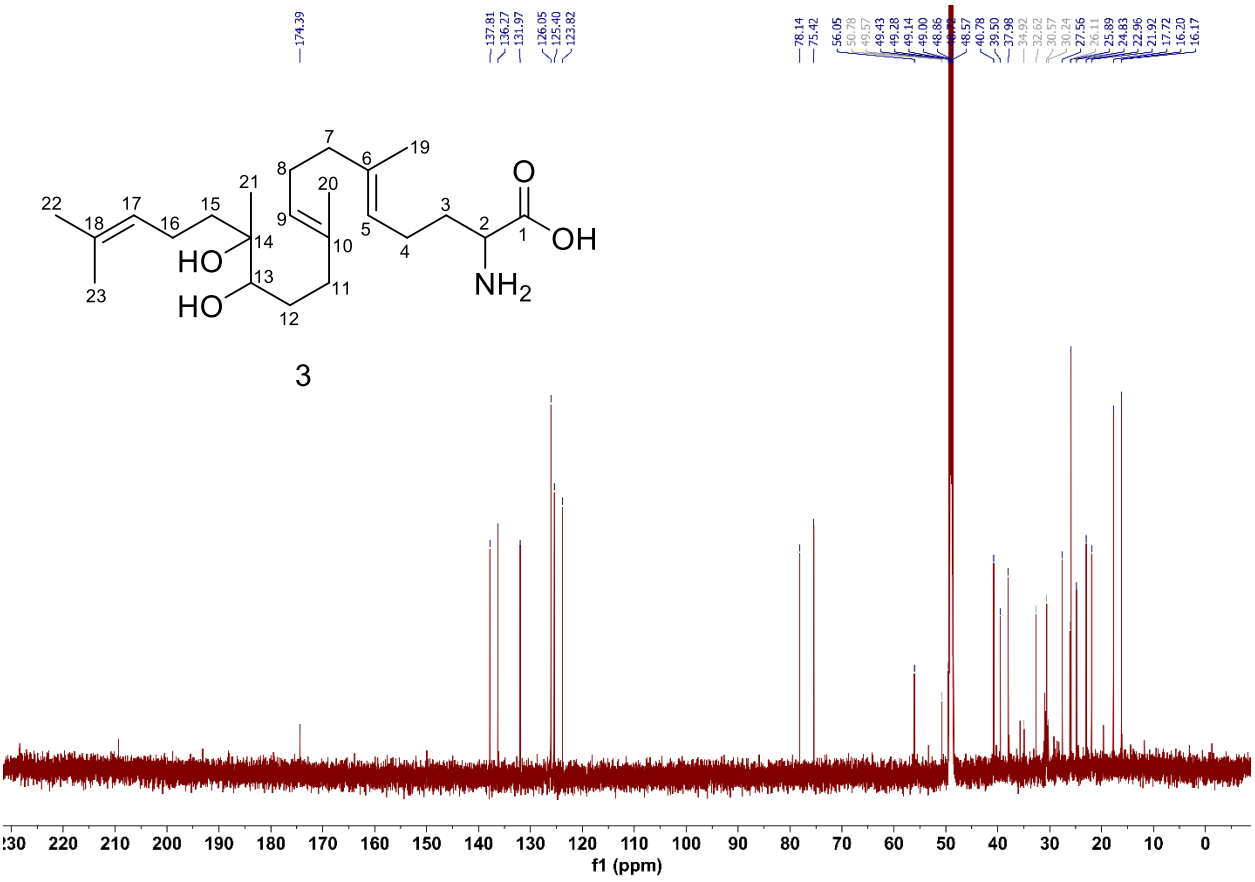

3

Figure S20. ^{1}H-^{13}C HSQC spectrum of **3** in CD_3OD.

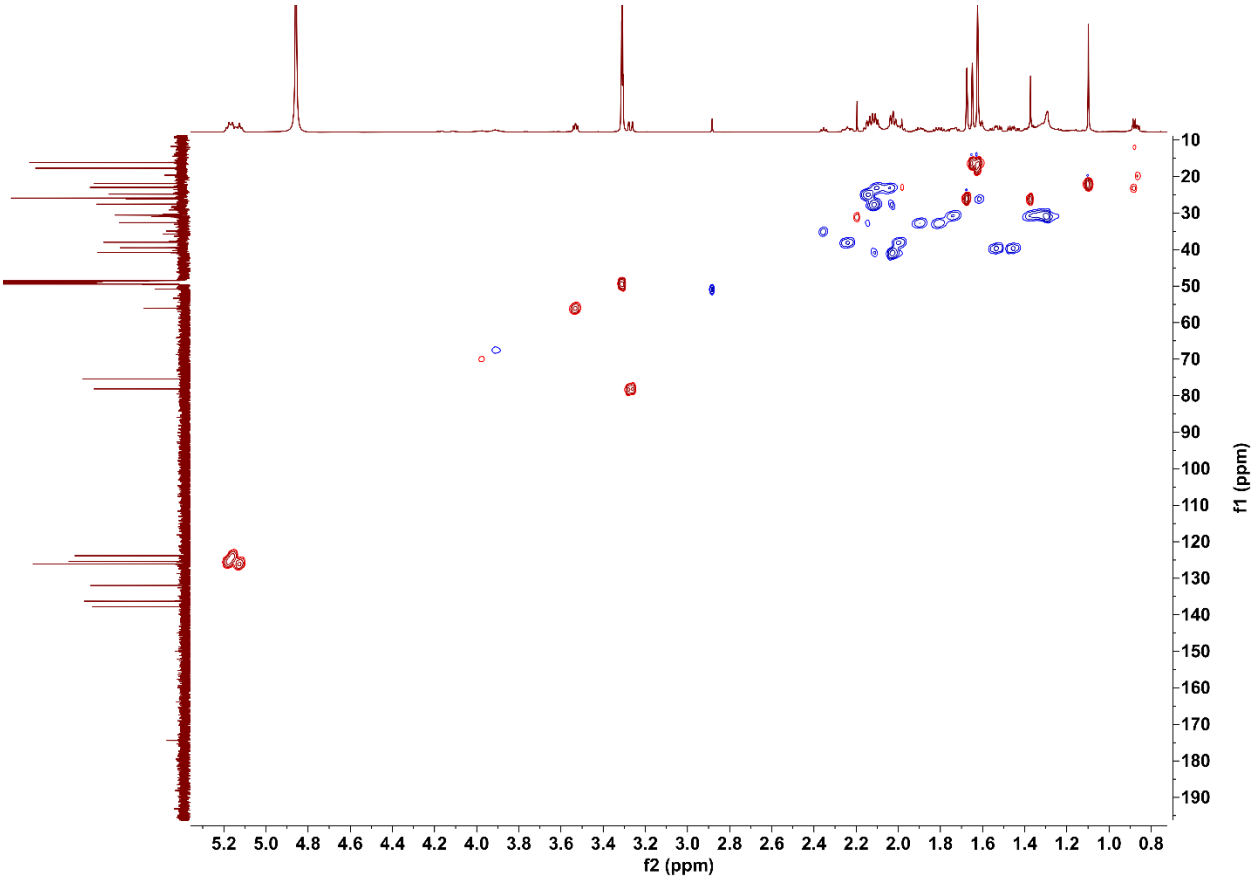

Figure S21. ^{1}H-^{13}C HMBC spectrum of **3** in CD_3OD.

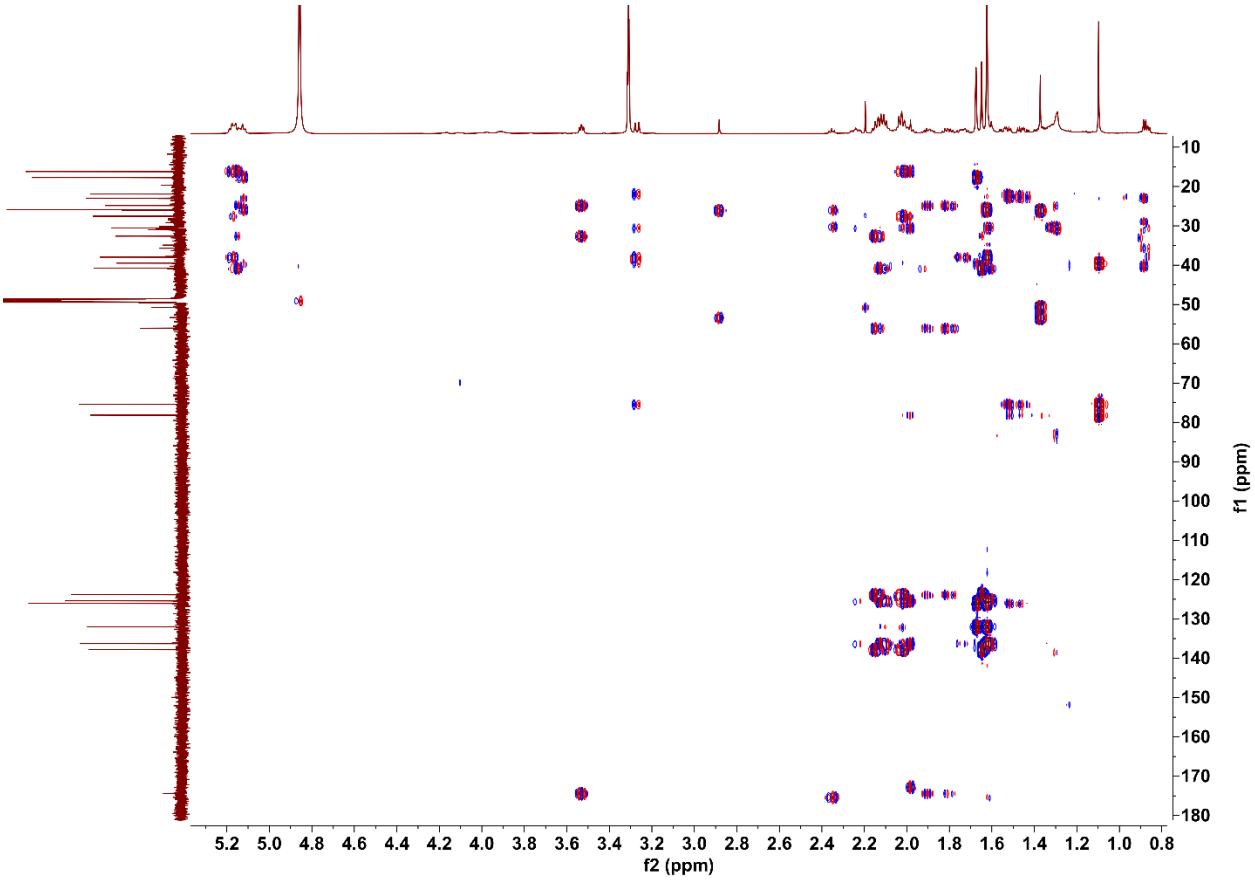

Figure S22. ^{1}H-^{1}H COSY spectrum of **3** in CD_3OD.

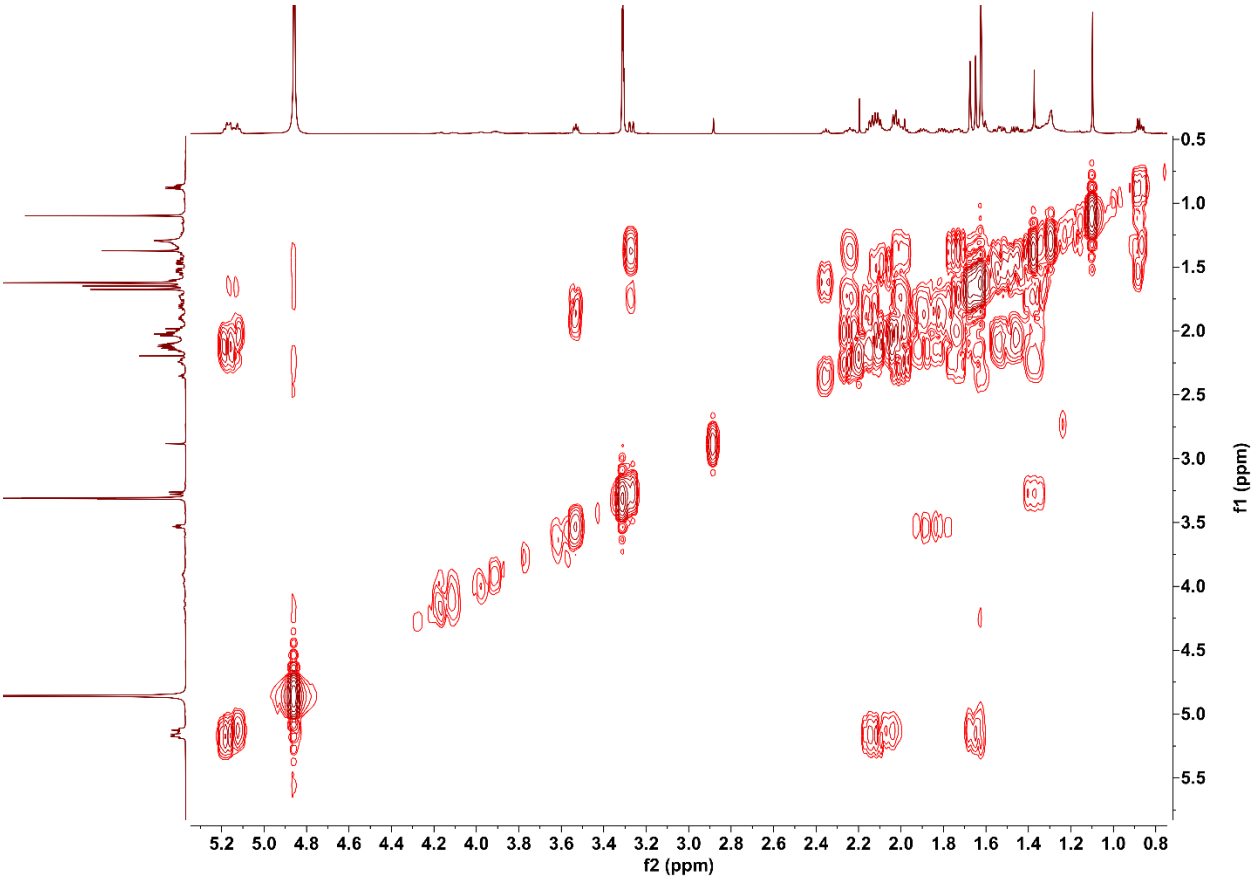

Figure S23. ^{1}H NMR spectrum of **4** in $CDCl_3$ (600 MHz).

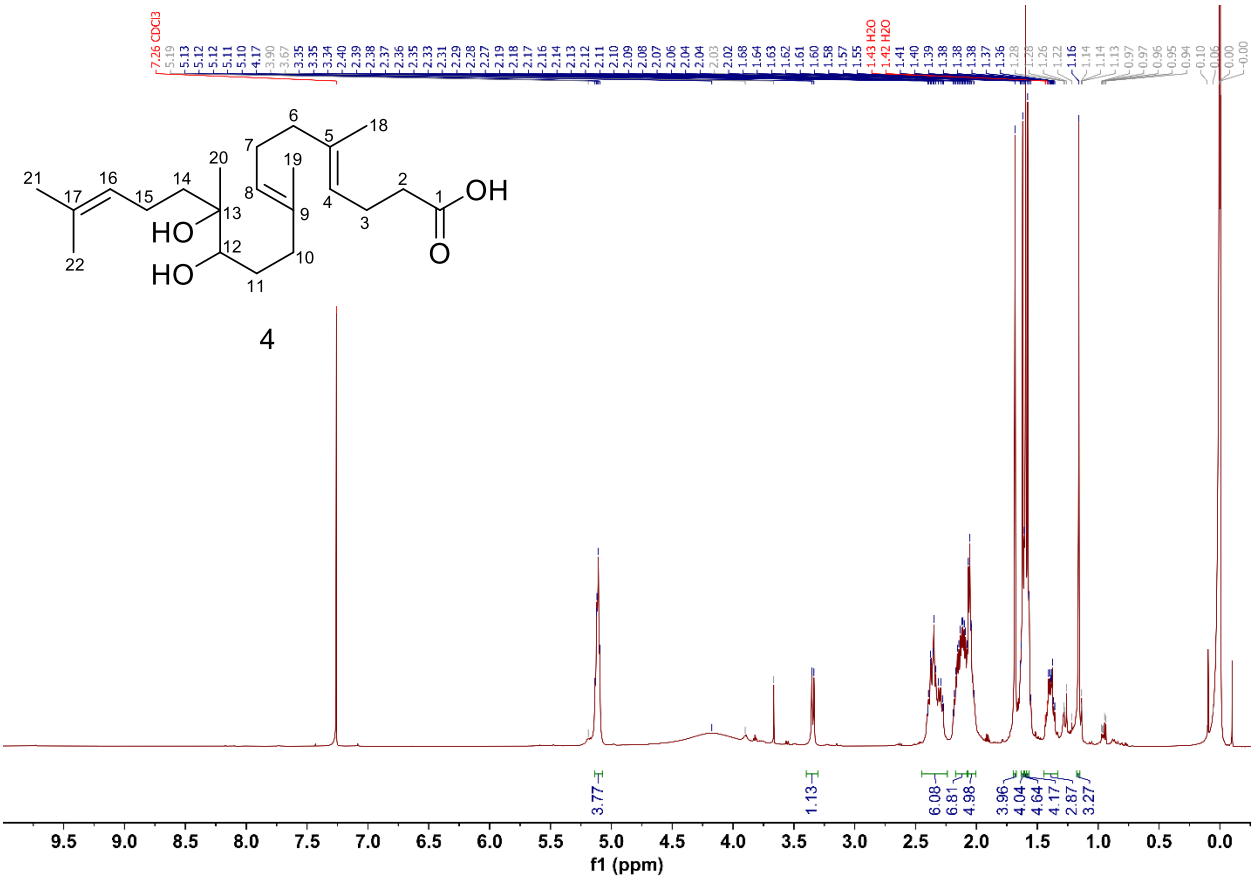

Figure S24. ^{13}C NMR spectrum of **4** in $CDCl_3$ (151 MHz).

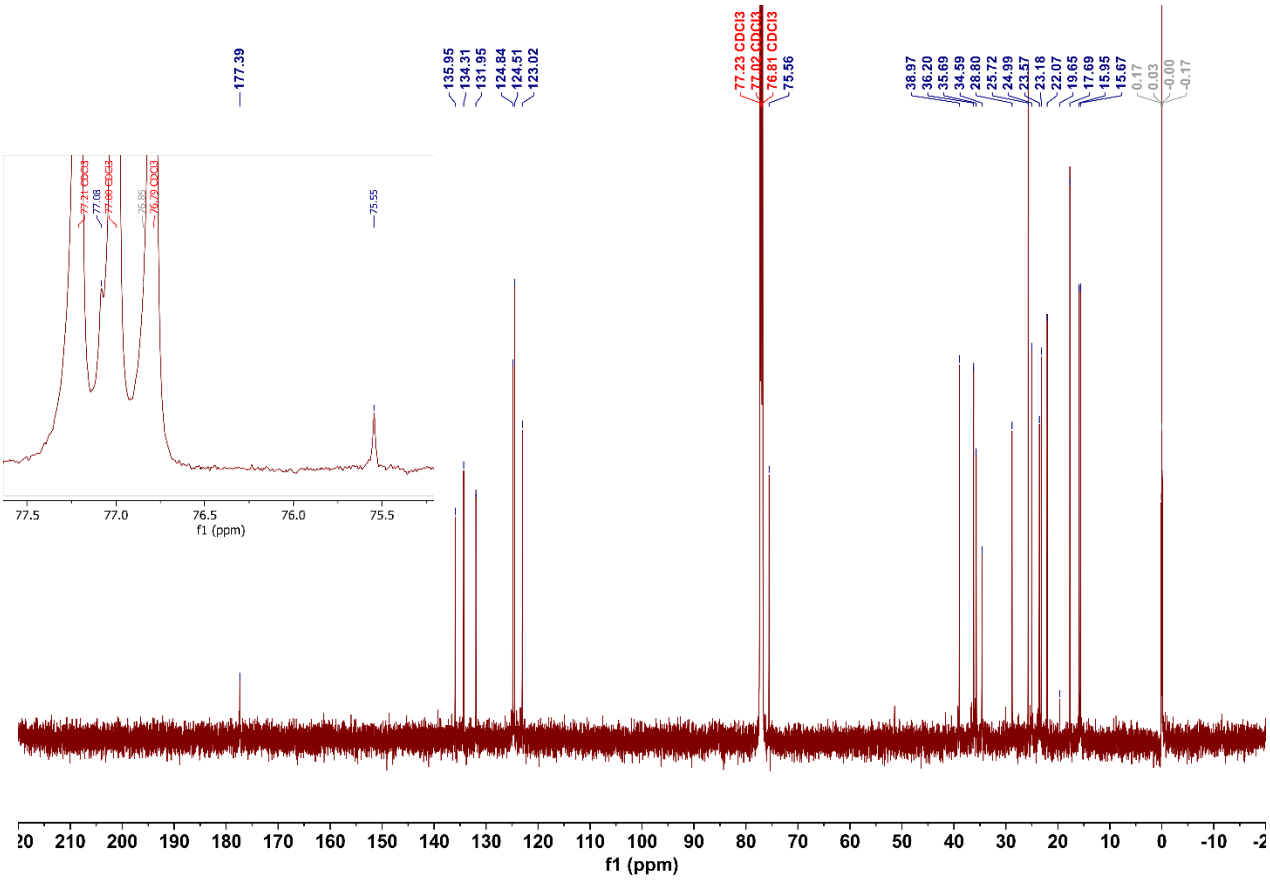

Figure S25. ^{1}H-^{13}C HSQC spectrum of **4** in $CDCl_3$.

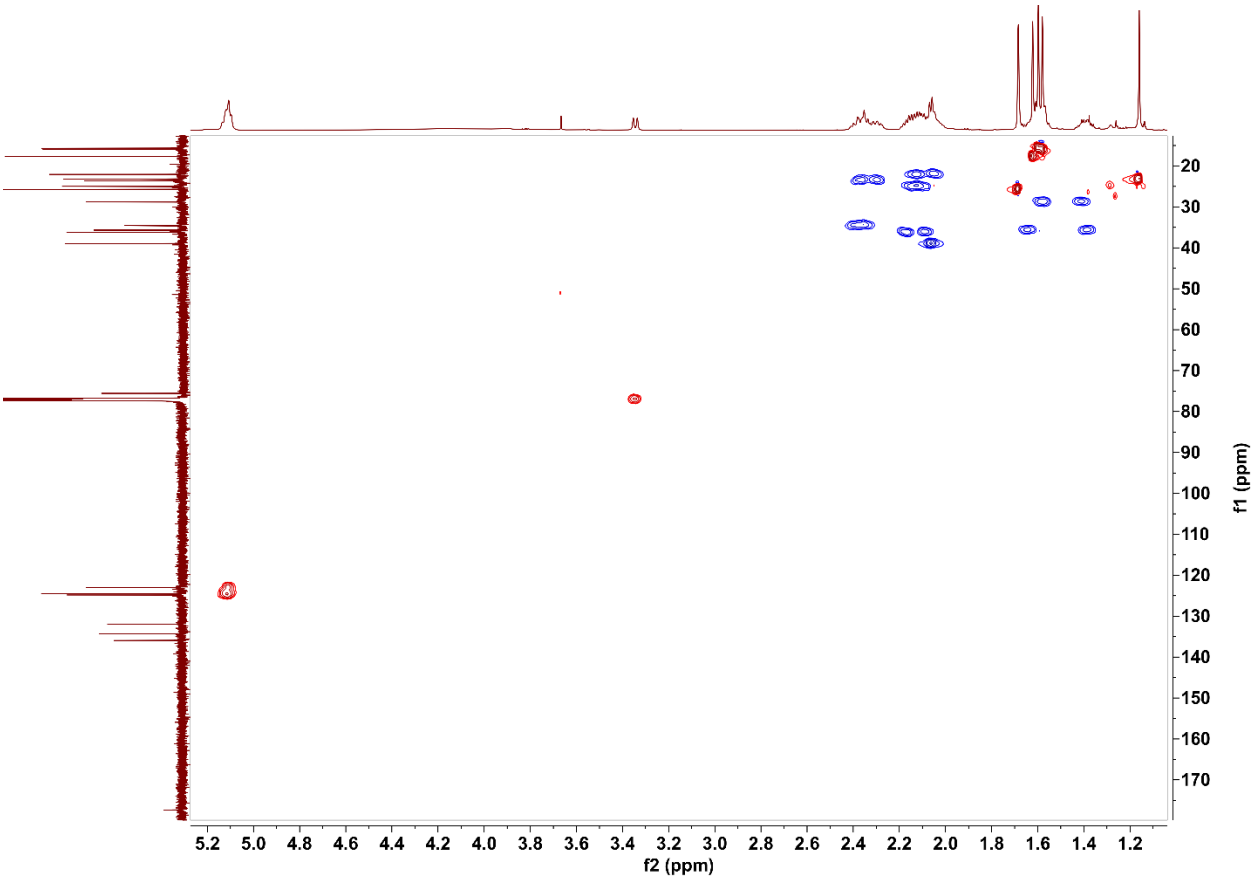

Figure S26. ^{1}H-^{13}C HMBC spectrum of **4** in $CDCl_3$.

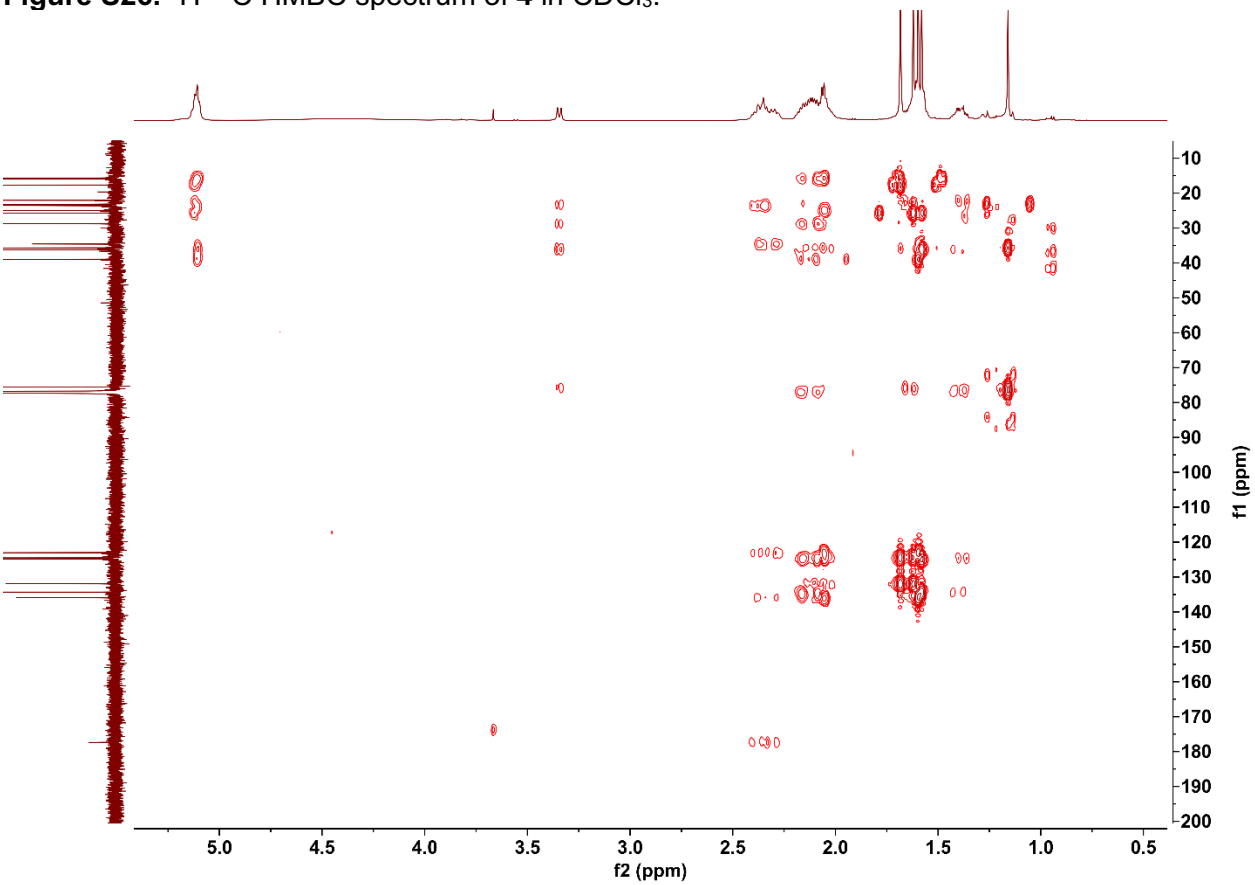

Figure S27. ^{1}H-^{1}H COSY spectrum of **4** in $CDCl_3$.

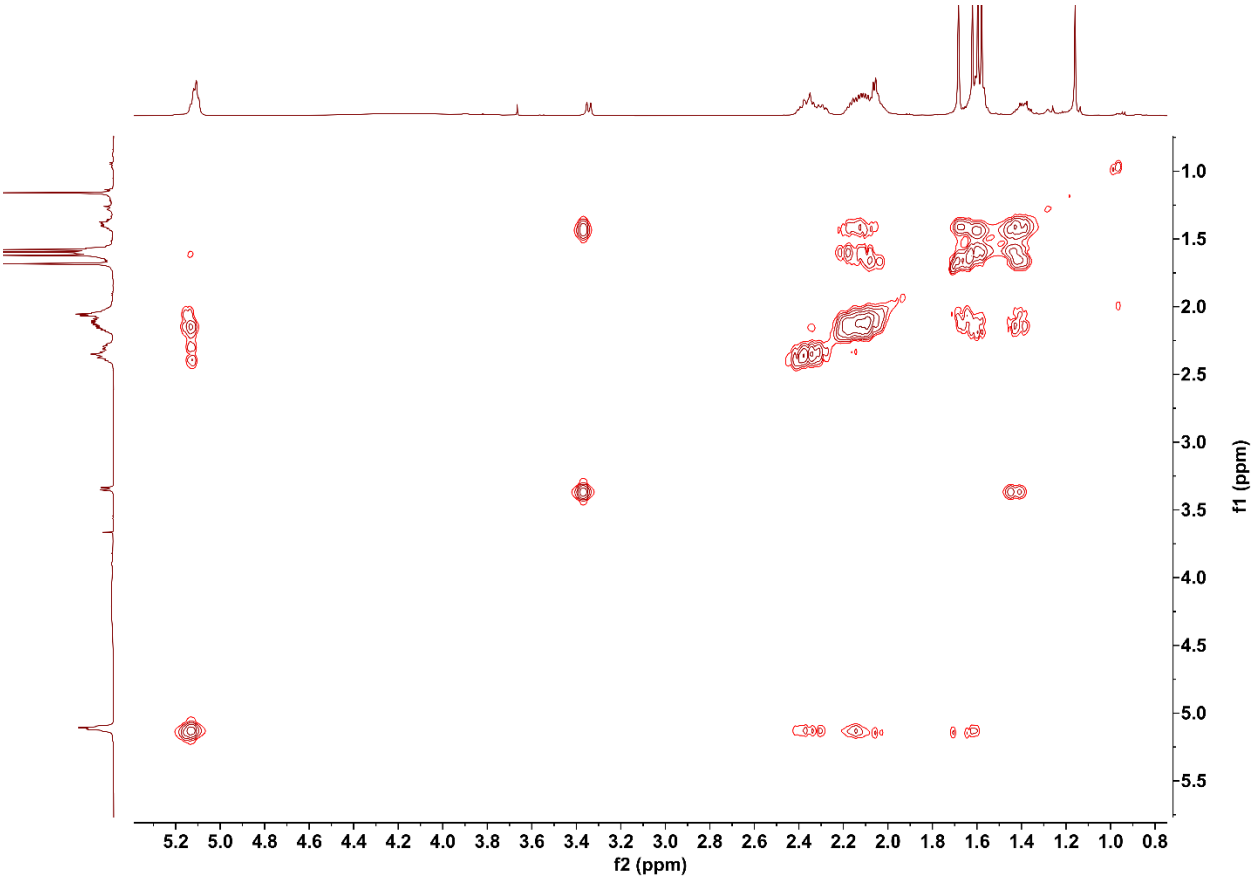

Figure S28. ^{1}H NMR spectrum of **5** in $CDCl_3$ (600 MHz).

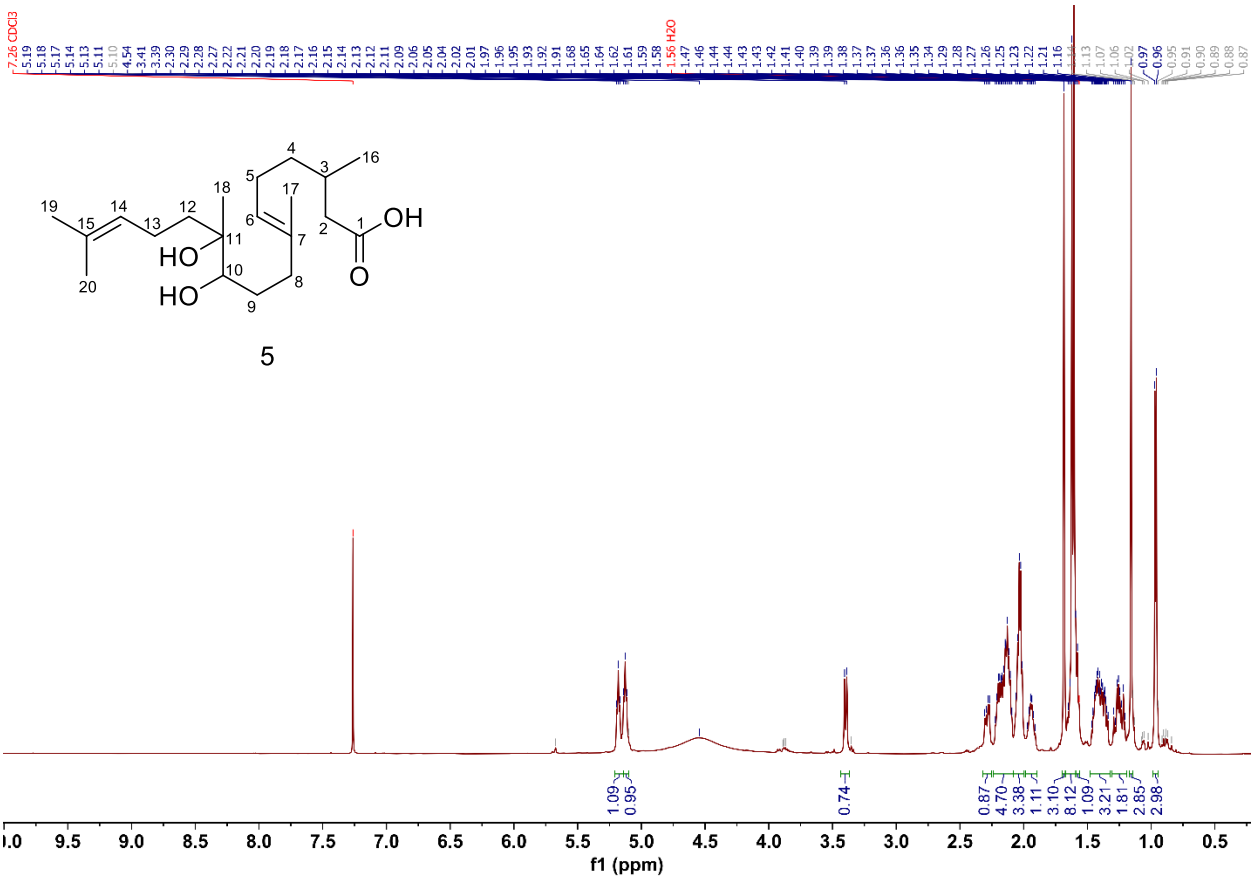

Figure S29. ^{13}C NMR spectrum of **5** in $CDCl_3$ (151 MHz).

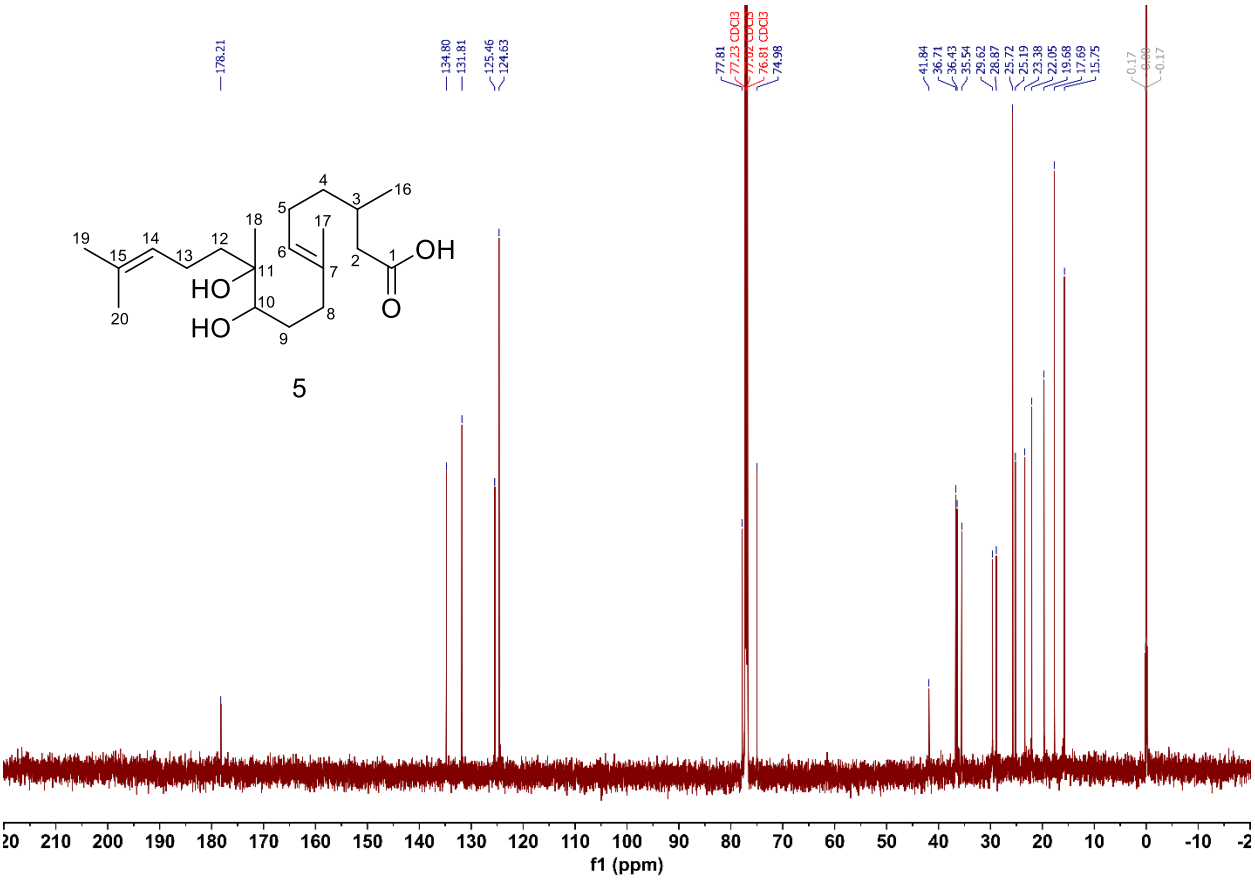

Figure S30. ^{1}H-^{13}C HSQC spectrum of **5** in $CDCl_3$.

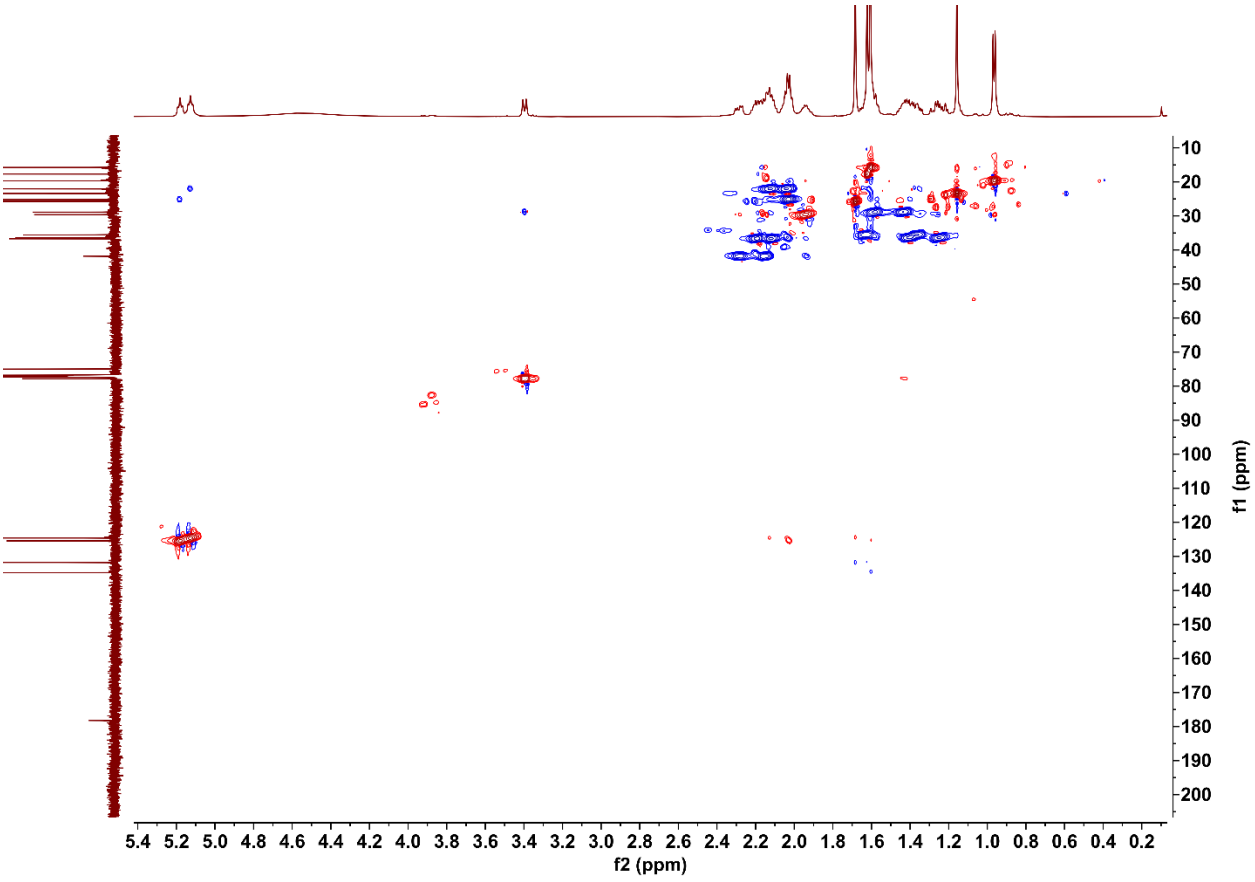

Figure S31. ^{1}H-^{13}C HMBC spectrum of **5** in $CDCl_3$.

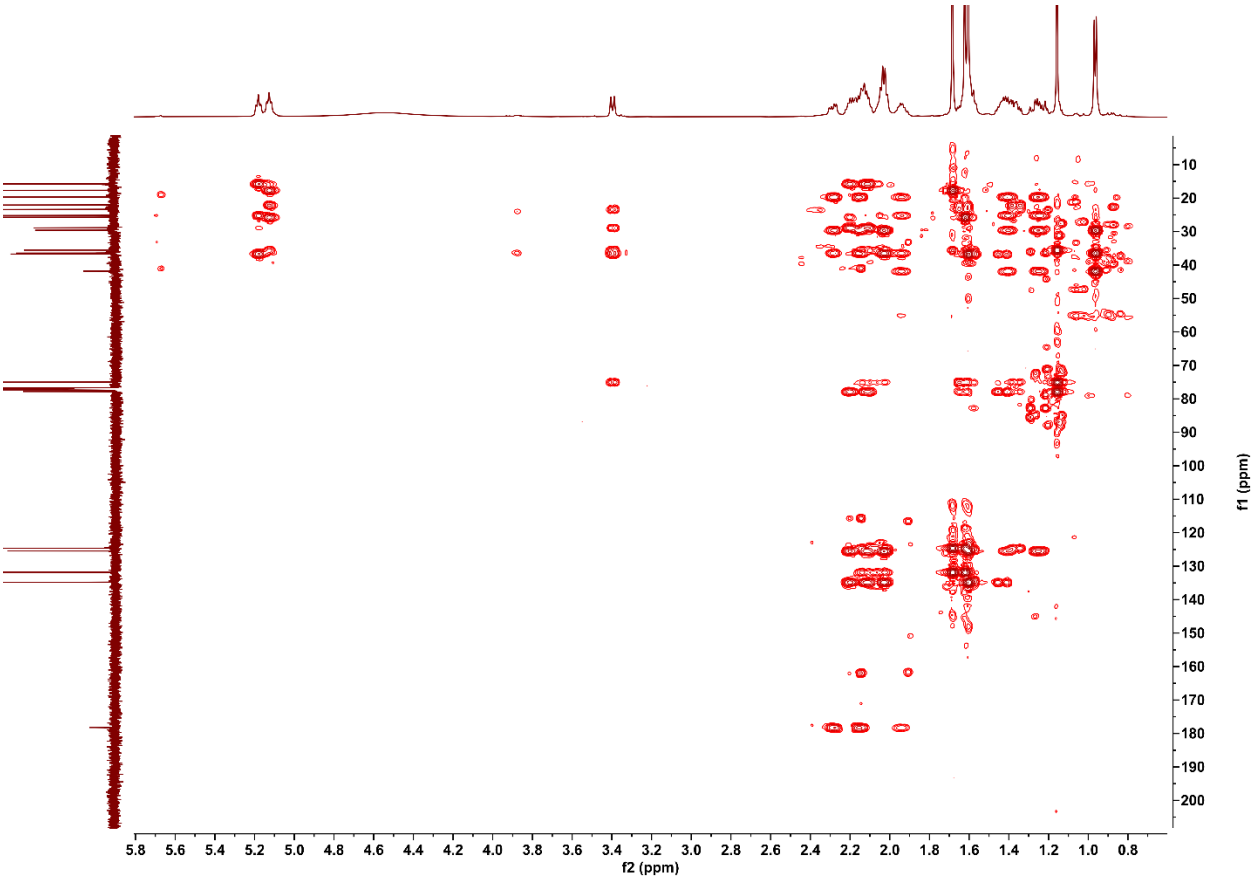

Figure S32. ^{1}H-^{1}H COSY spectrum of **5** in $CDCl_3$.

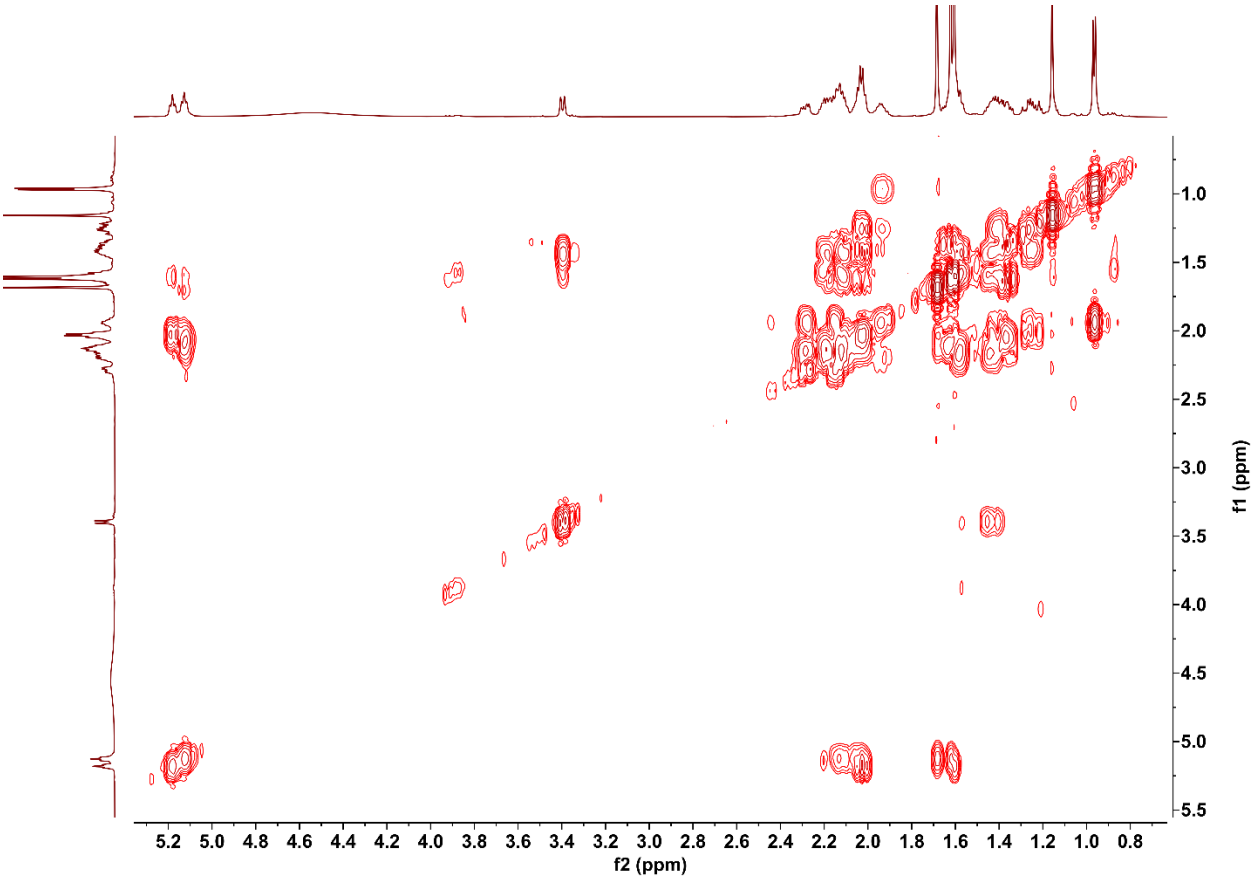

Figure S33. HRESIMS of **6** and **7** (negative mode).

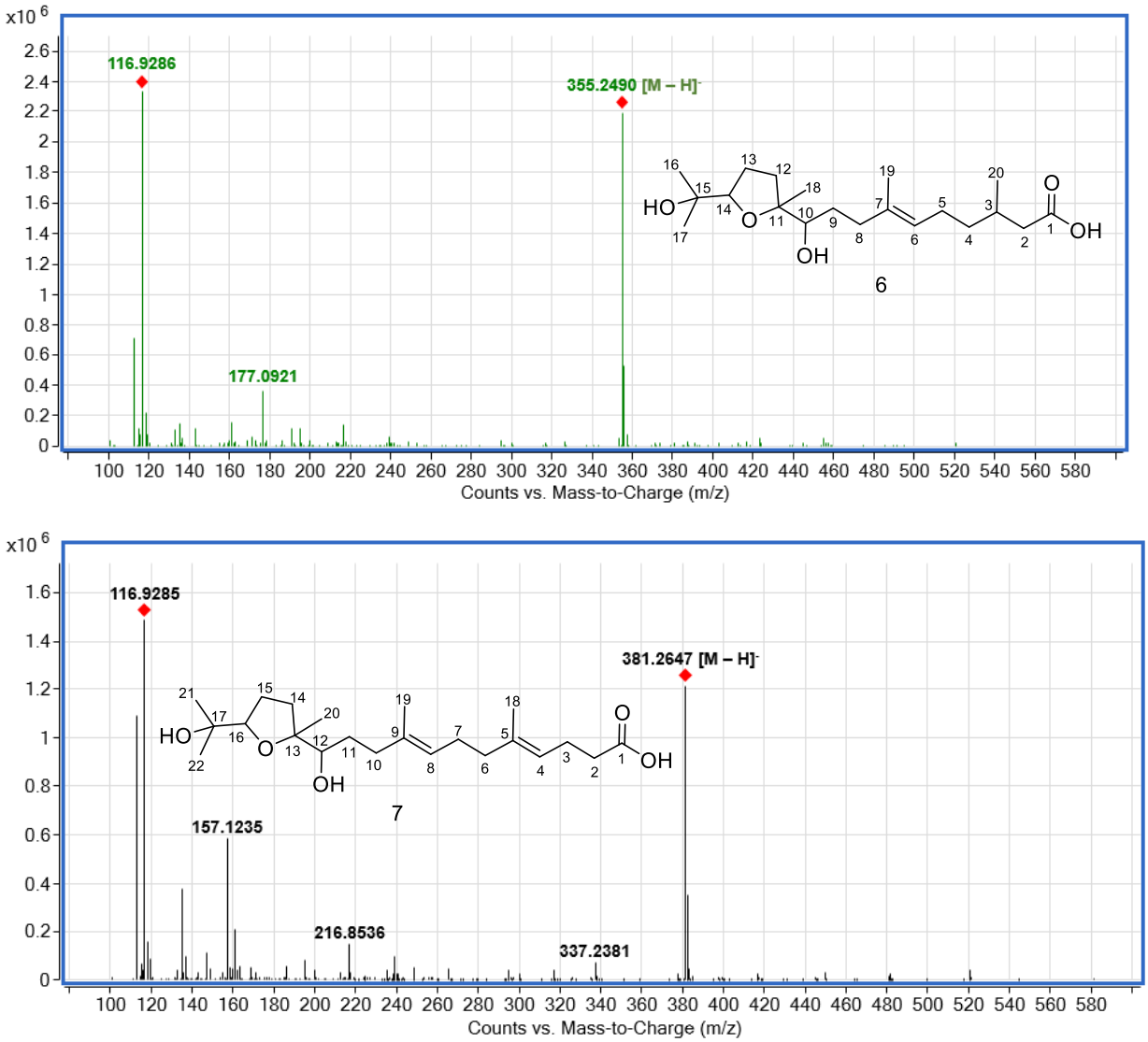

Figure S34. ^{1}H NMR spectrum of **6** in CD_3OD (600 MHz).

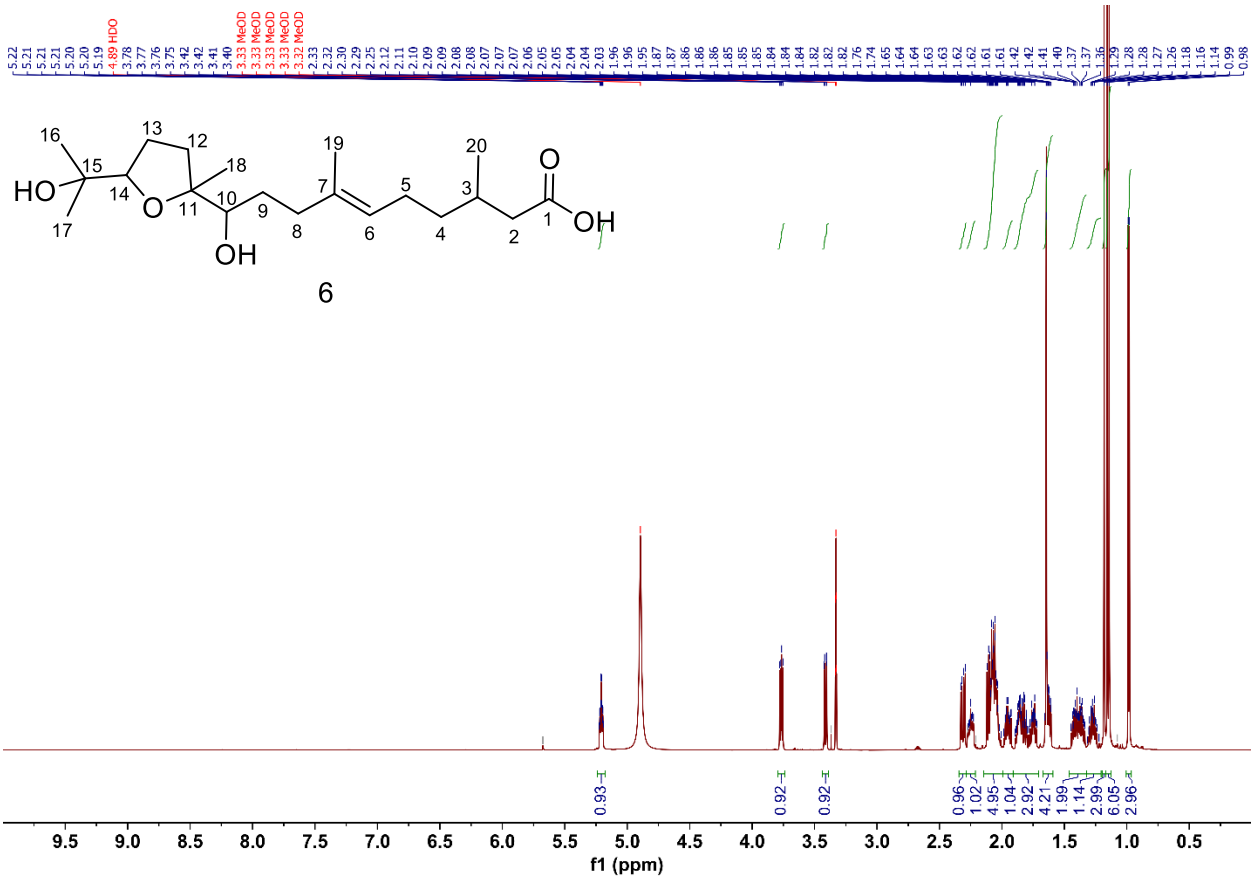

Figure S35. ^{13}C NMR spectrum of **6** in CD_3OD (151 MHz).

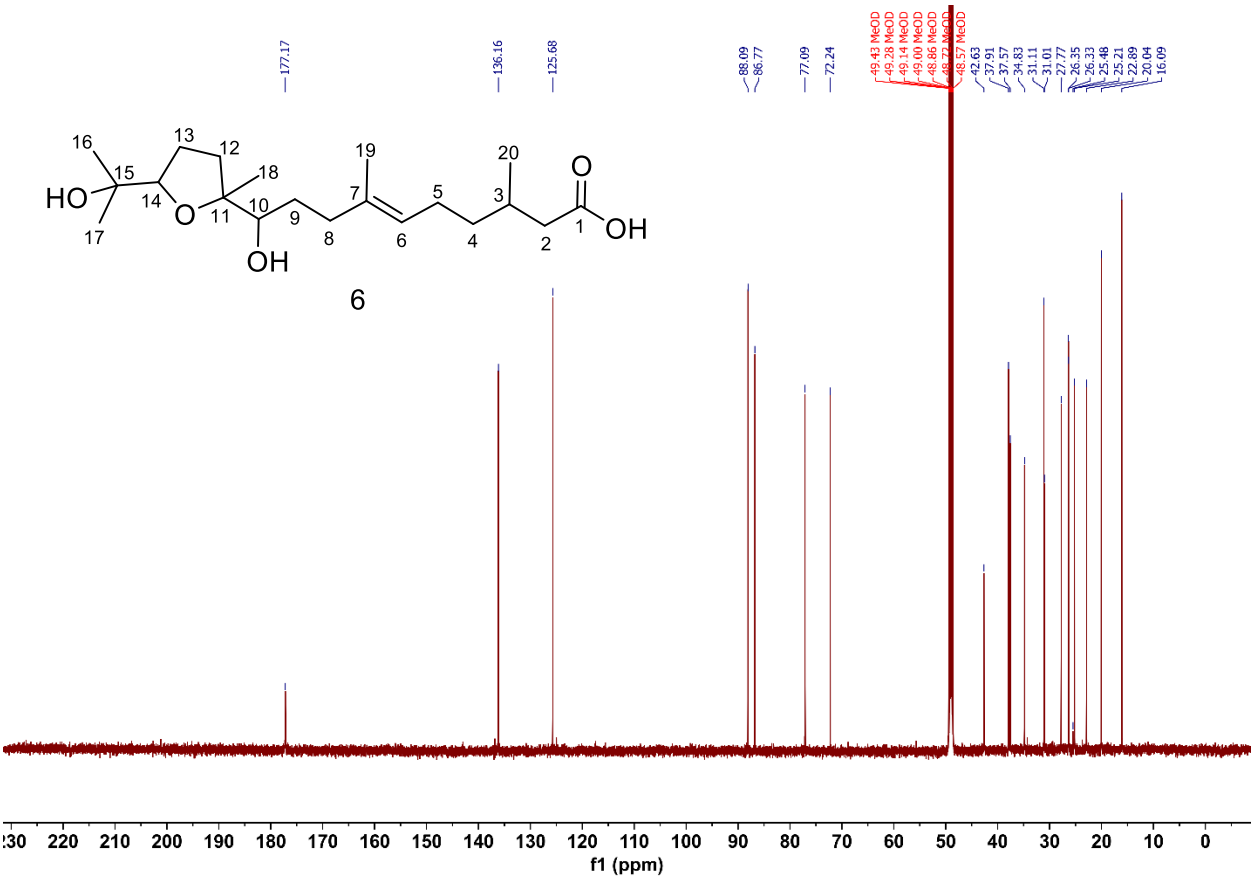

Figure S36. ^{1}H-^{13}C HSQC spectrum of **6** in CD_3OD.

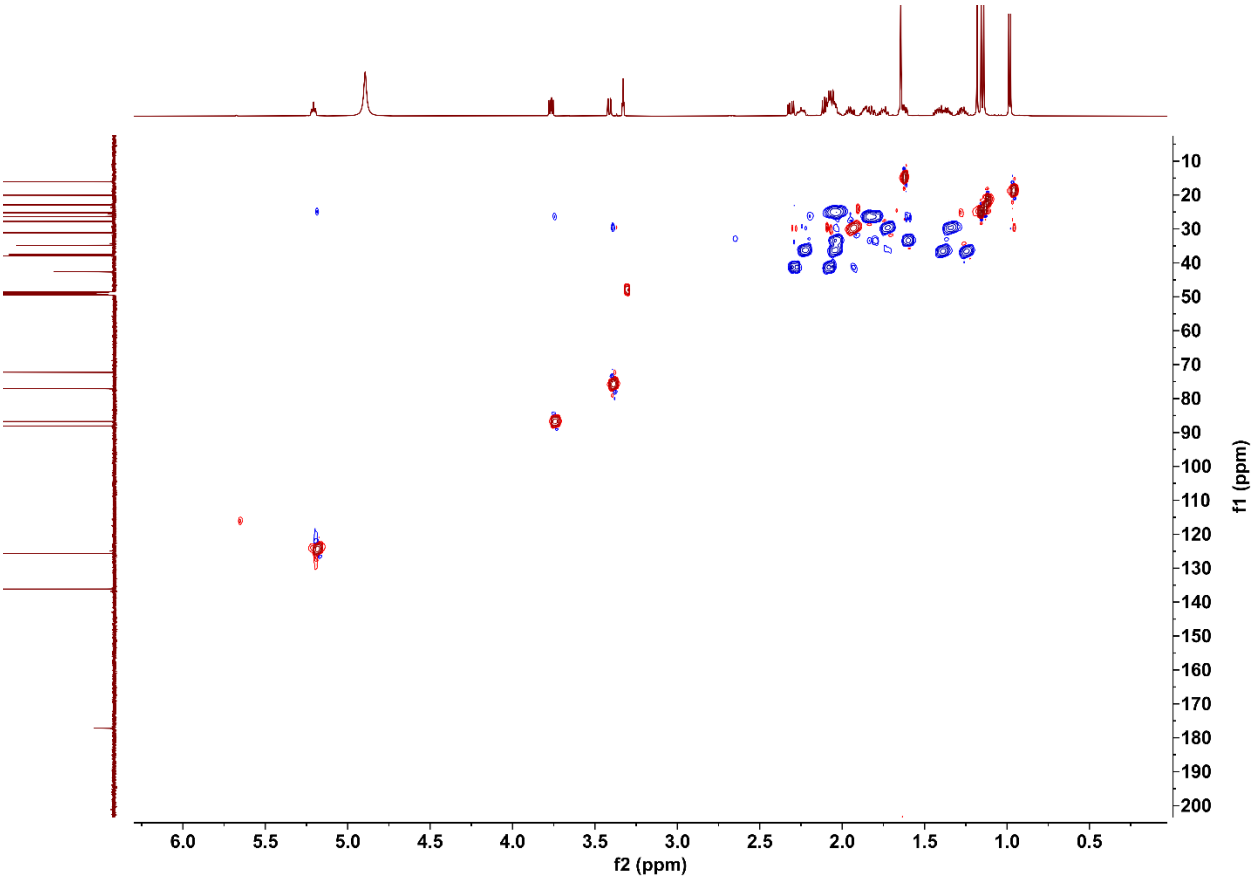

Figure S37. ^{1}H-^{13}C HMBC spectrum of **6** in CD_3OD.

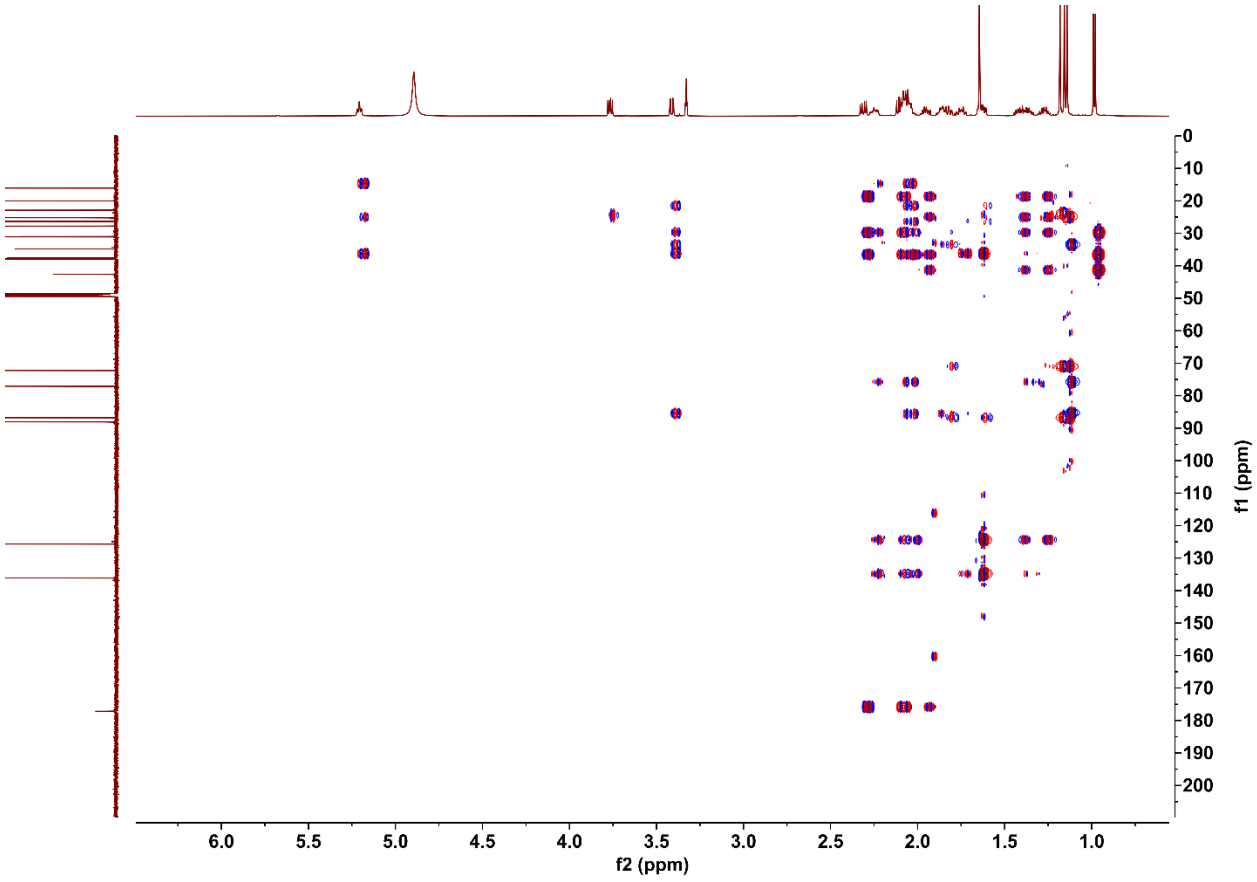

Figure S38. ^{1}H-^{1}H COSY spectrum of **6** in CD_3OD.

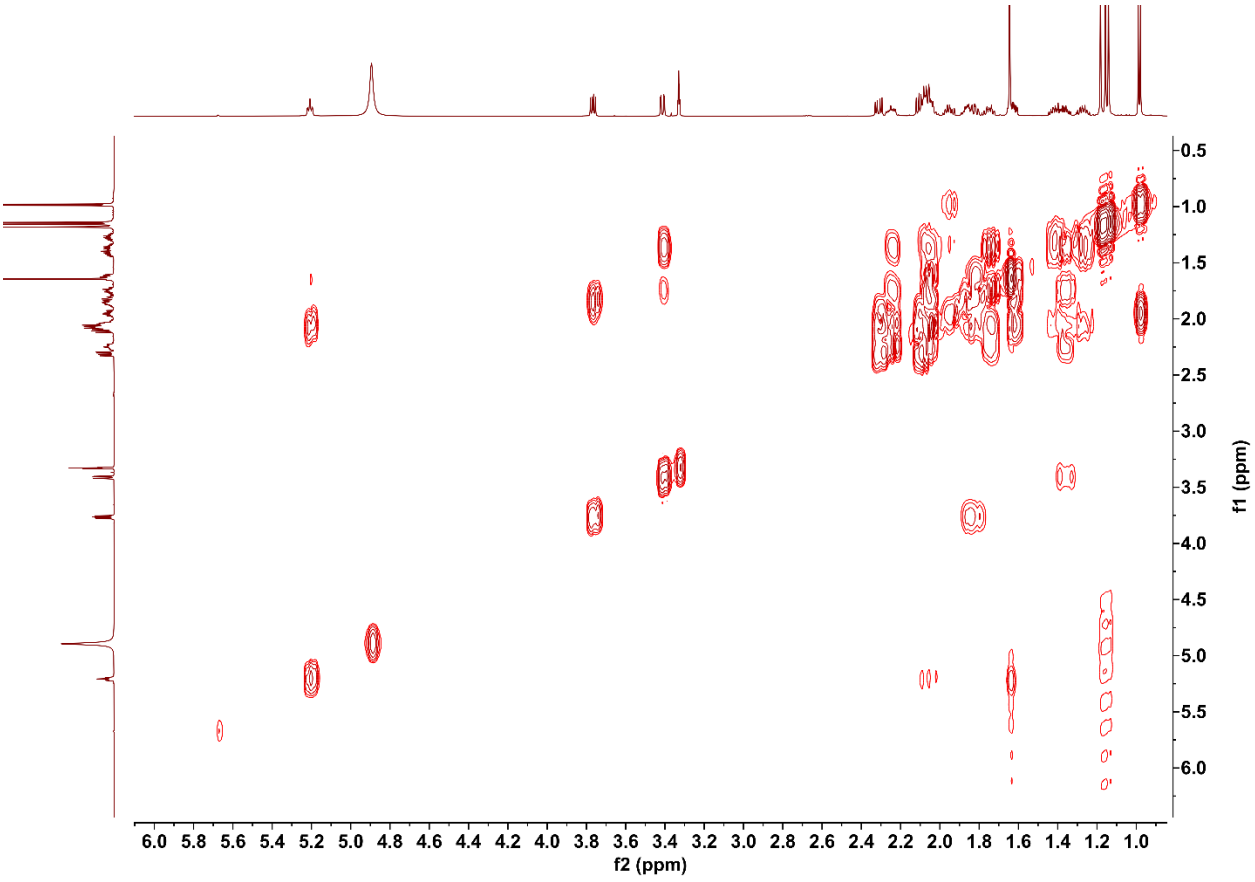

Figure S39. ^{1}H-^{1}H NOESY spectrum of **6** in CD_3OD.

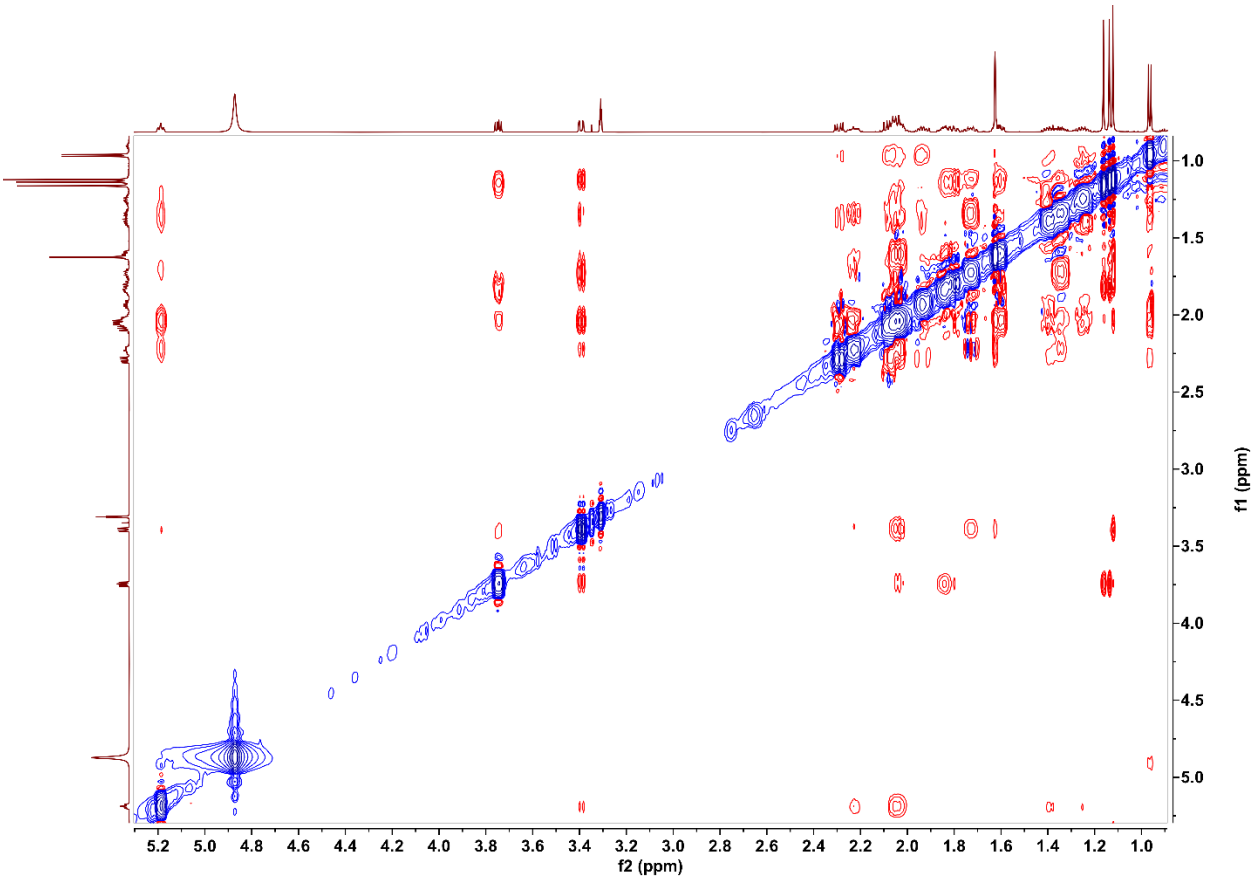

Figure S40. ^{1}H NMR spectrum of **7** in CD_3OD (600 MHz).

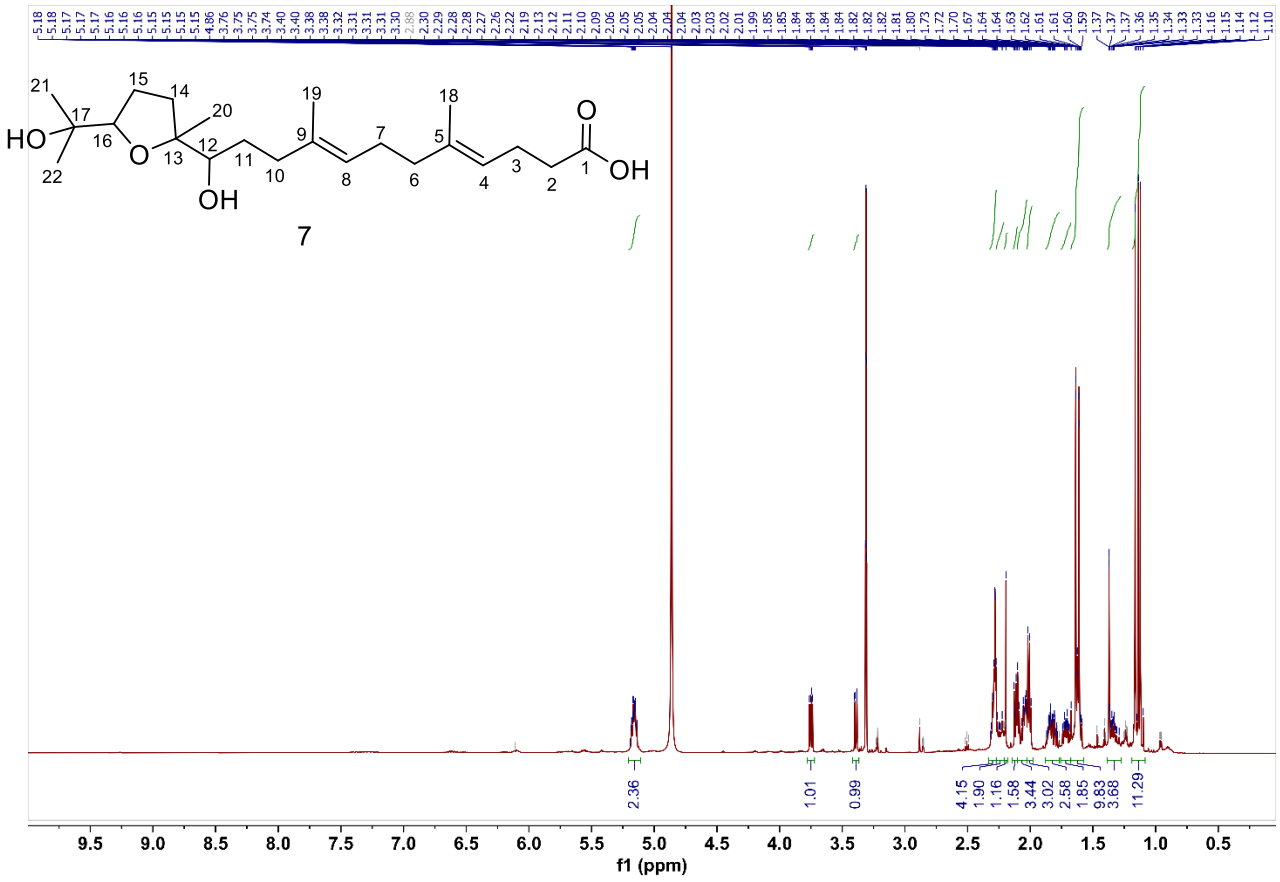

Figure S41. ^{13}C NMR spectrum of **7** in CD_3OD (151 MHz).

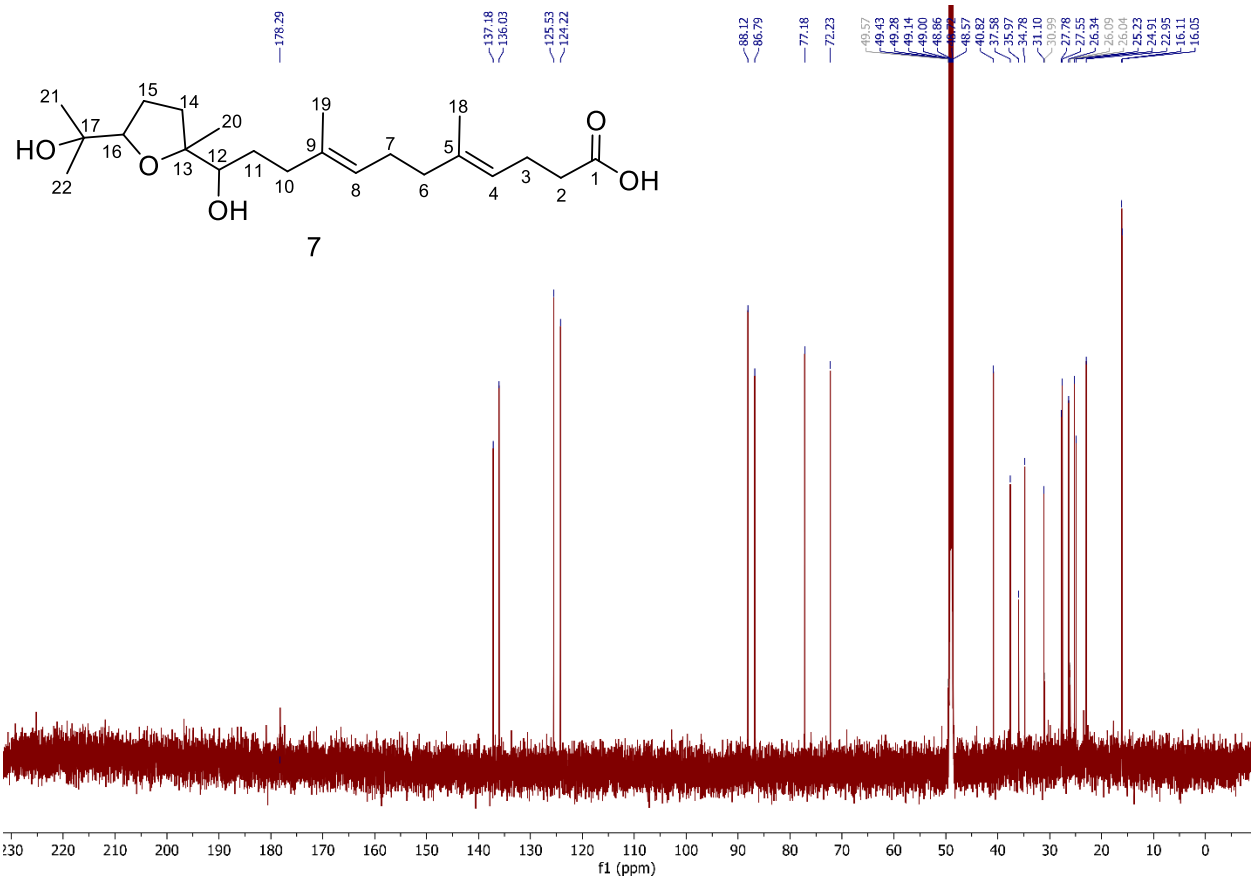

Figure S42. ^{1}H-^{13}C HSQC spectrum of **7** in CD_3OD.

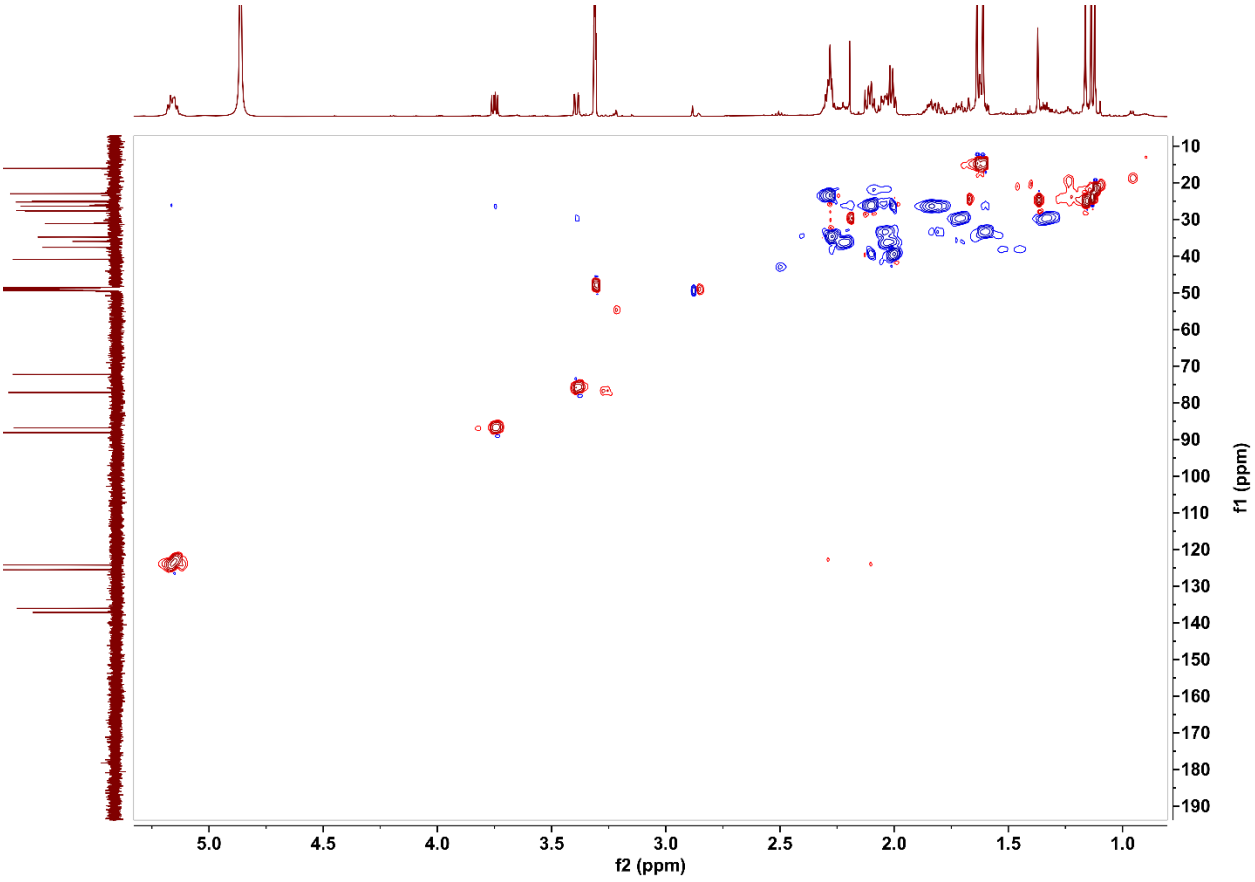

Figure S43. ^{1}H-^{13}C HMBC spectrum of **7** in CD_3OD.

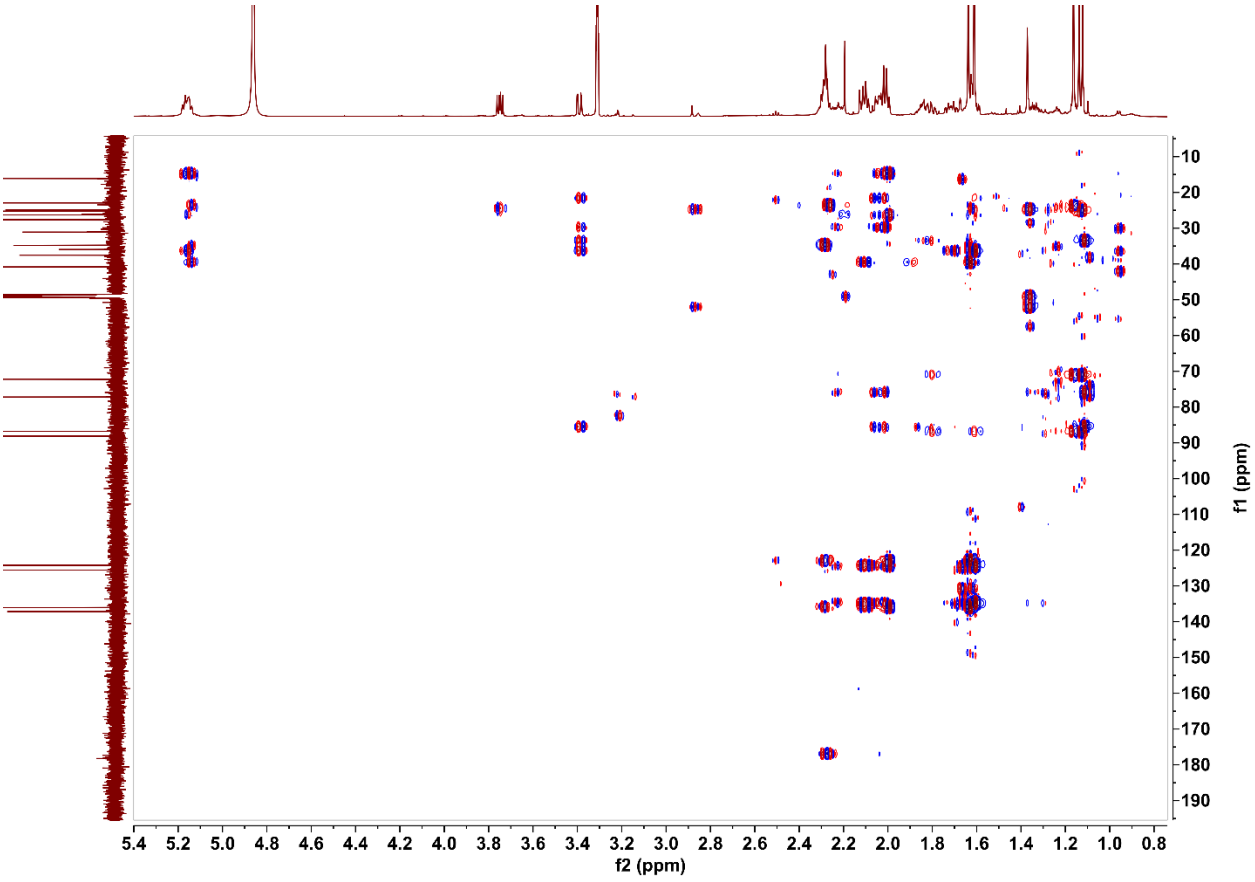

Figure S44. ^{1}H-^{1}H COSY spectrum of **7** in CD_3OD.

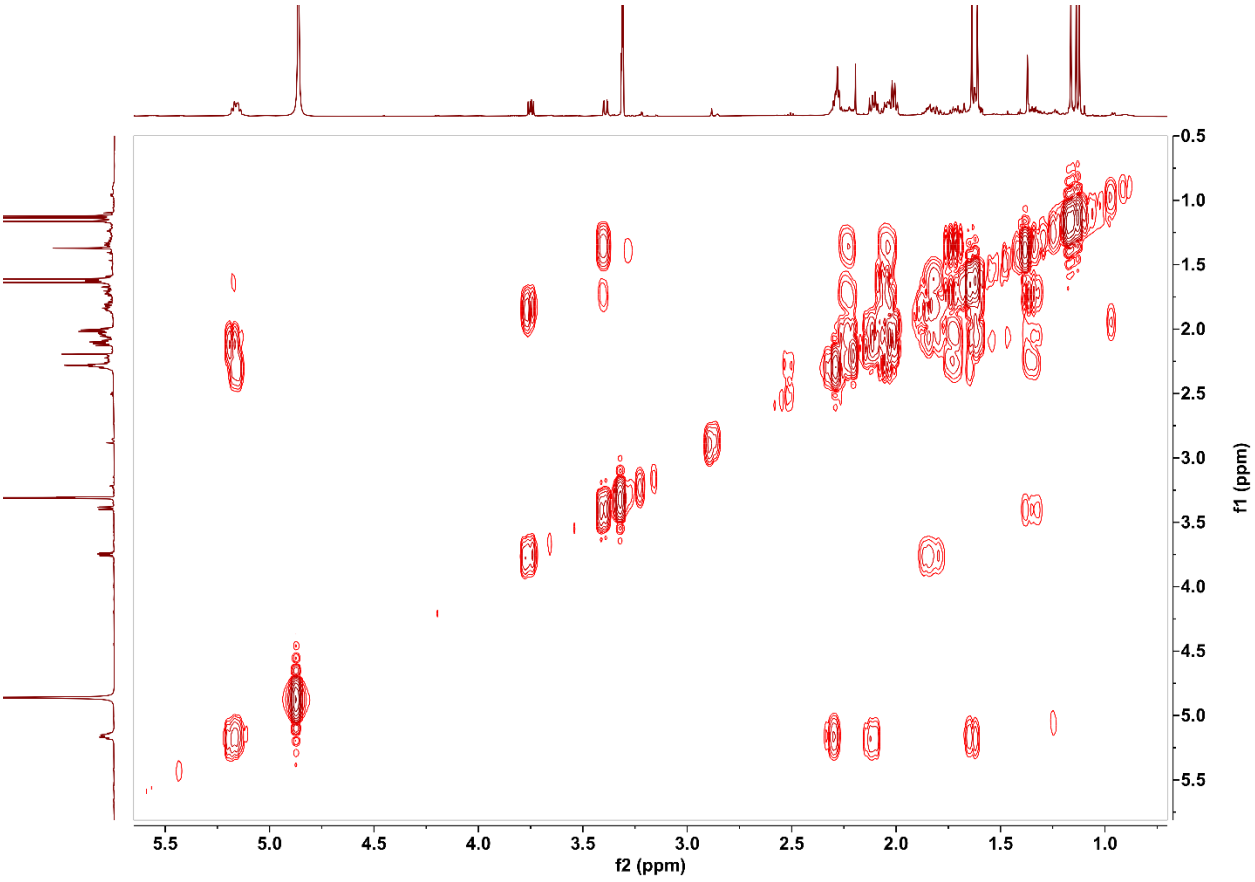

Figure S45. ^{1}H-^{1}H NOESY spectrum of **7** in CD_3OD.

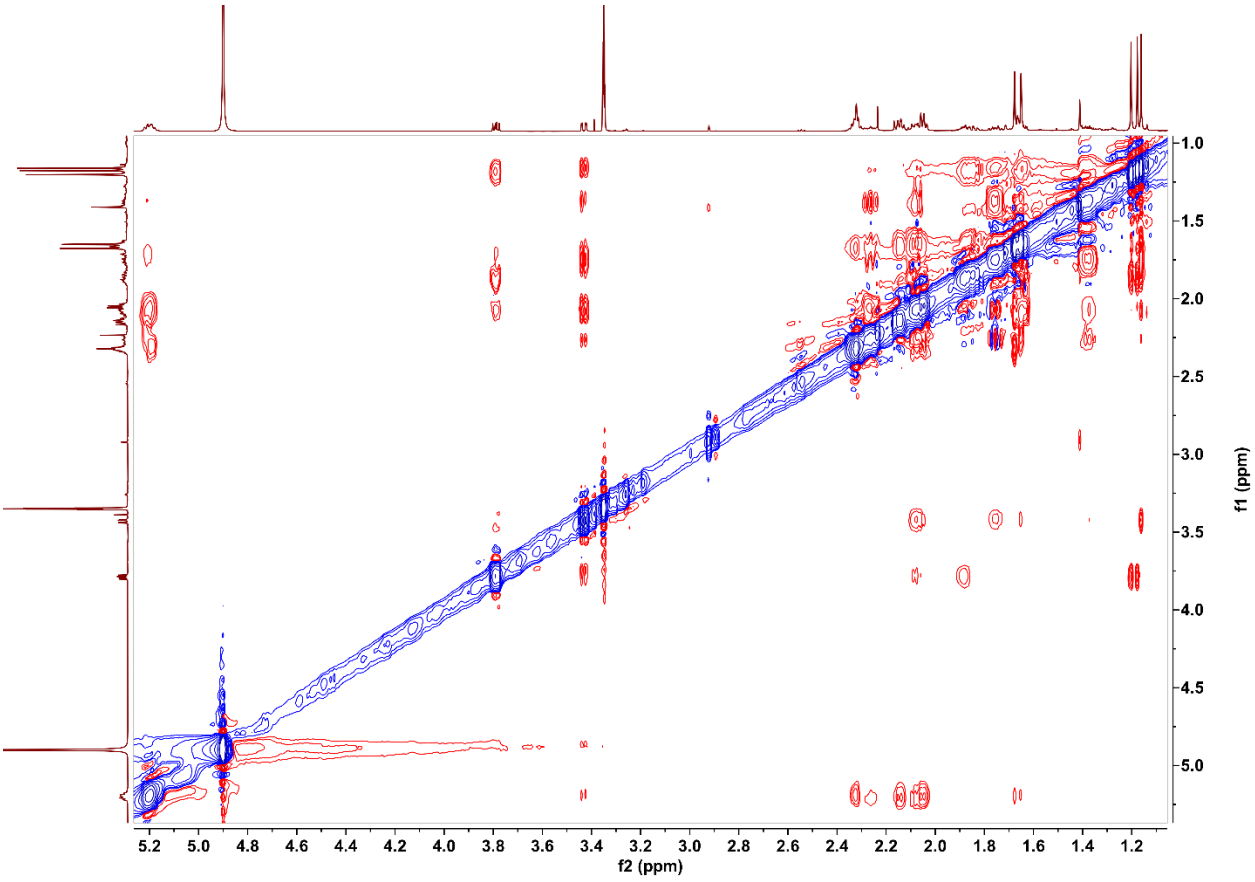

Figure S46. HRESIMS of **8** – **10** (negative mode).

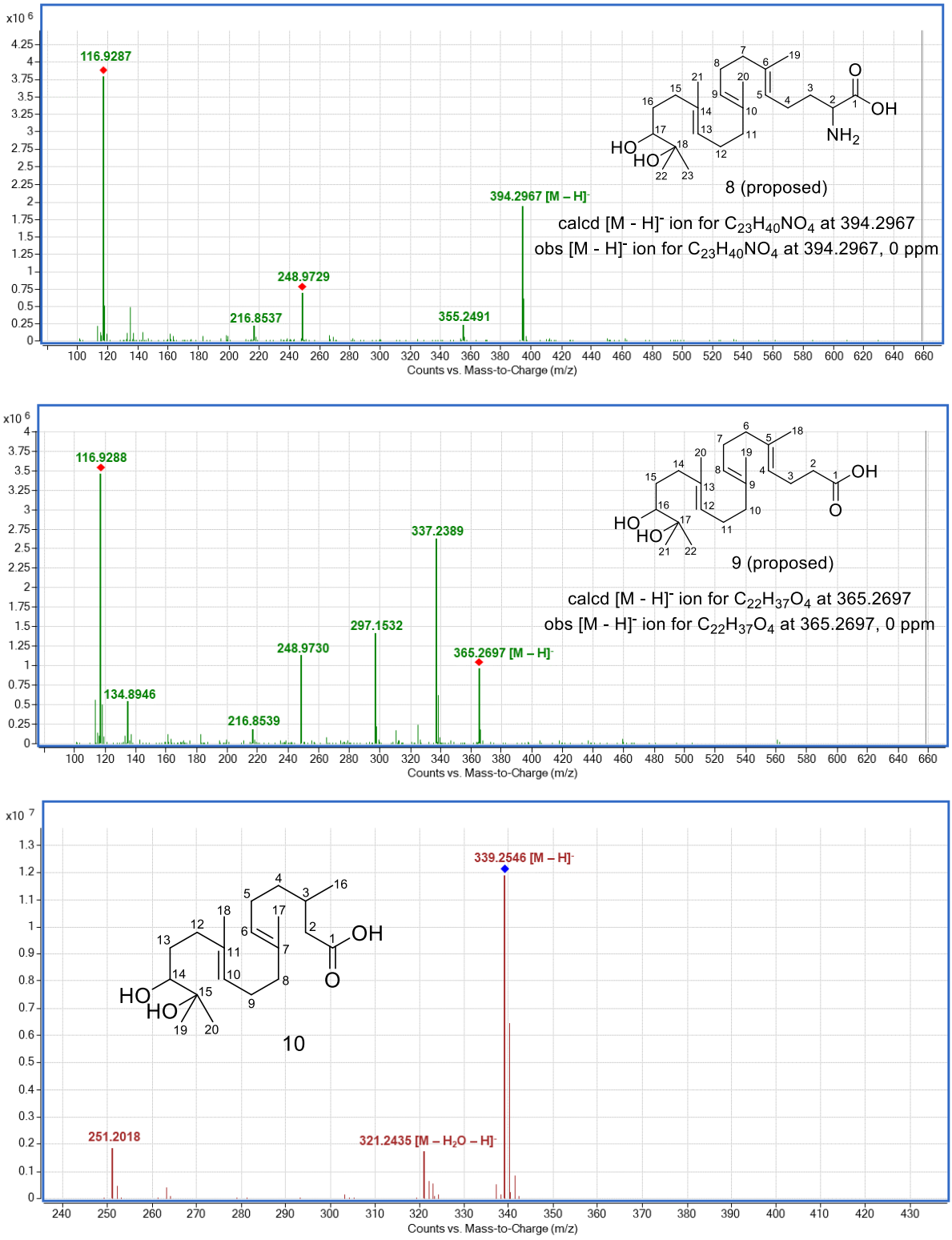

Figure S47. ^{1}H NMR spectrum of **10** in $CDCl_3$ (600 MHz).

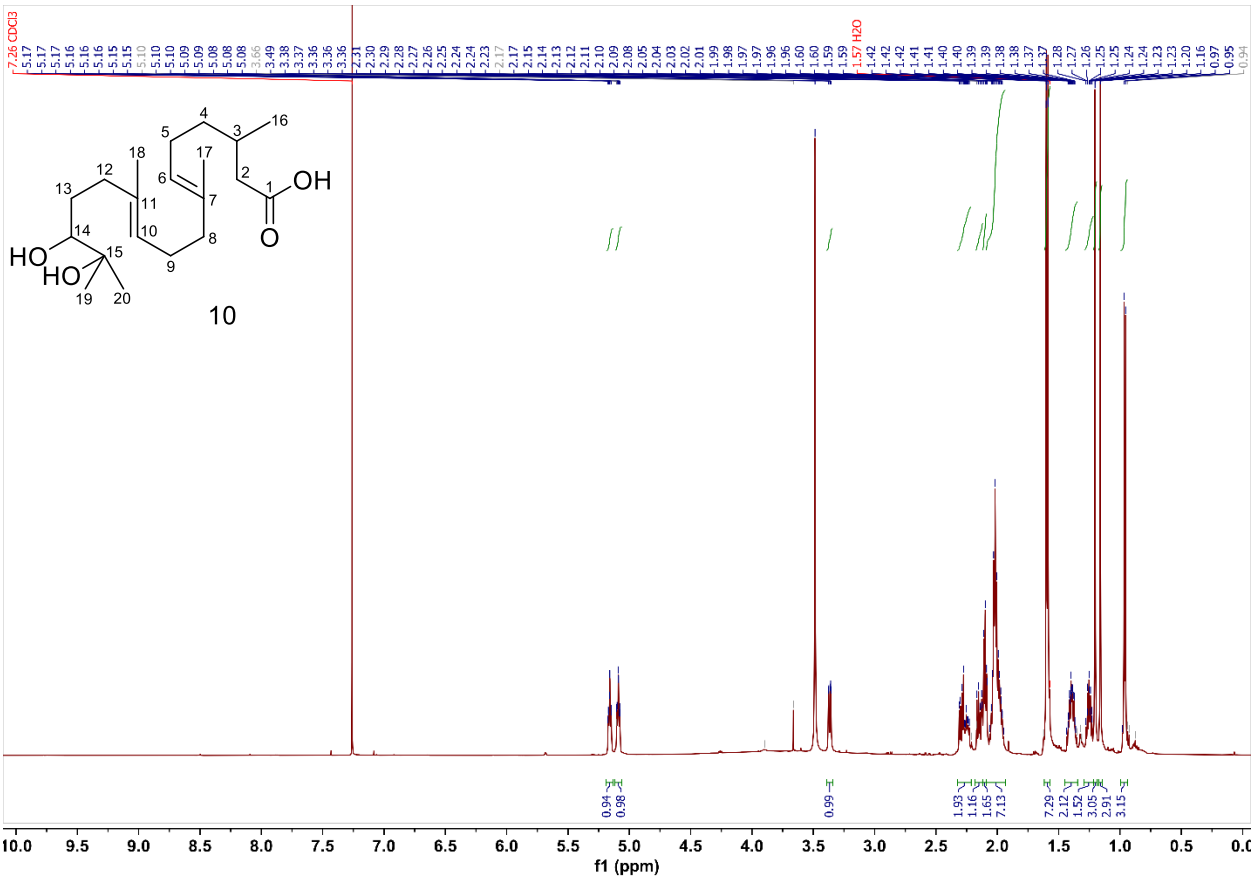

Figure S48. ^{13}C NMR spectrum of **10** in $CDCl_3$ (151 MHz).

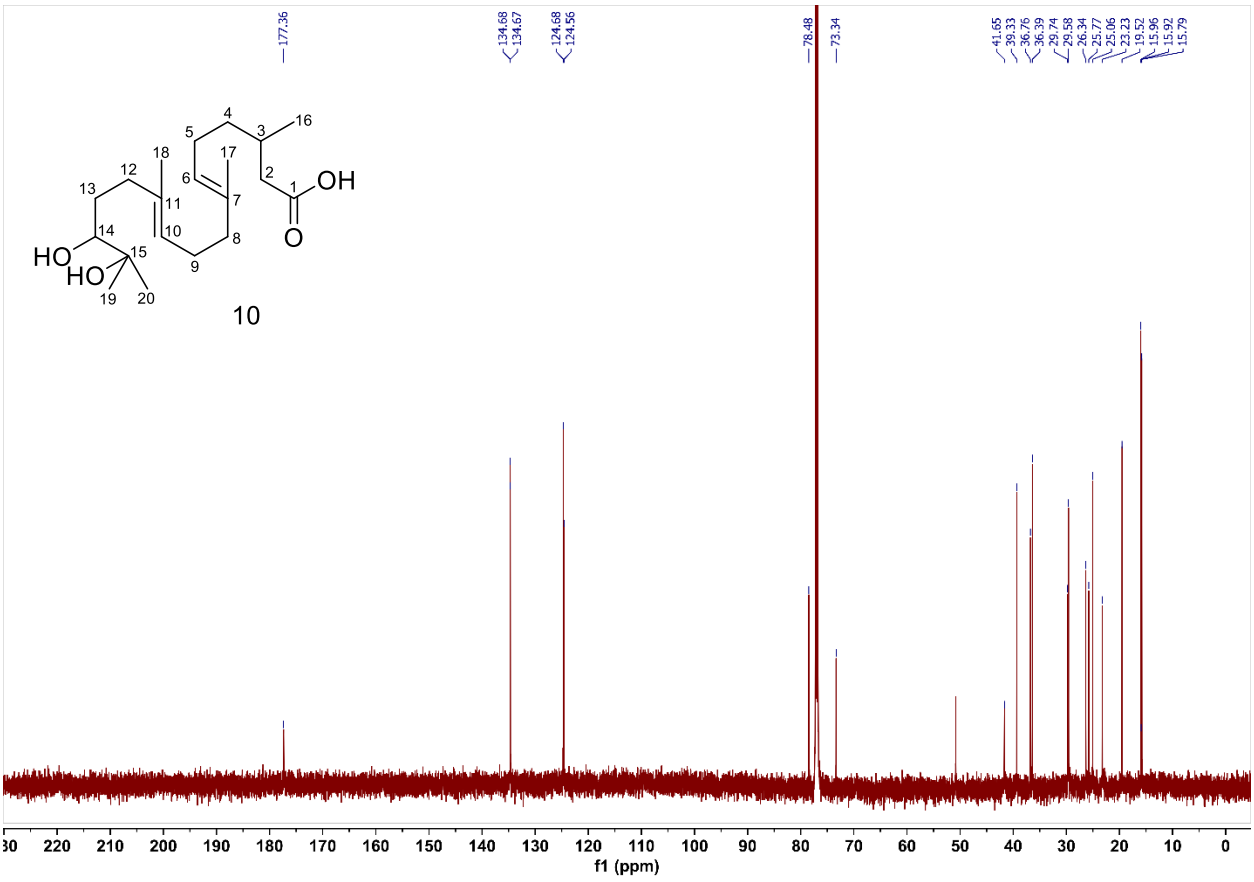

Figure S49. ^{1}H-^{13}C HSQC spectrum of **10** in $CDCl_3$.

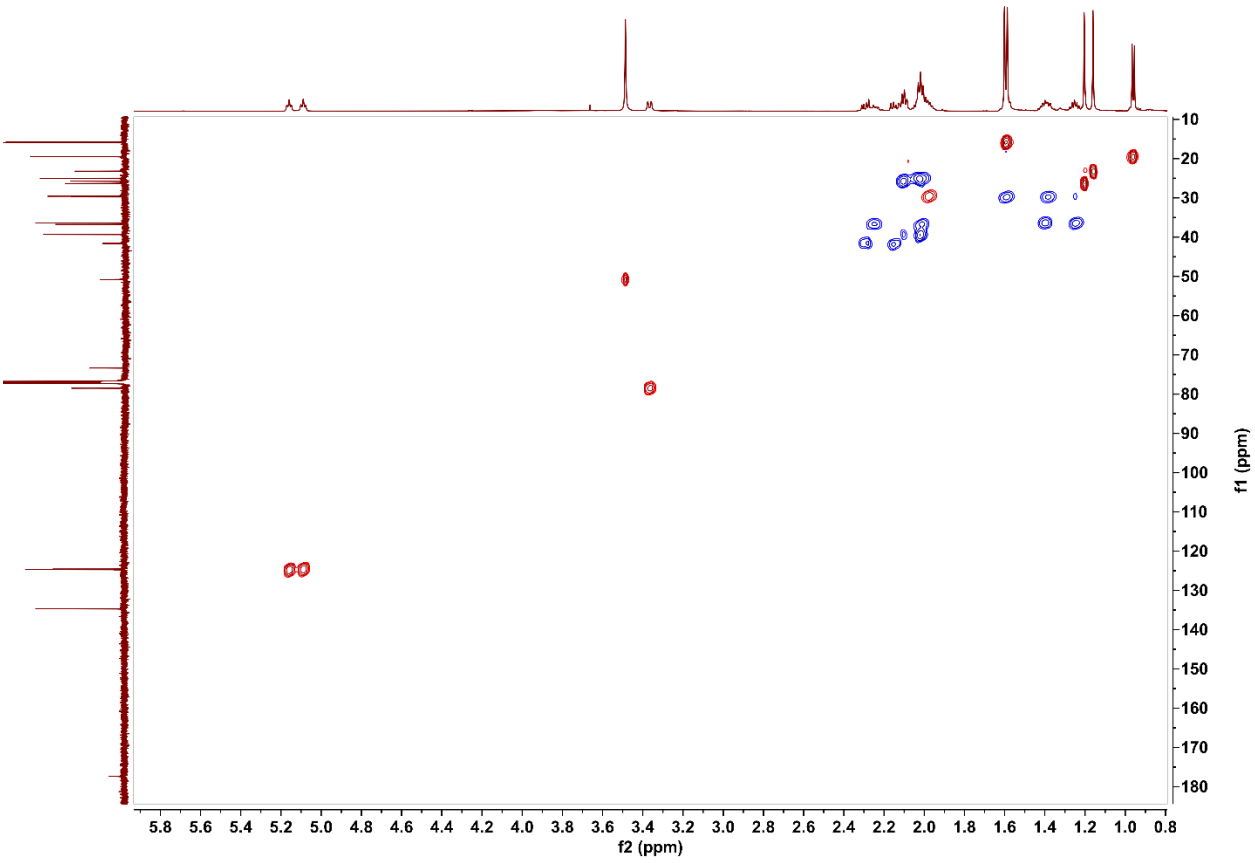

Figure S50. ^{1}H-^{13}C HMBC spectrum of **10** in $CDCl_3$.

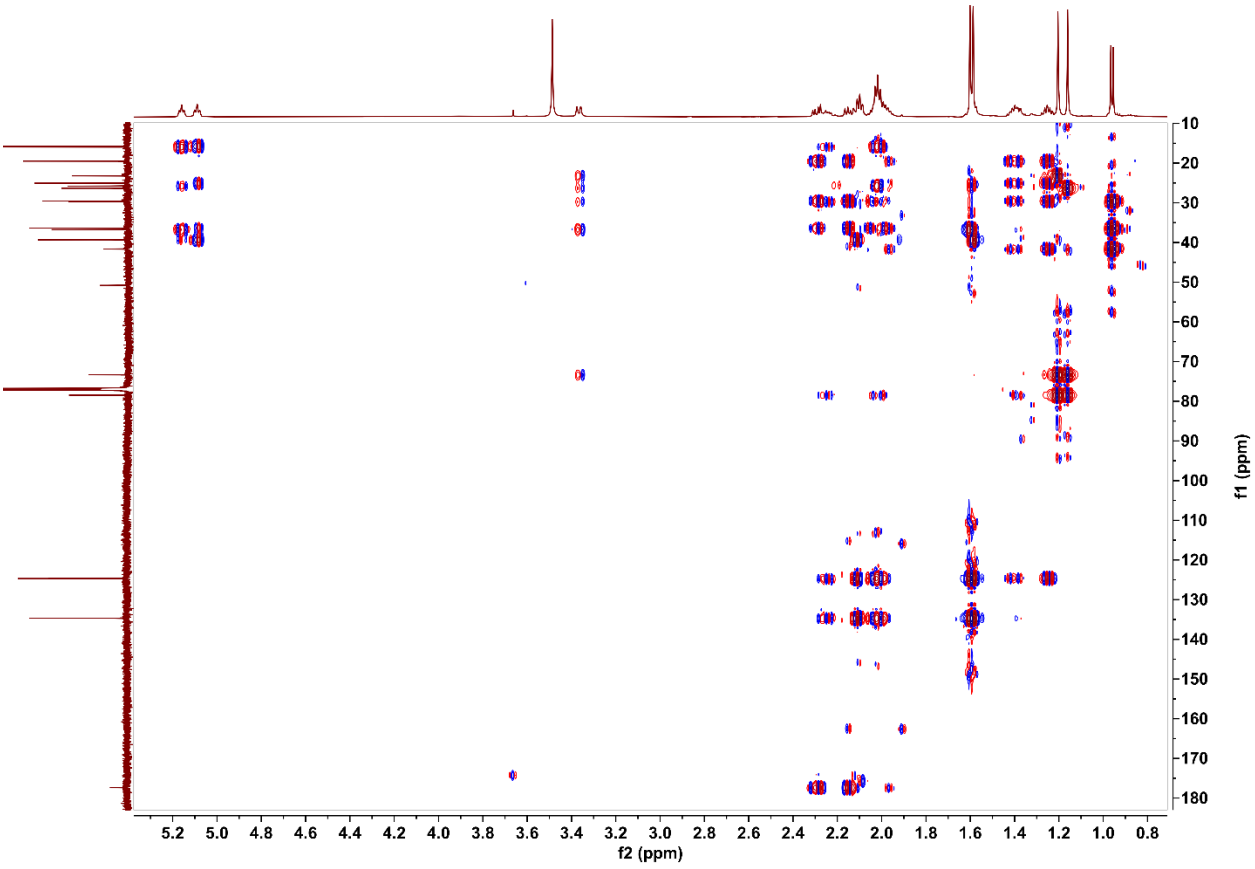

Figure S51. ^{1}H-^{1}H COSY spectrum of **10** in $CDCl_3$.

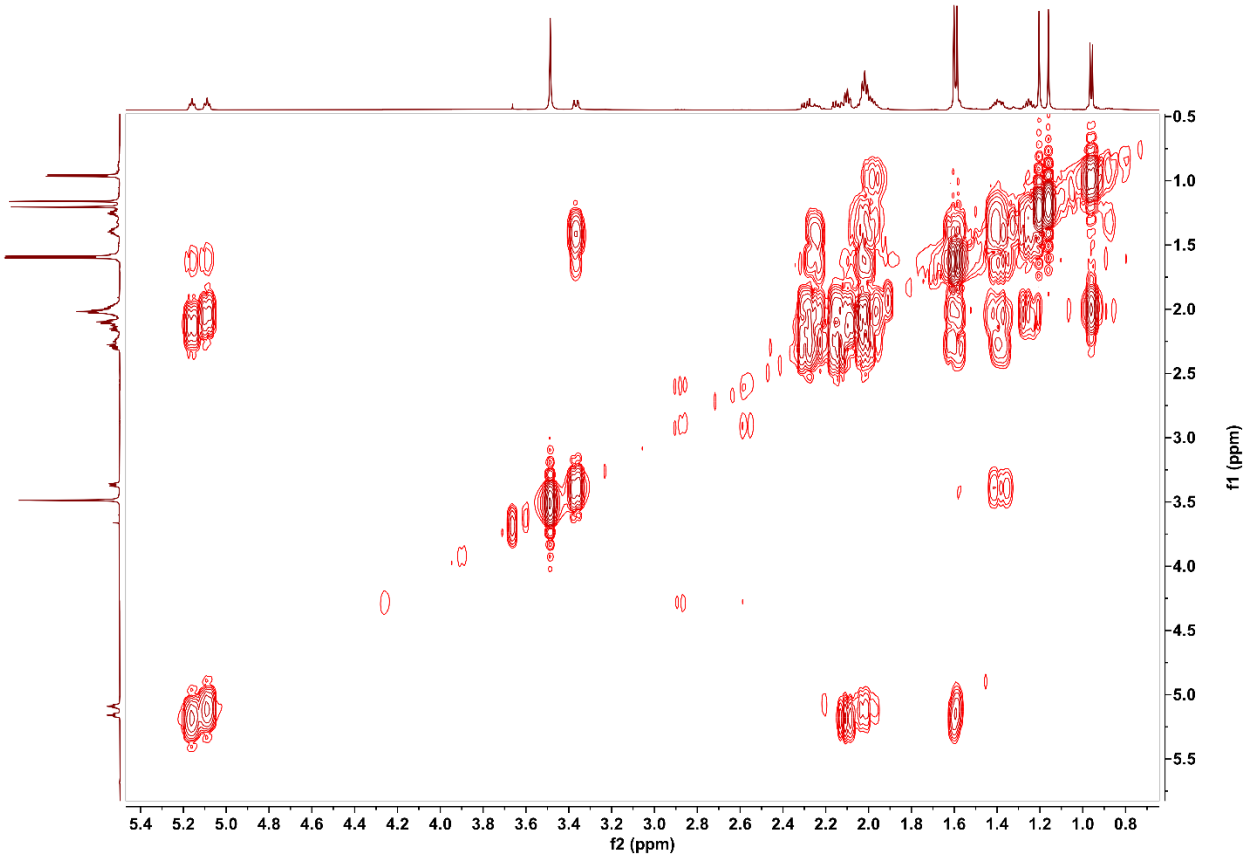

Figure S52. Proposed oxidation pathway in the heterologous hosts leading to degradation of acyclic terpenoid intermediates[8,9].

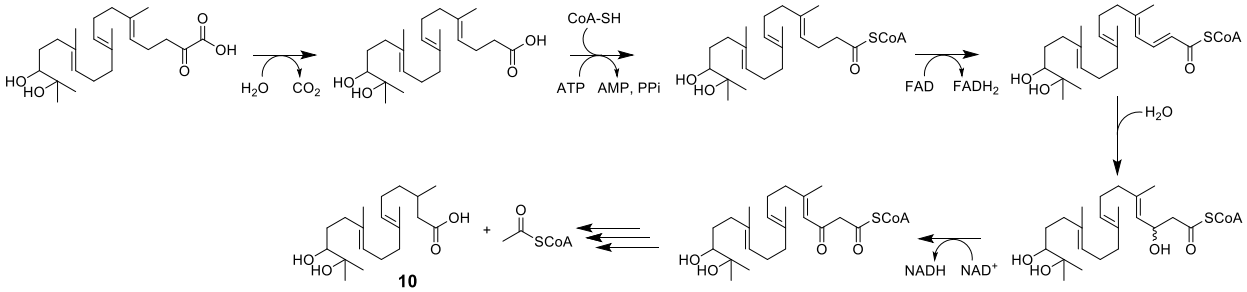

Figure S53. Proposed biosynthesis of shunt products **6** and **7**. The timing of the two epoxidations is unknown.

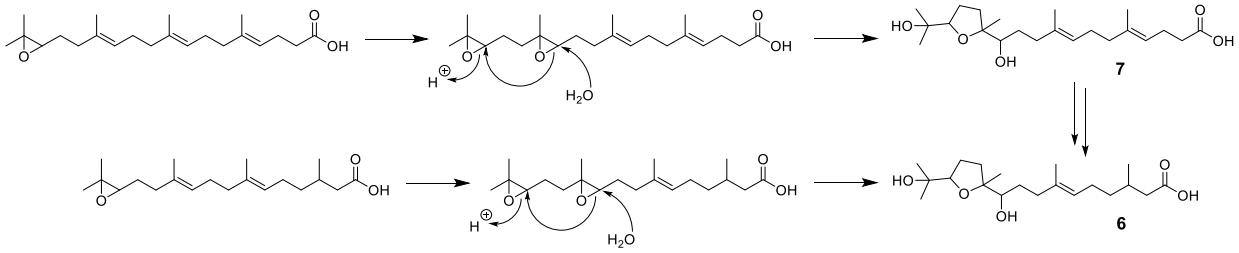

Figure S54. HRESIMS of **11** (negative mode).

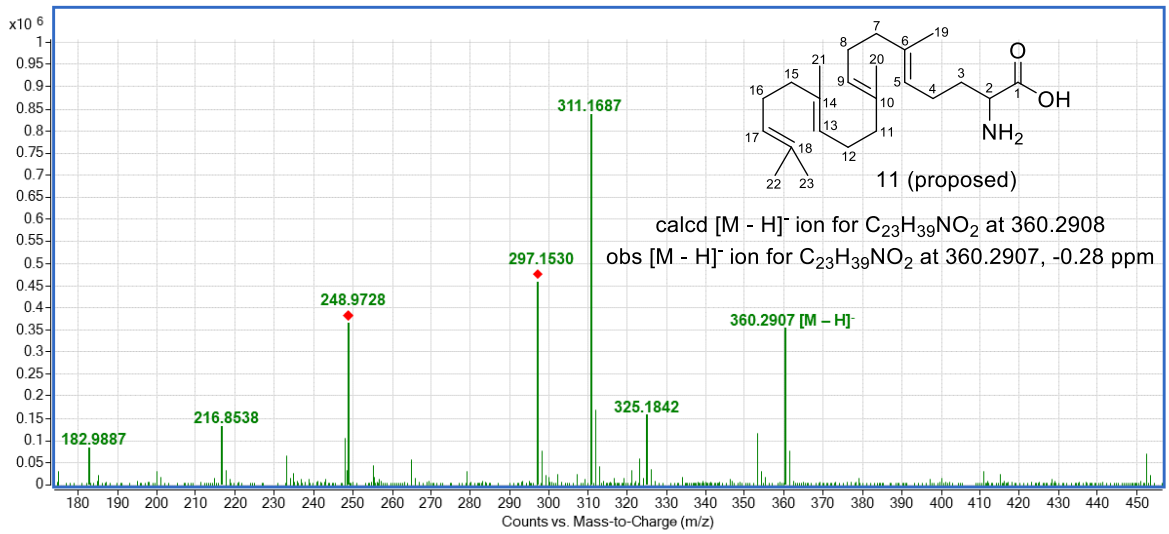

Figure S55. Comparison of phenalinolactone and fungal meroterpenoid biosynthesis. Bacteria and fungi utilize a similar chemical logic to biosynthesize terpenoids. Fungal meroterpenoid biosynthesis typically procedes by prenylation, epoxidation, and finally cyclization[10].

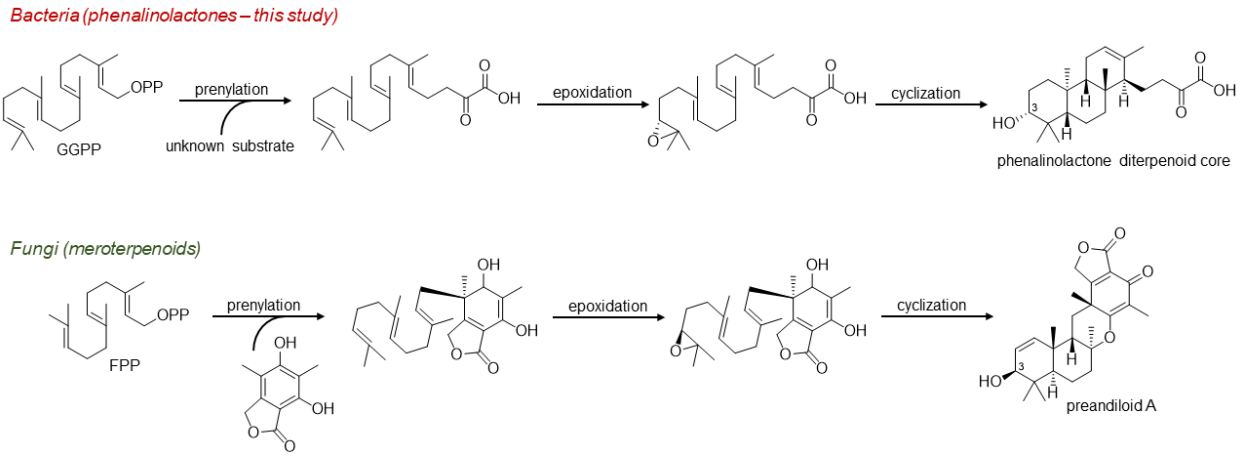

Supporting References

1. Y. Xia, K. Li, J. Li, T. Wang, L. Gu and L. Xun, *Nuc. Acids Res.*, 2018, **47** (3), e15.
2. Z. Li, B. Xu, T. A. Alsup, X. Wei, W. Ning, D. G. Icenhour, M. A. Ehrenberger, I. Ghiviriga, B.-D. Giang and J. D. Rudolf, *J. Am. Chem. Soc.*, 2023, **145** (41), 22361 – 22365.
3. A. Astulla, Y. Hirasawa, A. Rahman, I. Kusumawati, W. Ekasari, A. Widyawaruyanti, N. C. Zaini and H. Morita, *Nat. Prod. Commun.*, 2011, **6** (3), 323 – 326.
4. D. J. Macneil, K. M. Gewain, C. L. Ruby, G. Dezeny, P. H. Gibbons and T. MacNeil, *Gene*, 1992, **111** (1), 61 – 68.
5. K. Gebhardt, R. Pukall and H.-P. Fiedler, *J. Antibiot.*, 2001, **54** (5), 428 – 433.
6. K. Gebhardt, S. W. Meyer, J. Schinko, G. Bringmann, A. Zeeck and H.-P. Fiedler, *J. Antibiot.*, 2011, **64**, 229 – 232.
7. K. F. Chater and L. C. Wilde, *J. Bacteriol.*, 1976, **128** (2), 644 – 650.
8. K. Rose and A. Steinbüchei, *Appl. Environ. Microbiol.*, 2005, **71** (6).
9. W. Seubert, *J. Bacteriol.*, 1960, **79** (3), 426 – 434.
10. Y. Matsuda and I. Abe, *Nat. Prod. Rep.*, 2015, **33**, 26 – 53.